

A. I. Alikhanian National Science Laboratory
(Yerevan Physics Institute)

Sanasar G. Babajanyan

Thermodynamic work: from electromagnetism to adaptation

Thesis for acquiring the degree of candidate of physical-mathematical sciences
in division 01.04.02 (Theoretical Physics)

Scientific supervisor
A.E. Allahverdyan

YEREVAN 2017

Contents

Introduction and Motivation	9
1 Electromagnetic gauge-freedom and work	22
1.1 Introduction	22
1.2 Equations of motion and energy-momentum tensor	26
1.3 Two point-particles without self-interactions	30
1.4 Work and the first law	32
1.4.1 Formulation of the first law	32
1.4.2 Numerical validation	34
1.5 Gauge-freedom of non-relativistic time-dependent Hamiltonian	40
1.6 Standard forms of the energy-momentum tensor	41
1.7 Fermi's Lagrangian for free EMF	45
1.8 Angular momentum	46
1.9 Derivation of (1.34–1.37)	47
1.10 Solving self-consistently delay-differential equations	49
2 Work in presence of self-interaction	51
2.1 Two-particle retarded interaction in the presence of self-interaction	51
2.2 Energy momentum-tensor for free radiation	52
2.3 Energy transfer and work	54
3 Adaptive heat engine	59
3.1 Introduction	59

3.2	Working body	60
3.3	The controller	63
3.4	Adaptation	65
3.5	Restricted adaptation.	67
3.6	Full adaptation	68
3.7	Functioning regimes of the machine (heat-engine, refrigerator, heat-pump) . .	70
3.8	Derivation of the Fokker-Planck equation and justification of the slow limit . .	71
3.8.1	Fokker-Planck equation	71
3.8.2	Fokker-Planck equation for a negative temperature	74
3.8.3	Checking the slow limit	74
3.9	Feedforward does not provide advantages for adaptation	75
3.10	Heat-engine adaptation: symmetric vs. Kramers rates	77
3.11	Relations with the no-pumping theorem	80
3.12	Efficiency and power	81
3.12.1	Adaptation of efficiency	84
3.12.2	Adaptation of power	85
3.13	No-go statement for adaptation	87
3.14	Slow current	91
3.15	External force that generates negative friction	92
3.16	Non-equilibrium features and fragility	93
3.17	Coupling between heat-engine and controller has to be informative in the Bayesian sense	94
	Conclusion	96
	Bibliography	98

List of Figures

1	Carnot Cycle.	19
1.1	Repulsive motion with initially zero velocities. The curves are obtained via self-consistent solution of (1.34–1.39) for $m = 5$, $m' = 50$, $ee' = c = 1$, $l_0 = 5$, $\omega_0 = \omega'_0 = 0$. (a) The energy difference $\Delta_{t 0}E$ of the light particle (red) and the sum $\Delta_{t 0}(E + K')$ of this energy and the kinetic energy K' of the heavy particle (green); cf. (1.45, 1.46). (b) $\Delta_{t 0}(E + K')$ (green) and $\Delta_{t 0}(K + E')$ (brown). The former quantity is conserved better. (c) The velocity $\omega(t)$ ($\omega'(t)$) of the light (heavy) particle is shown by red (black) curve.	35
1.2	Attractive motion with initially zero velocities and $ee' = -1$, $c = 1$, $l_0 = 10$, $m = 10$, $m' = 50$, $\omega_0 = \omega'_0 = 0$; cf. (1.34–1.39). The inter-particle distance at the final time $x'(100) - x(100) = 1.2219$. (a) $\Delta_{t 0}E$ (red) and $\Delta_{t 0}(E + K')$ (green). (b) $\omega(t)$ (red) and $\omega'(t)$ (black); cf. Figs. 1.1(a)–1.1(c).	36
1.3	Repulsive motion: one particle (P') falls into another (P) that is at rest initially: $ee' = 1$, $c = 1$, $l_0 = 100$, $m = 10$, $m' = 50$, $\omega_0 = 0$, $\omega'_0 = -0.4$; cf. (1.34–1.39). The minimal inter-particle distance $x'(t) - x(t) = 1.2287$ is reached at $t = 255.87$. (a) $\Delta_{t 0}E$ (red) and $\Delta_{t 0}(E + K')$ (green). (b) $\omega(t)$ (red) and $\omega'(t)$ (black).	37

1.4	Scattering of particles with $ee' = 1$, $c = 1$, $l_0 = 200$, $m = 5$, $m' = 50$, $\omega_0 = 0.1$, $\omega'_0 = -0.0100499$; cf. (1.34–1.39). The parameter are chosen such that the initial (and the final) kinetic momentum is zero: $m\omega_0/\sqrt{1-\omega_0^2} + m'\omega'_0/\sqrt{1-\omega_0'^2} = 0$. The minimal inter-particle distance $x'(t) - x(t) = 30.57$ is reached at $t = 1944.13$. (a) Red (upper) curve $\Delta_{t 0}E$. Green (lower) curve: $\Delta_{t 0}(E + K')$; cf. Fig. 1.1(a). (b) Green (lower) curve: $\Delta_{t 0}(E + K')$. Brown (upper) curve: $\Delta_{t 0}(K + E')$	38
2.1	For all figures we employ $ee' = 1$, $m'/m = 10$ and the units of the light particle. The infinitely remote time is -10^3 . Cauchy solution for $t_f = 500$, where $v'(t_f) = 0.04$, $v(t_f) = -0.4$, $x'(t_f) - x(t_f) = 100$; $v'(0) = -0.04804$, $v(0) = 0.40117$. From up to down. Upper line $\Delta_{t 0}E$. Upper dotted line $\Delta_{t 0}(E' + K)$. Dashed line $\Delta_{t 0}(E + K')$; cf. (2.19, 2.20). Middle dotted line: the sum of the Larmor rates (2.22). Lower line $\Delta_{t 0}K'$. Lower dotted line $\Delta_{t 0}(K' + K)$	57
2.2	Cauchy solution for $t_f = 700$, where $v'(t_f) = -0.3$, $v(t_f) = -0.6$, $x'(t_f) - x(t_f) = 100$; $v'(0) = -0.364289$, $v(0) = 0.0102$. Upper line $\Delta_{t 0}E$. Lower line $\Delta_{t 0}K'$. Dashed line $\Delta_{t 0}(E + K')$	57
2.3	Cauchy solution for $t_f = 600$, where $v'(t_f) = 0.3$, $v(t_f) = -0.3$, $x'(t_f) - x(t_f) = 200$; $v'(0) = 0.187263$, $v(0) = 0.677107$. Lower line $\Delta_{t 0}E$. Upper line $\Delta_{t 0}K'$. Dashed line $\Delta_{t 0}(E + K')$. Dotted line: the sum of the Larmor rates (2.22).	58
3.1	A schematic representation of the model. There are three thermal baths at temperatures $T_{32}, T_{31} < T_{21} = \infty$; each one drives a single transition among three engine levels 1, 2, and 3. The bath with temperature $T_{21} = \infty$ is the source of work. A controller x interacts with energies, but does not couple directly with the baths.	61

- 3.2 Restricted adaptation scenario. $\Phi'(x)$ given by (3.17, 3.22) with $f_{ij}[y] = e^{\beta_{ij}y/2}$. (Similar results hold for all other physical choices of $f_{ij}[y]$; see (3.22) and 3.10) We assume $\hat{E}_3(x) = -x$, $\hat{E}_2(x) = x - 2$; see (3.18, 3.13). Now heat-engine conditions (3.20) hold for $x > 2$ if $\theta > 2$, and for $x \in (\frac{2}{2-\theta}, 2)$ if $\theta < 2$. Normal (resp. dashed) curves: $\Phi'(x)$ for x that support (3.20) under $\beta_{32} = 1$ (resp. $\beta_{32} = 0.7$) and various $\theta = \beta_{31}/\beta_{32}$. They are indicated from the top to the bottom in the right (resp. left). The magenta (bold) curve shows $-E'_1(x)$, where $E'_1(x) = 1.8(x - 2) + 0.680289$; cf. (3.13). Intersections of $-E'_1(x)$ with $\Phi'(x)$ determine \hat{x} . Conditions (3.19) hold for all normal curves, and none of dashed curves. 67
- 3.3 Full adaptation scenario ($\gamma < 0$). $\Phi'(x)$ with $f_{ij}[y] = e^{\beta_{ij}y/2}$ for varying β_{31} and fixed β_{32} ; cf. Fig. 3.2. We assume $\hat{E}_3(x) = x/2$, $\hat{E}_2(x) = x - 2$, and (3.20) holds for $x \in (\frac{4}{1+\theta}, 2)$. Normal (resp. dashed) curves: $\Phi'(x)$ for x that support (3.20) under $\beta_{32} = 1$ (resp. $\beta_{32} = 3$) and various $\theta = \beta_{31}/\beta_{32}$, as indicated from the top to the bottom in the left (resp. right). The magenta (bold) curve shows $-E'_1(x)$, where for the considered range of x , $E'_1(x) = -0.1(x - 2) - 0.5$. Adaptation conditions (3.23) hold for all curves, and for all β_{31}, β_{32} 68

- 3.4 (a) $\langle E \rangle = \sum_{i=1}^3 \sum_{\alpha=1}^N p_{i\alpha} E_{i\alpha}$ is the stationary average energy as a function of $\theta = \beta_{31}/\beta_{32}$ calculated from (3.28, 3.30, 3.31) for $\beta_{32} = 1$, $N = 100$, $\tau = 2$, $\beta = 0.5$ and $E_{i\alpha} = i\alpha^2$. $\langle \tilde{E} \rangle = \sum_{i=1}^3 \sum_{\alpha=1}^N \tilde{p}_{i\alpha} E_{i\alpha}$ is the stationary average energy calculated via the probabilities $\tilde{p}_{i\alpha}$ under the slow limit; see (3.43–3.45). Now (a) shows the relative difference $\frac{\langle E \rangle - \langle \tilde{E} \rangle}{\langle E \rangle}$ between $\langle E \rangle$ and $\langle \tilde{E} \rangle$. It is seen that the validity of the slow limit (as measured by the magnitude of $\frac{\langle E \rangle - \langle \tilde{E} \rangle}{\langle E \rangle}$) gets worst for $\theta \rightarrow 0$ and $\theta \rightarrow \infty$. This is natural because low temperatures of the heat-engine baths freeze some of its motions and tend to make it less fast, i.e. low temperatures act against the slow limit. (b) $p_{i\alpha}$ are the stationary probabilities calculated from (3.28, 3.30, 3.31) for the same parameters as in (a), but $\tau = 1$, $\beta = 2$. $\tilde{p}_{i\alpha}$ are the slow-limit stationary probabilities calculated from (3.43, 3.44, 3.45). The figure shows $\max_{i\alpha} |p_{i\alpha} - \tilde{p}_{i\alpha}|$, which is another measure for the validity of the slow limit. We again see that the validity of the slow limit gets worst for $\theta \rightarrow 0$ and $\theta \rightarrow \infty$ 72
- 3.5 A schematic representation of the model with the feedforward control. There are three thermal baths at temperatures $T_{32} < T_{31} < T_{21} = \infty$; each one drives a transition among three engine states 1, 2, and 3. x is a controller that changes energies of states, and also does interact directly with the two baths; 76

- 3.6 (a) $\Phi'(x)$ with $f_{ij}[y] = e^{\beta_{ij}y/2}$ for varying β_{31} and fixed $\beta_{32} = 1$ (restricted adaptation scenario). We assume $\hat{E}_3(x) = -x$, $\hat{E}_2(x) = x - 2$, and (3.20) holds for $x > 2$ if $\theta > 2$, for $\frac{2}{2-\theta} > x > 2$ if $1 < \theta < 2$, and for $\frac{2}{2-\theta} < x < 2$ if $\theta < 1$. $\Phi'(x)$ is shown for various $\theta = \beta_{31}/\beta_{32}$ and those x that support (3.20): $\theta = 0.1$ (red curve), $\theta = 0.25$ (green), $\theta = 0.5$ (blue), $\theta = 0.75$ (brown), $\theta = 0.95$ (black), $\theta = 1.2$ (black-dashed), $\theta = 1.5$ (brown-dashed), $\theta = 2.5$ (blue-dashed). The magenta curve shows $-E'_1(x)$, where $E'_1(x) = 1.8(x - 2) + 0.680289$. Intersections of $-E'_1(x)$ with $\Phi'(x)$ determine \hat{x} . (b) The same as in Fig. 3.6(a), but for $\beta_{32} = 0.7$. It is seen that for θ close to 1, no heat-engine functioning exists (i.e. (3.20) does not hold): the magenta curve does not cross the curves with $\theta = 0.95$, $\theta = 1.2$ and $\theta = 1.5$. (c) Adaptation for a negative friction $\gamma < 0$, $\beta_{32} = 3$ and varying β_{13} . The same parameters as in Fig. 3.6(a), but now $\hat{E}_3(x) = x/2$. Conditions (3.20) amount to $\frac{4}{1+\theta} > x > 2$ if $\theta < 1$, and to $\frac{4}{1+\theta} < x < 2$ if $\theta > 1$. $\Phi'(x)$ is shown for: $\theta = 0.1$ (red curve), $\theta = 0.25$ (green), $\theta = 0.5$ (blue), $\theta = 0.75$ (brown), $\theta = 0.95$ (black), $\theta = 1.2$ (black-dashed), $\theta = 1.5$ (brown-dashed), $\theta = 2.5$ (blue-dashed), $\theta = 4$ (green-dashed), $\theta = 6$ (red-dashed). The magenta curve shows $-E'_1(x)$, where for the considered range of x , $E'_1(x)$ is approximated as $E'_1(x) = -0.1(x - 2) - 0.5$ 78
- 3.7 (a) and (b) are the analogues of (resp.) Fig. 3.6(a) and Fig. 3.6(c), but with the Kramers rates (3.50) under $\Delta = 1$ 79
- 3.8 (a) and (b) are the analogues of (resp.) Fig. 3.6(a) and Fig. 3.6(c) [also, respectively, of Fig. 3.2 and Fig. 3.3], but with the rates given by (3.56) under $F_{ij} = 1$. (c) is the analogue of (b), but with $\beta_{32} = 3$. For (a): $\hat{E}_1(x) = 0.9(x - 2)^2 + 0.680289(x - 2)$, $\hat{E}_2(x) = x - 2$, $\hat{E}_3(x) = -x$. For (b) and (c): $\hat{E}_1(x) = -0.05(x - 2)^2 - 0.5(x - 2)$ (in the considered range of x), $\hat{E}_2(x) = x - 2$, $\hat{E}_3(x) = x/2$ 79
- 3.9 Functions $f_2(\theta)$ (dashed curve) and $f_3(\theta)$ (full curve) that determine the values of \hat{E}_2 and \hat{E}_3 which minimize J_{21} (i.e. maximize the power of the heat-engine); see (3.66). The minimized $J_{21}(\theta)$ for $\beta_{32} = 1$ (thick curve). 83

- 3.10 The efficiency $\eta(\theta)$ at the maximal power (full curve), the Carnot efficiency $\eta_C = 1 - \min(\theta, \frac{1}{\theta})$, and the minimized $J_{21}(\theta)$ at $\beta_{32} = 1$ (thick curve); see (3.62) and (3.60, 3.61). 83
- 3.11 Efficiency adaptation. $\Phi'(x)$ under rates (3.63) for varying β_{31} and fixed $\beta_{32} = 1$ (restricted adaptation scenario). We assume $\hat{E}_3(x) = -x$, $\hat{E}_2(x) = x - 2$, and (3.67) holds for $x > 2$ if $\theta > 2$, for $\frac{2}{2-\theta} > x > 2$ if $1 < \theta < 2$, and for $\frac{2}{2-\theta} < x < 2$ if $\theta < 1$. $\Phi'(x)$ is shown for various $\theta = \beta_{31}/\beta_{32}$, as indicated on the right from top to bottom. The magenta (dashed) curve shows $-E'_1(x)$; it is chosen so that both (3.67) and (3.68) hold. Intersections of $-E'_1(x)$ with $\Phi'(x)$ determine \hat{x} . The magenta curve passes on the edges of $\Phi'(x)$, i.e it passes through $\approx \frac{2}{2-\theta}$ that for the present choice of \hat{E}_2 and \hat{E}_3 fullfils (3.68). 86
- 3.12 Power adaptation. The same as for Fig. 3.11, but the magenta (dashed) curve $-E'_1(x)$ is chosen so that both (3.67) and (3.70) hold, i.e. the magenta curve passes through $\frac{4}{3-\theta}$ that for the present choice of $\hat{E}_2(x) = x - 2$ and $\hat{E}_3(x) = -x$ fullfils (3.70). Note that the adopted value $\beta_{32} = 1$ is sufficiently small for the high-temperature result (3.69) to apply. 86

Introduction and Motivation

Thermodynamics grew up as a theory of heat-engines with the raise of the Industrial Revolution in the XIX'th century [1]. Already in the middle of that century it matured into a phenomenological theory based on few explicit and many implicit assumptions. Fundamental contributions to thermodynamics were done by Carnot, Clausius, Thomson, Clayperon and others.

Since the works by Boltzmann, Maxwell and Gibbs thermodynamics became grounded on microscopic theories [2,3]: there appeared a general tendency of deriving (and not just postulating) various assumptions of thermodynamics [4]. Importantly, it also became related with a limited control, e.g. because thermodynamical relations emerge via an incomplete description of a many-body system [4]. This aspect of the limited control is frequently manifested via fluctuations [1]; hence the term statistical thermodynamics. However, neither fluctuations nor incomplete description exhaust deep relations of thermodynamics with ideas of control. One such relation was formalized as the maximum entropy principle [5]: basic distributions known in statistical thermodynamics can be recovered via maximizing the ignorance-i.e. maximizing the information-theoretic entropy-given certain plausible constraints, e.g. energy conservation. Another idea amounts to relating control and heat-engine physics within the concept of adaptation. This is one of the main subjects of this thesis.

Connections of thermodynamics with microscopic theories is an essentially two-way road. On one hand, the microscopic perspective does improve our understanding of thermodynamics and increase its applicability range even in its traditional domain of macroscopic systems. On the other hand, microscopic theories do benefit-and frequently even emerge-via thermo-

dynamics. Examples of the latter situation are well-known [1]: thermodynamic ideas played a crucial role in the inception of quantum mechanics via the Planck's approach to black-body radiation. Such ideas were also instrumental in black-hole physics, and hence in modern theories of quantum gravity [6].

These two aspects-two-way connection with microscopic theories and relations with control-will be the main themes of the present thesis. Below we provide an introduction to these themes using general arguments. They are developed in subsequent chapters.

Work and first law

We start our discussion with the first law of thermodynamics [1]. This law is frequently regarded as a trivial consequence of the energy conservation. While the energy conservation is indeed the ground of the first law, its relations with this law are far from trivial. Indeed, the first law introduces the fundamental concept of *energy quality*, because a change $\frac{dU}{dt}$ of internal energy is divided into two parts: high-graded $\frac{dW}{dt}$ (work) and low-graded $\frac{dQ}{dt}$ (heat) [1]:

$$\frac{dU}{dt} = \frac{dW}{dt} + \frac{dQ}{dt}, \quad (1)$$

In terms of the microscopic energy $H(x, \pi, f)$ -where x and π are (resp.) the sets of canonic coordinates and momenta, and where $f = f(t)$ is a time-dependent external field- U is presented as the average energy [1]:

$$U(t) = \int dx d\pi H(x, \pi, f(t)) P(x, \pi, t), \quad (2)$$

where t is the time, $P(x, \pi, t)$ is the probability density by which we describe the system. In particular, the description can be based a trajectory $\{x(t), \pi(t)\}$, where

$$P(x, \pi, t) = \delta_{\mathcal{D}}(x - x(t)) \delta_{\mathcal{D}}(\pi - \pi(t)), \quad (3)$$

and where $\delta_{\mathcal{D}}$ is the Dirac's function. Thus U involves both kinetic and potential energies of all particles that constitute the system. It is seen that the first law (1) is based on the energy

conservation: if no external influences are present (i.e. the system is left to itself) both the work and heat nullify and also the energy is conserved.

The work done by external field reads in (1) [1, 7, 8]:

$$\frac{dW}{dt} = \int dx d\pi P(x, \pi, t) \partial_t H(x, \pi, f(t)). \quad (4)$$

If the system couples only with an external source of work, i.e. when its evolution is governed by Hamiltonian equations of motion for x and π generated by $H(x, \pi, f(t))$, one can employ these equations to show that in (1) one has $\frac{dQ}{dt} = 0$, i.e. the heat is absent as expected [1]. The heat is defined from (1, 2, 4) as

$$\frac{dQ}{dt} = \int dx d\pi H(x, \pi, f(t)) \partial_t P(x, \pi, t). \quad (5)$$

Hence $\frac{dQ}{dt} \neq 0$ only if the system is open, i.e. (besides the source of work) it also couples with its environment. The latter need not be thermal. Hence the heat relates to the energy of degrees of freedom that are not under direct observation, i.e. they are not included in the system. Within this thesis we shall not dwell further into the features of heat. It suffices to say, however, that-in the regime, where the environment is not thermal and/or its coupling with the system is not weak- the detailed understanding of these features is mostly an open problem [9].

The source of work is a mechanic degree of freedom that holds certain conditions. First of all, its back-reaction on the system is neglected, i.e. the dynamics of the system can be described with given external fields. Note that the full reaction of the system to the source is not neglected, because the system can exchange energy with the source [1]. It is only the back-reaction is neglected in the sense that the dynamics of the system can be described as if the source does not feel the system. There is an important point in requiring that the back-reaction can be neglected: in thermodynamics the work-source is a mechanic degree of freedom (e.g. a wheel) that performs a well-controlled motion. If the back-reaction is not negligible, i.e. if we allow a full-scale coupling between the work-source and the thermalized system, then the work-source will cease to perform a mechanical motion, it will thermalize

as well and become a part of the system. Due to this controlled motion of the work-source, it is also possible to study slow, quasi-static processes.

Next pertinent feature of the work is that it is a local quantity [9]: let $x = (x_1, x_2)$ and $\pi = (\pi_1, \pi_2)$ be the coordinate and momenta of the full system, while (x_1, π_1) and (x_2, π_2) refer to two sub-systems of the system. We assume that external fields act only on one sub-system, i.e. we have in (2)

$$H(x, \pi, f(t)) = H_1(x_1, \pi_1, f(t)) + H_1(x_2, \pi_2) + H_{\text{int}}(x, \pi), \quad (6)$$

$$\partial_t H(x, \pi, f(t)) = \partial_t H_1(x_1, \pi_1, f(t)), \quad (7)$$

where $H_{\text{int}}(x, \pi)$ is the interaction Hamiltonian that does not depend on the external field $f(t)$. Also, $H_1(x_2, \pi_2)$ does not depend on $f(t)$. Then the global definition (4) can be re-written locally with help of (6, 7)

$$\frac{dW}{dt} = \int dx_1 d\pi_1 P_1(x_1, \pi_1, t) \partial_t H_1(x_1, \pi_1, f(t)), \quad (8)$$

i.e. involving only the marginal density $P_1(x_1, \pi_1, t)$ of the first sub-system. Eq. (8) is necessary when defining the work for systems with unknown and/or uncontrolled environment.

Work and second law

An important property of work is that its definition does not rely on any local-equilibrium assumption. In that sense the work differs from e.g. entropy, whose definition as a state function is closely tied to quasi-equilibrium states [8]. Hence the work should be involved in non-equilibrium formulations of thermodynamic laws instead of entropy. Let us illustrate this point in the context of the second law [8].

Consider a system with n sub-systems, which are (probabilistically) independent from each other at the initial time:

$$P(x, \pi, 0) = \prod_{k=1}^n P_k(x_k, \pi_k, 0). \quad (9)$$

Moreover, we shall assume that initially the sub-systems are in Gibbsian equilibrium:

$$P_k(x_k, \pi_k, 0) = \frac{e^{-\beta_k H_k(x_k, \pi_k, f(0))}}{Z_k}, \quad Z_k = \int dx_k d\pi_k e^{-\beta_k H_k(x_k, \pi_k, f(0))}, \quad k = 1, \dots, n. \quad (10)$$

where Z_k is the statistical sum, and where $\beta_k = 1/(T) > 0$ is the inverse temperature, which can differ from one sub-system to another. We take $k_B = 1$, i.e. the temperature is measured in energy units.

The considered system is thermally isolated for $t > 0$, i.e. it interact only with the source of work. Given (9, 10), we construct the relative entropy or the Leibler-Kullback divergence:

$$S_{\text{KL}}[P(t)||P(0)] \equiv \int dx d\pi P(x, p, t) \ln \frac{P(x, p, t)}{P(x, p, 0)} \geq 0, \quad (11)$$

where $P(x, p, t)$ is the probability density of the full system at time t . Among many important features of $S_{\text{KL}}[P(t)||P(0)]$ (see [7, 8]) we shall need only its non-negativity.

The above assumption on the thermal isolation leads to the conservation of the (microscopic or fine-grained) entropy

$$- \int dx d\pi P(x, p, t) \ln P(x, p, t) = - \int dx d\pi P(x, p, 0) \ln P(x, p, 0). \quad (12)$$

Eq. (12) follows from the Liouville equation for the probability density $P(x, p, t)$.

Our last assumption is that the external field acting on the system is cyclic, in the sense that its sub-systems are non-interacting both initially (at time $t = 0$) and finally (at time $t = \tau$):

$$H(x, \pi, f(0)) = \sum_{k=1}^n H_k(x_k, \pi_k, f(0)) = \sum_{k=1}^n H_k(x_k, \pi_k, f(\tau)) = H(x, \pi, f(\tau)). \quad (13)$$

Note however that (13) by no means implies that the final state $P(x, p, t)$ is also factorized like (9). In fact, $P(x, p, t)$ can be arbitrarily correlated between its sub-systems and arbitrary far from equilibrium. One scenario by which (13) can be realized is that the initially non-interacting sub-systems are subject to interaction, which is switched off for $t \geq \tau$. Using (12,

13) in (11) and also employing (9, 10) we end with:

$$\sum_{k=1}^n \beta_k \Delta U_k = S_{\text{KL}}[P(t)||P(0)] \geq 0, \quad (14)$$

$$\Delta U_k \equiv \int dx d\pi_k H_k(x_k, \pi_k, f(0)) [P_k(x_k, \pi_k, t) - P_k(x_k, \pi_k, 0)], \quad (15)$$

where ΔU_k is the energy increase of the sub-system k . We shall now explore consequences of (14). For $k = 1$ we get noting that $\beta_1 > 0$ and using (1):

$$W = \Delta U_1 \geq 0. \quad (16)$$

Since the evolution was thermally isolated (i.e. no environment was present) the whole energy change amounts to work; cf. (1, 4). Eq. (16) is the statement of the Thomson's formulation of the second law [8]: no work can be extracted from an initially equilibrium (Gibbsian) system via a cyclic change of the external field. In contrast to the Thomson's formulation within the phenomenological thermodynamics, (16) was deduced without any assumption on local equilibrium, i.e. only the initial state was assumed to be in equilibrium.

Let us now take $k = 2$ and $\beta_2 > \beta_1$. Now (1, 4) produce $\Delta U_1 + \Delta U_2 = W$ and (14) leads to

$$W = \frac{1}{\beta_2} S_{\text{KL}}[P(t)||P(0)] + (1 - \frac{\beta_1}{\beta_2}) \Delta U_1. \quad (17)$$

Now the work-extraction, i.e. $W < 0$, is already possible, because the temperatures are different. Eq. (17) shows that $W < 0$ (together with $\beta_2 > \beta_1$) leads to $\Delta U_1 \leq 0$: the sub-system, which initially had a higher temperature loses energy. Eq. (17) also implies

$$\frac{|W|}{|\Delta U_1|} = 1 - \frac{\beta_1}{\beta_2} - \frac{S_{\text{KL}}[P(t)||P(0)]}{\beta_2 |\Delta U_1|} \quad (18)$$

Now $|\Delta U_1|$ can be related to the incoming energy, and hence $\frac{|W|}{|\Delta U_1|}$ is the efficiency of the work-extraction defined as the results $|W|$ divided over the effort (input energy $|\Delta U_1|$). Eqs. (18, 11) show that this efficiency is smaller than the Carnot bound $1 - \frac{\beta_1}{\beta_2}$. This known result of

thermodynamics is derived without the local-equilibrium assumption [1, 8].

The role and definition of entropy in (18, 17) is not clear. It is seen from (18) that $S_{\text{KL}}[P(t)||P(0)]$ can play the role of entropy production, because it limits the approach to the Carnot bound. But this is in a sense "entropy production" without "entropy". Put differently, in non-equilibrium processes, work has definite advantages over the entropy.

Work done by the electromagnetic field

As we saw, the above definition of work has several advantages, and it does improve our understanding of thermodynamics. But this definition still contain a serious caveat: (2) does not specify the Hamiltonian $H(x, \pi, f(t))$ that appears in the definition. Indeed, any system of differential equations can be written in a Hamiltonian form with a suitable (and generally non-unique) Hamiltonian [10]. This can be done even for systems that are clearly dissipative, and should not have a conserved energy according to their physical meaning.

Frequently, this problem can be overcome on a phenomenological ground, because it is *a priori* clear what is the proper energy function. However, the situation is quite different for a charged particle driven by an external electromagnetic field (EMF). First of all recall that the influence of an EMF on a charged particle can be described either via electric and magnetic fields (\mathbf{E}, \mathbf{B}) or via potentials ϕ and \mathbf{A} [11]. Within this part of the thesis we shall use Gaussian units, $c = 1$ and metrics $g_{ik} = \text{diag}[1, -1, -1, -1]$ [11]. The potentials are joined into a four-vector $A^i = (\phi, \mathbf{A})$, while instead of (\mathbf{E}, \mathbf{B}) one can employ the asymmetric tensor $F_{ik} = \partial_i A_k - \partial_k A_i$, where $\partial_i \equiv \partial/\partial x^i = (\partial_t, \nabla)$ [11].

Although the description via potentials is easier, this description is not unique, since equations of motion for the charged particle-as well as the fields (\mathbf{E}, \mathbf{B}) -are invariant under the gauge-transformation [11]

$$A^i \rightarrow A^i + \partial^i \chi : \quad \varphi \rightarrow \varphi + \partial_t \chi, \quad \mathbf{A} \rightarrow \mathbf{A} - \nabla \chi, \quad (19)$$

where $\chi = \chi(t, \mathbf{x})$ is an arbitrary smooth function. The gauge-transformation is regarded as an additional freedom that can be tuned by convenience, since it does not affect observable

quantities [11]. They can be of two types: quantities that depend on A^i , but still stay invariant under the gauge-transformation, e.g. F_{ik} . Another type of observables are those which do not (directly) depend on A^i , e.g. x^i [11]. However, even gauge-non-invariant A^i can become an observable, if it can be expressed via gauge-invariant or gauge-independent quantities. Examples of this type are discussed in chapter I of the thesis.

We return to the definition of work for a charged particle in an EMF. Naturally, we suppose as the first step that the particle with mass m and charge e is thermally-isolated and we then attempt to define work via a time-dependent Hamiltonian, as (4) suggests. The standard Hamiltonian formalism is given by the canonic momentum $\boldsymbol{\pi} = \boldsymbol{p} + e\boldsymbol{A}$, kinetic momentum $\boldsymbol{p} = \frac{m\boldsymbol{v}}{\sqrt{1-\boldsymbol{v}^2}}$, velocity \boldsymbol{v} , and Hamiltonian [11]:

$$H = \sqrt{(\boldsymbol{\pi} - e\boldsymbol{A}(\boldsymbol{x}, t))^2 + m^2} + e\phi(\boldsymbol{x}, t). \quad (20)$$

But here we meet a problem, since H in (20) is not gauge-invariant due to the scalar potential ϕ that changes during a gauge-transformation; see (19).

One can naturally wonder whether this problem is not due a bad choice of the Hamiltonian formalism, i.e. can one look for an explicitly gauge-invariant Hamiltonian formalism for the considered situation of a single particle in an EMF? Such a formalism is known in literature [10], but it is useless for our purposes. Let us see why. While Hamiltonian (20) produces the equations of motion via the standard Poisson bracket, we can modify the definition of this brackets for two functions A and B , making it explicitly relativistically-invariant [10]:

$$[A, B] = \frac{\partial A}{\partial \pi_i} \frac{\partial B}{\partial x^i} - \frac{\partial A}{\partial x_i} \frac{\partial B}{\partial \pi^i}. \quad (21)$$

Now can take the simplest relativistically-invariant generalization of (20) [10]:

$$\tilde{\mathcal{H}} = -\frac{1}{2m}(\pi_i - eA_i)(\pi^i - eA^i) + \frac{m}{2}, \quad (22)$$

which also appears to be explicitly gauge-invariant for the same reason as the kinetic part of (20). Now equations of motion for a particle in an EMF can be written via the Poisson

brackets (21) as

$$\frac{dx_i}{d\tau} = [x_i, \tilde{\mathcal{H}}], \quad \frac{d\pi_i}{d\tau} = [\pi_i, \tilde{\mathcal{H}}], \quad (23)$$

where τ is the local-time of the particle. Note that (23) cannot be directly generalized to interacting particles, since generally there is no unique local time for them. Still they are a legitimate representation of the equations of motion for a single particle.

But here we meet another problem: due to the kinematic relation

$$p_i p^i = \left[\frac{m}{\sqrt{1 - \mathbf{v}^2}} \right]^2 - \mathbf{p}^2 = m^2, \quad (24)$$

the Hamiltonian (22) is zero along any physical trajectory. Hence it does not change from one phase-space point to another, and it also cannot change in the course of time. Thus it is completely useless for the physical purpose of calculating energy changes.

Paradoxically, it appears that we cannot proceed with the straightforward definition of work (4) even in such a basic set-up as the work done by an external EMF.

This problem is solved in chapter I of the thesis. Moreover, in the above treatment we completely neglected electromagnetic radiation produced by the particle. Chapter II shows that the problem of defining work can be solved even if the radiation and its back-reaction are taken into account. Here we do not re-tell the solution, but only mention that it closely relates to deep problems in the energetics of the EMF. There is a well-known expression for the energy current of the EMF given by Poynting [11]:

$$\mathbf{S} = \frac{1}{4\pi} \mathbf{E} \times \mathbf{B}. \quad (25)$$

Eq. (25) emerged directly from the Maxwell's equation, or from the standard Belinfante-Rosenfeld energy-momentum tensor of the EMF [11].

For a generic configuration of a fixed charge and a permanent magnet (25) predicts a constant flow of electromagnetic energy. This is surprising, since the configuration does not seem to require any specific energy cost for its maintenance, hence the constant flow appears as a

kind of a perpetuum mobile. Expectedly, it was never seen experimentally. In his book Feynman discusses this surprising prediction of (25) and offers for it the following resolution [12]: since the permanent magnetic field is eventually created by moving charges, there is an aspect of non-equilibriumness hidden in the above configuration. At very least, the "perpetuum mobile" aspect is not anymore surprising, because it is related to permanently moving charges that create the magnetic field [12]. This argument is not conclusive, because the picture of permanently moving charges is outdated: a constant magnetic field can be generated by a system in its ground state (e.g. a spin magnet) without requiring any permanent classical motion. Of course, this example is generically quantum, while we are discussing classical electrodynamics. But it is clear that a quantum system can generate a classical magnetic field, to which the classical electromagnetism should apply. Another resolution was offered by Mandelshtam [13], who suggests that the energy current (25) becomes observable only after space-averaging over the wave-length. The latter is infinite for static fields, which amounts to integrating (25) over the whole space. This produces zero. However, it is not clear why the space-averaging of (25) is conceptually necessary, moreover that (25) is also the momentum density of EMF [11].

Hence we are back to explaining the surprising prediction of (25) and in particular to explaining why it was never seen in experiments. As chapter I shows, this problem intrinsically relates to the problem of defining the work: both demand a careful reconsideration of the standard energetics of the EMF and both can be resolved simultaneously.

Controlled versus adaptive heat-engines

Control and information-theoretic ideas show up in many different aspects of thermodynamics [4]. Frequently, such questions are relegated to foundations of statistical thermodynamics that mostly produce a better understanding of its general rules [5]. In contrast, below we remind that already the simplest heat-engines do need an external control that makes their functioning vulnerable to environmental variations; see also [14] in this context.

Fig. 1 shows the entropy-temperature diagram of the famous Carnot cycle that combines two thermally isolated (adiabatic or entropy-conserving) and two isothermal processes. These

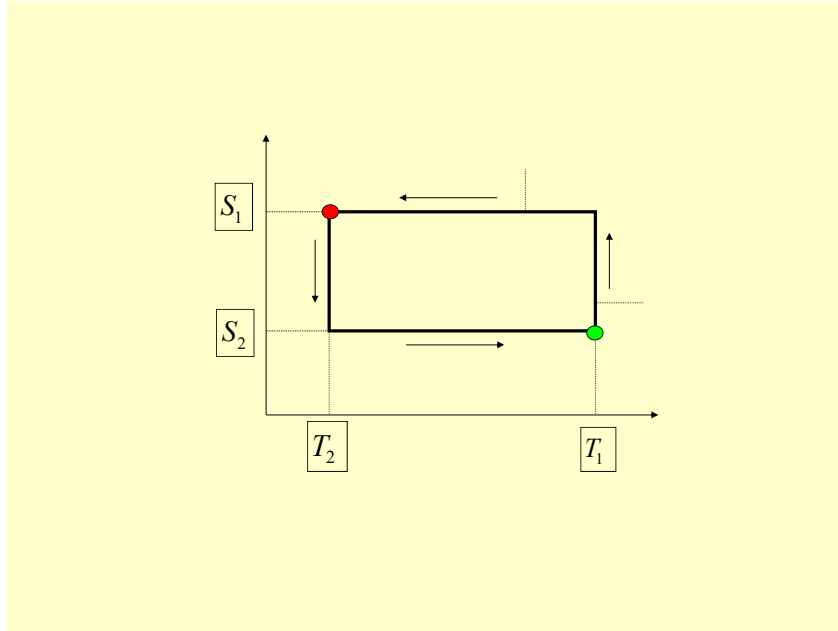


Figure 1: Carnot Cycle.

four processes must be slow for the working body (that undergoes these processes) to stay in equilibrium. We do not need the equation of state of the working body, since it is well-known that the work and efficiency of the Carnot cycle can be deduced directly from Fig. 1 assuming that at the end of the four-stage process the working body returns to its initial state [1]. We shall now follow this analysis in detail so as to underline its hidden points.

We start from the green point in Fig. 1. First the system is subject to an isothermal process at temperature T_1 . This means that the working body is attached to a thermal bath at temperature T_1 (hence both the working body and the thermal bath have the same temperature) and the volume of the working body is increased externally so that it does work against externally controlled pressure. At the end of this process the working body is detached from the bath, and now the expansion continues adiabatically again doing work. The purpose of this second adiabatic process (besides doing work) is that the temperature of the working body decreases from T_1 to a predetermined value T_2 ($T_2 < T_1$). Next, this body is attached to a thermal bath at this smaller temperature T_2 . In the third isothermal process, the volume of the working body is squeezed so that its entropy gets back to S_1 at the end of this process. During this third process the external pressure does work on the working body.

The squeezing continues adiabatically (the fourth and last process), where the working body is back to its original state. Once the evolution of the working body is cyclic and since the heat entered to the system only during the isothermal processes, we calculate the extracted work as $|W| = |Q_1| - |Q_2| > 0$, where $|Q_1| = T_1(S_1 - S_2)$ and $|Q_2| = T_2(S_1 - S_2)$. The efficiency $|W|/|Q_1|$ of the Carnot cycle is evidently given by the Carnot value.

While the above analysis is well-known, it is rarely emphasized how much control the above cycle needs: coupling and decoupling with thermal baths, precise control of temperature at the end of each process (so as to know where to finish) *etc.* In addition, the adiabatic processes have to be slow, but not too slow, otherwise the working body will interact with its environment. Now we stress that we started from the green point in Fig. 1. If the starting point is not chosen correctly (e.g. it is given by the red point in Fig. 1), then the Carnot cycle will consume the work from the external source and not extract it!

Such a strong dependence on external control is not a specific feature of the Carnot cycle. Many other thermodynamic cycles require it as well. In particular, they can operate only under specific temperatures of thermal baths; otherwise their performance is poor. There are certainly autonomous heat-engines that do not need external control. But, as recalled in chapter III, such engines need a fine-tuning of their parameters, since the same device can work (for suitable range of parameters) as a heat-engine, refrigerator or heater. The parameters have to be fine-tuned and this fine-tuning has to depend on bath temperatures since these three functions just contradict to each other.

Given the above arguments, it is natural to ask: is it possible to build a truly autonomous-*i.e. adaptive*-heat engine that will work for arbitrary bath temperatures by putting itself into the heat-engine regime? What are thermodynamic limitations on the functioning of such an engine? Is it possible that this device adapts to the heat-engine functioning and simultaneously improves its efficiency? These questions are answered in chapter III of the present thesis.

Here we only mention that such questions can be relevant for biophysics. There are at least two different aspects here. First, the fundamental biophysical process of photosynthesis is eventually a heat engine that operates between the hot thermal bath created by Sun and

a much colder Earth environment [15]. This heat-engine does have adaptive features that govern its functioning under changing environmental conditions (e.g. shadow); see chapter III for details. However, the photosynthesis is an extremely complex process that involves physics (including quantum effects) and biochemistry [16]. Developing physical models for adaptive engines may clarify aspects of this complex process.

Second, there is a body of knowledge on the origin of life that relates primary (and relatively primitive) organisms with heat engines (and possibly also with chemical engines that are anyhow conceptually similar to heat-engines) [17–22]. Such an approach seems to be plausible, because work-extraction from a non-equilibrium environment-and most importantly employing this work for improving the very work-extraction ability and hence extracting even more work-can be taken as one of defining features of life [23]. Then the major question of this approach is how such engine emerged without an external designer [24–27]? It is natural to expect that adaptive heat-engines-once their theory is developed and well-understood-can shed light also to this question.

Chapter 1

Electromagnetic gauge-freedom and work

1

1.1 Introduction

Equilibrium statistical thermodynamics is based on notions of work, heat, entropy and temperature [1, 4, 8]. The primary concept of non-equilibrium statistical mechanics is work, because its definition is relatively straightforward [1, 4, 8]. This is witnessed by recent activity in non-equilibrium (classical and quantum) physics that revolves around the work and the laws of thermodynamics [4, 8, 28–43].

We recall the definition of the thermodynamic work and its feature. Consider a non-relativistic particle with coordinate x , canonic momentum π and Hamiltonian $\mathcal{H}(x, \pi; f(t))$, where $f(t)$ is an external field. The thermodynamic work done on the particle by the field's source in the time-interval $[t_1, t_2]$ is [1, 4, 8]:

$$W = \mathcal{H}(x(t_2), \pi(t_2); f(t_2)) - \mathcal{H}(x(t_1), \pi(t_1); f(t_1)). \quad (1.1)$$

W equals the energy increase of the particle. No work is done if f is time-independent.

¹The results considered in this chapter are published in Ref. [178].

Definition (1.1) generalizes to statistical situations, where the description goes via probability densities or via density matrices [1, 4, 8]. It appears in the laws of thermodynamics.

There is an alternative definition of the thermodynamic work [1, 4, 8]

$$W = \int_{t_1}^{t_2} dt \frac{df}{dt} \partial_f \mathcal{H}(x(t), \pi(t); f(t)). \quad (1.2)$$

It applies to the open-system situation, e.g. particles interacting with baths [1, 4, 8]. Eq. (1.2) leads to (1.1) due to the Hamilton equations of motion.

If f is a coordinate of the source, the full time-independent Hamiltonian of the system and source reads²

$$\mathcal{H}(x, \pi; f) + \mathcal{H}'(f, \pi_f), \quad (1.3)$$

where π_f is the momentum of the source, and $\mathcal{H}'(f, \pi_f)$ is its Hamiltonian. The time-dependent Hamiltonian $\mathcal{H}(x, \pi; f(t))$ of the system in (1.1, 1.2) results from (1.3), if the reaction of the system to the source is neglected, e.g. because the source is heavy.

Two important features of the thermodynamic work (1.1) are displayed via (1.2, 1.3). First, since the total energy (1.3) is conserved, the thermodynamic work (1.1) relates to the energy change $\mathcal{H}'(f, \pi_f)$ of the source [1, 4, 8]. Second, (1.2, 1.3) show that $-\partial_f \mathcal{H}(x(t), \pi(t); f(t))$ is the potential force acting (from the particle) to the source. Then (1.2) relates to the mechanic concept of work: force times the displacement $dt \frac{df}{dt}$ [29].

Let now the external field be electromagnetic (EMF). The relativistic Hamiltonian of a particle reads [11, 44]

$$H = \sqrt{c^2 \mathbf{p}^2 + m^2 c^4} + e\phi(\mathbf{x}, t), \quad (1.4)$$

$$\mathbf{p} = m\mathbf{v}/\sqrt{1 - v^2/c^2}, \quad \boldsymbol{\pi} = \mathbf{p} + e\mathbf{A}(\mathbf{x}, t)/c, \quad (1.5)$$

where $A^i = (\phi, \mathbf{A})$ is the 4-potential of EMF, \mathbf{p} ($\boldsymbol{\pi}$) is the kinetic (canonic) momentum, \mathbf{x} ,

²Even if f is not a coordinate, (1.1, 1.2) stay consistent as far as the system and the work-source form a closed system.

m and e are the coordinate, mass and charge, respectively. For a non-relativistic particle, $\sqrt{c^2 \mathbf{p}^2 + m^2 c^4}$ is replaced by $\frac{\mathbf{p}^2}{2m}$.

The thermodynamic work cannot be read directly from (1.1, 1.2, 1.4), because neither H nor its time-difference stay invariant under a gauge-transformation defined via a function $\chi(\mathbf{x}, t)$ [45–50]:

$$A^i \rightarrow A^i + \partial^i \chi: \quad \phi(\mathbf{x}, t) \rightarrow \phi(\mathbf{x}, t) + \partial \chi(\mathbf{x}, t) / \partial (ct), \quad (1.6)$$

$$\mathbf{A}(\mathbf{x}, t) \rightarrow \mathbf{A}(\mathbf{x}, t) - \partial \chi(\mathbf{x}, t) / \partial \mathbf{x}. \quad (1.7)$$

The kinetic momentum \mathbf{p} in (1.4) is gauge-invariant. But ϕ is not [45–47]³. The same problem exists for a quantum particle interacting with EMF [45–47].

One response to the EMF gauge-freedom problem is that the gauge in (1.4) is to be selected as (temporal gauge) [11, 44, 46, 47]:

$$\phi = 0. \quad (1.8)$$

This definition is indirectly supported by the standard EMF energy-momentum tensor, which suggests that particles do not have potential energy [11, 44]; see section 1.6. Eq. (1.4) under $\phi = 0$ implies that the sought thermodynamic work would amount to the particle’s kinetic energy change, i.e. to the mechanic work done on the particle by the Lorentz force [11]. This cannot be the correct definition of the thermodynamic work. First, because it implies that time-independent fields do thermodynamic work [51, 52] Consider a constant electric field $\mathbf{E} = \partial_{\mathbf{x}} \phi(\mathbf{x})$. The temporal gauge is achieved by taking $\chi = -ct\phi(\mathbf{x})$ in (1.6), which brings in a time-dependent $\mathbf{A}(\mathbf{x}, t)$ and shows from (1.1, 1.4) that the work done is not zero and equals to the change of the kinetic energy. The latter is non-zero, since *only* $\sqrt{c^2 \mathbf{p}^2 + m^2 c^4} + e\phi(\mathbf{x})$ is conserved in time [11]. The proposal can apply *only* for a particular (and self-obvious) case, where all fields are absent both initially and finally. Second, because this work (1.2) relates to the force acting on the source, and not to the force acting on the particle.

³ This differs from a formally similar gauge-freedom issue that appears even for the non-relativistic situation (1.1) [39–42]. This issue is resolved easily by choosing $f(t)$ as e.g. the coordinate of a physical source of work [39–43]; see (1.3) and section 1.5.

Another possibility for resolving the gauge-freedom is to employ in (1.4) the Coulomb gauge [53, 54]:

$$\operatorname{div}\mathbf{A}(\mathbf{x}, t) = 0. \quad (1.9)$$

But the scalar potential $\phi_C(\mathbf{x}, t)$ in the gauge (1.9) propagates with infinite speed [55–57]. The Maxwell equation $\operatorname{div}\mathbf{E} = 4\pi\rho$ reads [11]: $\Delta\phi(\mathbf{x}, t) + \frac{1}{c}\partial_t\operatorname{div}\mathbf{A}(\mathbf{x}, t) = -4\pi\rho(\mathbf{x}, t)$. Upon using (1.9) we get for time-dependent $\phi_C(\mathbf{x}, t)$ in the Coulomb gauge the “static” equation $\Delta\phi_C(\mathbf{x}, t) = -4\pi\rho(\mathbf{x}, t)$ implying that $\phi_C(\mathbf{x}, t)$ responds instantly to changes in the charge density $\rho(\mathbf{x}, t)$ [55–57].

While this is consistent with electric $\mathbf{E}(\mathbf{x}, t)$ and magnetic $\mathbf{B}(\mathbf{x}, t)$ fields propagating with speed c [55–57], it also means that $\phi_C(\mathbf{x}, t)$ -and the Hamiltonian (1.4) defined via it-cannot be given a direct physical meaning.

For both proposals it is unclear how the work defined via (1.4) relates to the energy of the source (heavy body).

Noting the difficulties with the temporal and Coulomb gauge, it is natural to look at the Lorenz gauge,

$$\partial_i A^i \equiv \frac{1}{c} \frac{\partial\phi}{\partial t} + \operatorname{div}\mathbf{A} = 0, \quad (1.10)$$

which is relativistic invariant and causal, i.e. ϕ and \mathbf{A} defined from (1.10) propagate with speed c [58, 59]. Given (1.10) and standard boundary conditions of decaying at spatial infinity, A^i is uniquely expressed via gauge-invariant electromagnetic field (\mathbf{E}, \mathbf{B}) , and hence it is observable [58]. If the photon is found to have a small (but finite) mass, (1.10) will hold automatically [60]. These features are suggestive, but they do not suffice for defining the thermodynamic work.

Our results validate the usage of (1.4, 1.10), and also show that main features of the thermodynamic work generalize to the relativistic, electromagnetic situation:

- The definition of the (thermodynamic) work based on (1.4, 1.10) results from a separation of overall (source + particle(s) + EMF) energy into specific components. This separation is

not arbitrary, but emerges from a relativistically covariant energy-momentum tensor \mathbb{T}^{ik} for the overall system; see section 1.2. \mathbb{T}^{ik} necessarily differs from the standard energy-momentum tensor (e.g. because \mathbb{T}^{ik} has to account for a potential energy), but it leads to the same values of the overall energy. It consistently relates to an angular momentum (tensor). Certain aspects of \mathbb{T}^{ik} are known from [61, 62], but in its entirety it is proposed for the first time ⁴.

– The approach leads to a formulation of the first law for a relativistic thermally isolated situation, which we demonstrate for point charges with retarded electromagnetic interactions. According to this formulation, the thermodynamic work can be defined through the *gauge-invariant* kinetic energy of the source, but it is also equal to the change of (1.4) in the Lorenz gauge. As compared to the non-relativistic first law—which is an automatic consequence of energy conservation [1, 4, 8, 28, 29] [cf. (1.3)]—the formulation is necessarily approximate, since some energy is stored in the (near) EMF, even if the radiated energy is negligible. Once the thermodynamic work amounts to the kinetic energy of the source, it directly relates it to the mechanic work done by the Lorentz force acting on the source. Thus the two important features (described after (1.3)) generalize to the relativistic, electromagnetic situation.

Several recent studies looked at the work done by EMF in the context of fluctuation theorems [63–67]. But the problem of the EMF gauge-freedom was not addressed, partially due to implicitly assumed magnetostatic limit, where the gauge (1.9) is employed by default, and where (1.10) and (1.9) are approximately equal [68, 69].

1.2 Equations of motion and energy-momentum tensor

Consider electromagnetic field (EMF) coupled with a charged continuous matter with mass density $\mu(\mathbf{x}, t)$, charge density $\rho(\mathbf{x}, t)$ and 4-velocity

$$u^i(\mathbf{x}, t) = \frac{(1, \mathbf{v}(\mathbf{x}, t)/c)}{\sqrt{1 - v^2(\mathbf{x}, t)/c^2}}, \quad u_i u^i = 1. \quad (1.11)$$

⁴Energy-momentum tensors are not uniquely defined, and different situations may require different definitions. An example of this is the dielectric media (not considered here), where different experiments demand different forms of this tensor [49].

The comoving frame mass density and charge density read, respectively (omitting (\mathbf{x}, t)):

$$\mu_0 = \mu\sqrt{1 - \mathbf{v}^2/c^2}, \quad \rho_0 = \rho\sqrt{1 - \mathbf{v}^2/c^2}. \quad (1.12)$$

Dealing with a continuous matter allows us to postpone the treatment of infinities related to point particles.

The mass and charge conservation read, respectively

$$\partial_k(\mu_0 u^k) = \partial_k J^k = 0, \quad J^k \equiv c\rho_0 u^k. \quad (1.13)$$

where J^k is the charge current. Equations of motion for matter+EMF in the gauge (1.10) read [11, 44]⁵:

$$\partial_k \partial^k A^i = \frac{4\pi}{c} J^i, \quad (1.14)$$

$$\mu_0 c^2 \frac{du^i}{ds} \equiv \mu_0 c^2 u^l \partial_l u^i = \frac{1}{c} F^{ik} J_k, \quad (1.15)$$

where $F^{ik} = \partial^i A^k - \partial^k A^i$, and s/c is the proper time.

The energy-momentum of matter reads [11]

$$\tau_i{}^k = c^2 \mu_0 u_i u^k, \quad (1.16)$$

where the pressure has been neglected. Eq. (1.15) implies

$$\partial_k \tau_i{}^k = \frac{1}{c} J^k F_{ik}. \quad (1.17)$$

We now deduce a conserved energy-momentum tensor \mathbb{T}^{ik} from (1.13–1.17). Guided by the analogy with a free scalar, massless field φ whose energy-momentum tensor is $\propto \partial^i \varphi \partial^k \varphi -$

⁵Eqs. (1.14, 1.15) are normally obtained via (1.10). But one can employ (1.14) and (1.13) for deriving the Lorenz gauge (1.10) [70–72].

$\frac{1}{2}g^{ik}\partial_l\varphi\partial^l\varphi$ [62], we suggest

$$\mathbb{T}^{ik} = T^{ik} + \tau^{ik} + \frac{1}{c}A^i J^k, \quad (1.18)$$

$$T^{ik} = -\frac{1}{4\pi}\partial^i A_l \partial^k A^l + \frac{1}{8\pi}g^{ik}\partial_n A_m \partial^n A^m, \quad (1.19)$$

where (1.19) is the energy-momentum tensor of the free EMF, τ^{ik} is given by (1.16), and $\frac{1}{c}A^i J^k$ in (1.18) is due to the interaction. Eqs. (1.13–1.17) lead to 4 conservation laws

$$\partial_k \mathbb{T}^{ik} = \partial_0 \mathbb{T}^{i0} + \partial_\alpha \mathbb{T}^{i\alpha} = 0. \quad (1.20)$$

Eqs. (1.20, 1.18) imply that \mathbb{T}^{00} is the energy density

$$\mathbb{T}^{00} = -\frac{1}{4\pi}\partial^0 A_l \partial^0 A^l + \frac{1}{8\pi}\partial_n A_m \partial^n A^m \quad (1.21)$$

$$+ \frac{c^2\mu}{\sqrt{1-v^2/c^2}} + \rho\phi. \quad (1.22)$$

Eq. (1.21) is the energy density of EMF, while (1.22) amounts to the energy of the matter that consists of kinetic and the interaction term. The latter will be shown to be the particle's potential energy in section 1.4. The possibility of this interpretation is confirmed by the form of energy current:

$$c\mathbb{T}^{0\alpha} = -\frac{c}{4\pi}\partial^0 A_l \partial^\alpha A^l \quad (1.23)$$

$$+ \left(\frac{c^2\mu}{\sqrt{1-v^2/c^2}} + \rho\phi\right)v^\alpha, \quad (1.24)$$

where (1.23) is the energy current of EMF.

Eq. (1.19) for the free EMF was previously derived from the Fermi's Lagrangian [62, 70, 73]; see section 1.7. Eqs. (1.21–1.24) were discussed in [61] as alternatives to standard expressions (i.e. the Poynting vector), but were not derived from a consistent energy-momentum tensor. Various proposals for the energy flow of (free) EMF are given in [95–100]. Their general drawback is that they do not start from a consistent energy-momentum tensor.

All above expressions-including \mathbb{T}^{ik} -that contain A^i (in the Lorenz gauge (1.10)) are gauge-

invariant, because A^i can be expressed via $F^{ik} = \partial^i A^k - \partial^k A^i$ [58]:

$$A^i(x) = \partial_k \int d^4x' G(x-x') F^{ki}(x'), \quad (1.25)$$

$$\partial_k \partial^k G(x-x') = \delta_{\mathcal{D}}(x-x'), \quad (1.26)$$

$$G(x-x') = \frac{1}{2\pi} \theta(x^0 - x'^0) \delta_{\mathcal{D}}((x^i - x'^i)(x_i - x'_i)), \quad (1.27)$$

where $G(x, x')$ is the retarded Green's function, $x \equiv (ct, \mathbf{x})$, $x' \equiv (ct', \mathbf{x}')$, $\theta(x^0 - x'^0) = \theta(ct - ct')$ is the step function, and $\delta_{\mathcal{D}}(x)$ is the Dirac's delta-function. Eq. (1.25) relates to the retarded solution of (1.14). Its derivation from (1.26) is straightforward, e.g. by employing (1.10) in F^{ik} and integrating by parts.

The main reason for introducing \mathbb{T}^{ik} is to verify that the potential energy $\rho\phi$ can emerge from a consistent energy-momentum tensor; the standard energy-momentum tensor of EMF does not allow such an interpretation; see section 1.6. Without a potential energy we cannot define the thermodynamic work via (1.1, 1.2); cf. the discussion around (1.8).

Both (1.18) and the standard tensor lead to the same expressions for energy (and momentum) of the matter+EMF [see 2.2]:

$$\int d^3x \left[\frac{\mathbf{E}^2 + \mathbf{B}^2}{8\pi} + \tau^{00} \right] = \int d^3x \mathbb{T}^{00}, \quad (1.28)$$

where the integration over the full 3-space is taken (assuming that all fields nullify at infinity), $\frac{\mathbf{E}^2 + \mathbf{B}^2}{8\pi}$ is the Larmor's electromagnetic energy density expressed via the electromagnetic field (\mathbf{E}, \mathbf{B}) (it follows the standard energy-momentum tensor [11]), and $\tau^{00} = \frac{c^2 \mu}{\sqrt{1-v^2}}$ is the kinetic energy density for the matter; see (1.16, 1.12). The same τ^{00} enters also \mathbb{T}^{00} ; cf. (1.21, 1.22). Thus whenever only the total energy matters, \mathbb{T}^{00} agrees with the standard predictions (1.28). However, generally the density $\frac{\mathbf{E}^2 + \mathbf{B}^2}{8\pi}$ is not equal to T^{00} given by (1.19). Differences and similarities between (1.18) and the standard energy-momentum tensor of EMF are discussed in sections 1.6 and 2.2; e.g. for spherical waves (1.19) produces the same expression as the standard tensor.

Note that the free EMF tensor (1.19) is symmetric, $T^{ik} = T^{ki}$, as it should, because

this ensures the known relation between the energy current $cT^{0\alpha}$ and the momentum density $T^{\alpha 0} = T^{0\alpha}$; cf. (1.23). But the full tensor (1.18) is not symmetric, $\mathbb{T}^{ik} \neq \mathbb{T}^{ki}$, due to the EMF-matter coupling. Section 1.8 discusses the meaning of this asymmetry and relates \mathbb{T}^{ik} to the angular momentum and spin tensor. These relations are necessary to establish, because the angular momentum is employed for explaining the energy of EMF [12, 74, 95–100].

1.3 Two point-particles without self-interactions

For two point particles P and P' we take in (1.12–1.15):

$$\mu(\mathbf{r}, t) = m\delta_{\mathcal{D}}(\mathbf{r} - \mathbf{x}(t)) + m'\delta_{\mathcal{D}}(\mathbf{r} - \mathbf{x}'(t)), \quad \rho(\mathbf{r}, t) = e\delta_{\mathcal{D}}(\mathbf{r} - \mathbf{x}(t)) + e'\delta_{\mathcal{D}}(\mathbf{r} - \mathbf{x}'(t)), \quad (1.29)$$

where $\mathbf{x}(t)$, e and m are the trajectory, charge and mass of P (resp. for P'), and where $\delta_{\mathcal{D}}$ is the delta-function. It is known that for point particles equations of motion (1.15) and energy-momentum tensor are not well-defined, since they contain diverging terms [11, 44]. One needs to renormalize the masses by infinitely large counter-terms [44]. The next-order (finite) terms refer to the self-force that includes the back-reaction of the emitted radiation [11, 44].

For clarity, we first focus on the point-particle case, where the self-force is neglected, but the situation is still relativistic, i.e. retardation effects are essential [75–83]. In this situation particles influence each other via the Lorentz forces generated by the Lienard-Wichert potentials; see section 1.9.

A sufficient condition for neglecting the self-force is that the characteristic lengths are larger than the “classical radius” [11, 75–79]

$$\max\left[\frac{e^2}{mc^2\sqrt{1-v^2/c^2}}, \frac{e'^2}{m'c^2\sqrt{1-v'^2/c^2}}\right]. \quad (1.30)$$

Section 1.9 recalls how to get equations of motion for point particles from (1.15) by selecting in (1.14) retarded solutions, and relates them to the tensor (1.18).

We focus on the 1D situation, where the particles P and P' move on a line, since their

initial velocities were collinear. We checked that physical results obtained in sections 1.4 hold as well for the full 3D situation, but the 1D case is chosen for its relative simplicity. For all times t_1 and t_2 , we set for the coordinates of P and P' (respectively)

$$x(t_1) \leq x'(t_2). \quad (1.31)$$

We denote for the delays $\delta(t)$ and $\delta'(t)$ that emerge due to retarded interactions:

$$c\delta(t) \equiv x' - x(t - \delta(t)), \quad (1.32)$$

$$c\delta'(t) \equiv x'(t - \delta'(t)) - x, \quad (1.33)$$

and introduce dimensionless velocities: $\omega \equiv \dot{x}/c$, $\omega' \equiv \dot{x}'/c$. The equations of motion read [see 1.9]

$$\dot{\omega}(t) = [1 - \omega^2(t)]^{3/2} \left(\frac{-ee'}{mc^3} \right) \frac{1}{\delta'^2(t)} \frac{1 - \omega'(t - \delta'(t))}{1 + \omega'(t - \delta'(t))}, \quad (1.34)$$

$$\dot{\omega}'(t) = [1 - \omega'^2(t)]^{3/2} \left(\frac{ee'}{m'c^3} \right) \frac{1}{\delta^2(t)} \frac{1 + \omega(t - \delta(t))}{1 - \omega(t - \delta(t))}, \quad (1.35)$$

$$\dot{\delta}'(t) = \frac{\omega'(t - \delta'(t)) - \omega(t)}{1 + \omega'(t - \delta'(t))}, \quad (1.36)$$

$$\dot{\delta}(t) = \frac{\omega'(t) - \omega(t - \delta(t))}{1 - \omega(t - \delta(t))}. \quad (1.37)$$

The factor $\delta'^{-2}(t)$ in (1.35) is the retarded Coulomb interaction; cf. (1.32). Eqs. (1.34–1.37) were considered in [75, 80, 84, 85], and from a mathematical viewpoint in [82, 86–89]. But the energy exchange was not studied.

Eqs. (1.34–1.37) are delay-differential equations due to the retardation of the inter-particle interaction. Their initial conditions are not trivial [81, 87–91]. We focus on the simplest scenario, where the two-particle system is prepared via strong external fields for $t < 0$ [86, 90]. These fields do not enter into (1.34–1.37) and they are suddenly switched off at the initial time $t = 0$. They define (prescribed) trajectories of the particles for $t < 0$. For simplicity we

shall take them as

$$x(t) = \omega_0 c t, \quad x'(t) = \omega'_0 c t + l_0, \quad l_0 > 0, \quad t \leq 0, \quad (1.38)$$

where ω_0 , ω'_0 and l_0 are constants. Eqs. (1.32, 1.33, 1.38) imply

$$\delta(0) = \frac{l_0/c}{1 - \omega_0}, \quad \delta'(0) = \frac{l_0/c}{1 + \omega'_0}. \quad (1.39)$$

Conditions (1.38, 1.39) do determine uniquely the solution of (1.34–1.37) for $t > 0$ [82, 83, 86, 90]. An iterative method of solving (1.34–1.37) is described in section 1.10.

1.4 Work and the first law

1.4.1 Formulation of the first law

The standard (non-relativistic) work has two aspects: the kinetic energy change of the work-source (a heavy body whose motion is only weakly perturbed by the interaction)⁶, and the energy change of the lighter particle; cf. the discussion around (1.3). The equality between them is the message of the first law (in the thermally isolated situation, when no heat is involved) [1, 4, 8]. The task of identifying two aspects of work will be carried out for the relativistic dynamics (1.34–1.37). To make P' a source of EMF whose motion is perturbed weakly, we assume that it is much heavier than P:

$$m' \gg m. \quad (1.40)$$

In practice, $m'/m \simeq 5 - 10$ already suffices; see below.

⁶If the work-source is subject to an external potential, the latter will add to the kinetic energy.

The energy E of P is defined via (1.4) in the Lorenz gauge, or with help of (1.22):

$$\begin{aligned} E(t) &= \frac{mc^2}{\sqrt{1-\omega^2(t)}} + e\phi'(x(t), t) \\ &= \frac{mc^2}{\sqrt{1-\omega^2(t)}} + \frac{ee'}{c\delta'(t)[1+\omega'(t-\delta'(t))]}, \end{aligned} \quad (1.41)$$

where $\phi'(x(t), t)$ is the Lorenz-gauge scalar potential generated by P'; see (1.32, 1.33) and section 1.9.

The change of E reads:

$$\Delta_{t_2|t_1} E \equiv E(t_2) - E(t_1). \quad (1.42)$$

The kinetic energy change of P' is

$$\Delta_{t_2|t_1} K' \equiv K'(t_2) - K'(t_1), \quad (1.43)$$

$$K'(t) \equiv m'c^2/\sqrt{1-v'^2/c^2}. \quad (1.44)$$

We validate below that under reasonable conditions $|\Delta_{t_2|t_1} E + \Delta_{t_2|t_1} K'|$ can be negligible, and hence the thermodynamic work can be defined via $\Delta_{t_2|t_1} E$, or via the *gauge-invariant* $-\Delta_{t_2|t_1} K'$:

$$W = -\Delta_{t_2|t_1} K', \quad \text{if} \quad (1.45)$$

$$|\Delta_{t_2|t_1} E + \Delta_{t_2|t_1} K'| \ll |\Delta_{t_2|t_1} E|, |\Delta_{t_2|t_1} K'|. \quad (1.46)$$

Eq. (1.46) can be interpreted as an approximate conservation law ensuring the energy transfer between P and P'. The validity of (1.46) confirms that $e\phi'(x, t)$ is the time-dependent potential energy for P. Defining the work via the kinetic energy of P' is consistent the fact that this energy can be fully transferred to heat [28], e.g. by stopping the particle by a static target.

Eqs. (1.45, 1.46) amount to the first law. Importantly, (1.45, 1.46) are written in finite differences: in the relativistic situation the energy transfer does take a finite time, since the energy has to pass through the EMF. Hence (1.46) cannot hold for a small $|t_2 - t_1|$.

Note that, as implied by (1.35), there is only the Lorentz force acting on P' . Hence the kinetic energy difference (1.43) can be also recovered as the (time-integrated) mechanic work done by the Lorentz force acting on P' .

Recall the non-relativistic situation, where two particles interact directly via the Coulomb potential. There we have an exact relation (conservation of energy)

$$\frac{mv^2(t)}{2} + \frac{ee'}{|x'(t) - x(t)|} = -\frac{m'v'^2(t)}{2} + \text{const.} \quad (1.47)$$

If (1.40) holds, the left-hand-side of (1.47) is identified with the time-dependent Hamiltonian of P , and we get an exact correspondence between the two aspects of work; cf. the discussion around (1.3). But since (1.47) is a non-relativistic relation, it implies an instantaneous transfer of energy, hence it is written as a conservation relation that holds at any time.

The quantities in (1.42, 1.43) are calculated-in the considered lab-frame-at the same times (t_2 and t_1 , respectively), but at different coordinates. Though events that are simultaneous in one reference frame will not be simultaneous in another, the relativity theory does employ such reference frame-specific quantities, the length being the main example [92, 93].

Since the correct expression of the first law is open, we tried to use instead of E and K' in (1.45, 1.46) other quantities, e.g. (resp.) $K(t) = mc^2/\sqrt{1 - v^2/c^2}$ and $E'(t)$, where $E'(t)$ is the analogue of (1.41) for P'

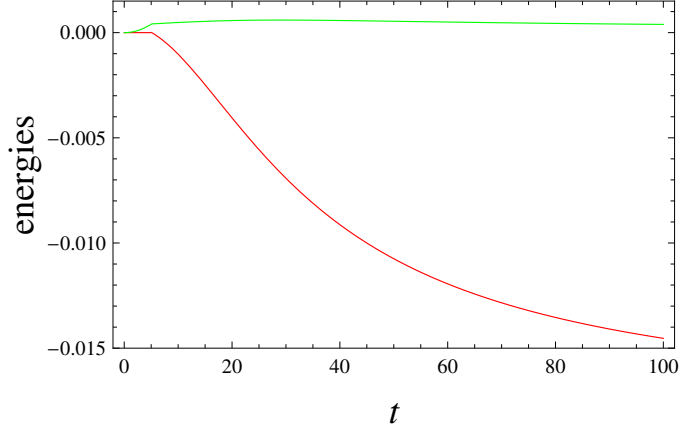
$$\begin{aligned} E'(t) &= \frac{m'c^2}{\sqrt{1 - \omega'^2(t)}} + e'\phi(x'(t), t) \\ &= \frac{m'c^2}{\sqrt{1 - \omega'^2(t)}} + \frac{ee'}{c\delta(t)[1 - \omega(t - \delta(t))]} \end{aligned} \quad (1.48)$$

In contrast to (1.46), this choice (as well as several other choices) did not lead to a sufficiently precise conservation law, i.e. $|\Delta_{t_2|t_1} E' + \Delta_{t_2|t_1} K|$ is not negligible; see below.

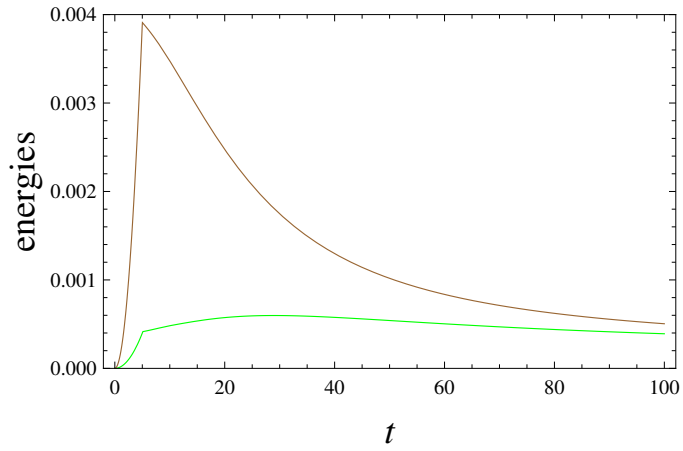
1.4.2 Numerical validation

We studied (1.34–1.37) numerically. Figs. 1.1–1.4 show four representative examples.

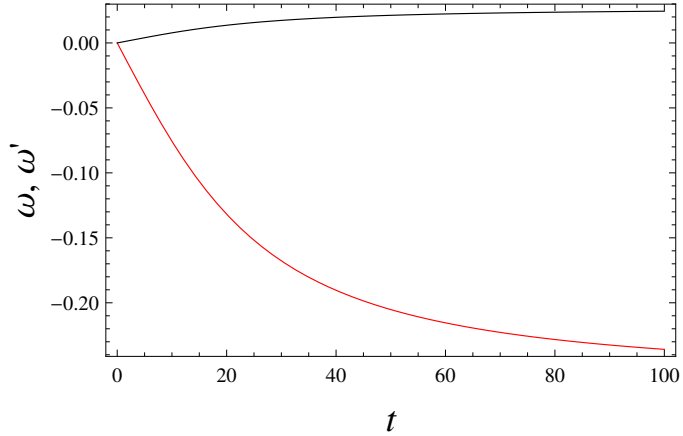
Figs. 1.1 refer to repelling P and P' that start to move from a fixed distance, with zero



(a)



(b)



(c)

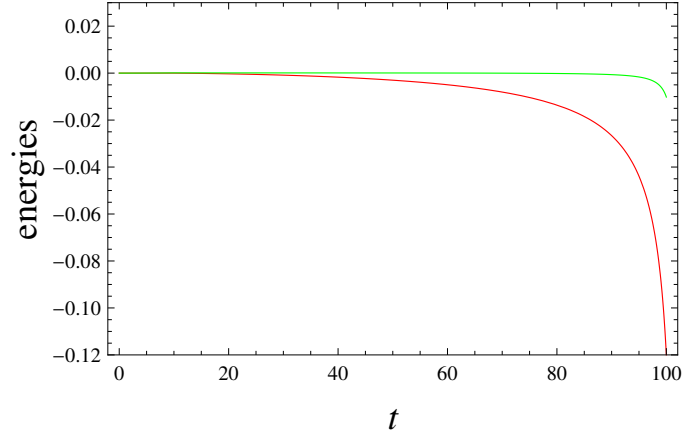
Figure 1.1: Repulsive motion with initially zero velocities. The curves are obtained via self-consistent solution of (1.34–1.39) for $m = 5$, $m' = 50$, $ee' = c = 1$, $l_0 = 5$, $\omega_0 = \omega'_0 = 0$.

(a) The energy difference $\Delta_{t|0}E$ of the light particle (red) and the sum $\Delta_{t|0}(E + K')$ of this energy and the kinetic energy K' of the heavy particle (green); cf. (1.45, 1.46).

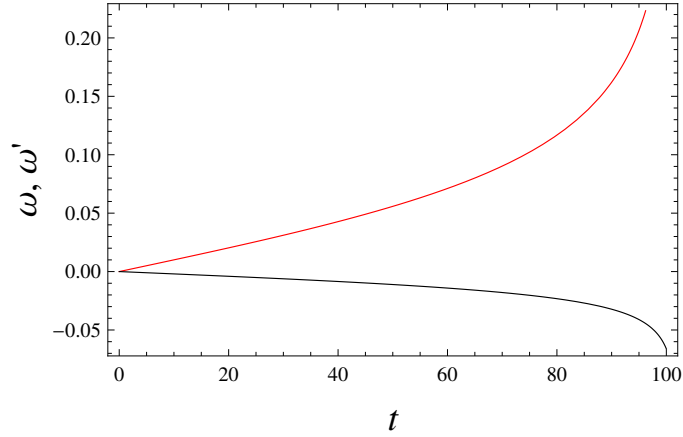
(b) $\Delta_{t|0}(E + K')$ (green) and $\Delta_{t|0}(K + E')$ (brown). The former quantity is conserved better.

(c) The velocity $\omega(t)$ ($\omega'(t)$) of the light (heavy) particle is shown by red (black) curve.

velocities for $t \leq 0$, i.e. $\omega_0 = \omega'_0 = 0$ in (1.38). (Here the full 3d case reduces to the considered 1d situation.)



(a)



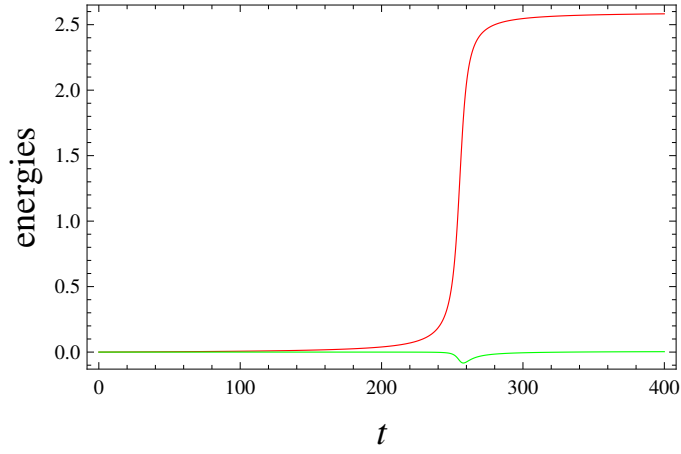
(b)

Figure 1.2: Attractive motion with initially zero velocities and $ee' = -1$, $c = 1$, $l_0 = 10$, $m = 10$, $m' = 50$, $\omega_0 = \omega'_0 = 0$; cf. (1.34–1.39). The inter-particle distance at the final time $x'(100) - x(100) = 1.2219$.

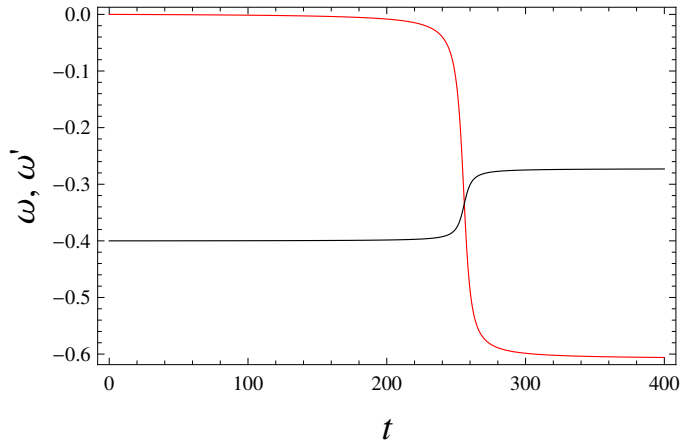
(a) $\Delta_{t|0}E$ (red) and $\Delta_{t|0}(E + K')$ (green).

(b) $\omega(t)$ (red) and $\omega'(t)$ (black); cf. Figs. 1.1(a)–1.1(c).

Figs. 1.2 describe a classical analogue of the annihilation process: two attractive particles P and P' fall into each in a finite time; their evolution again starts from a fixed distance and with zero velocities.



(a)



(b)

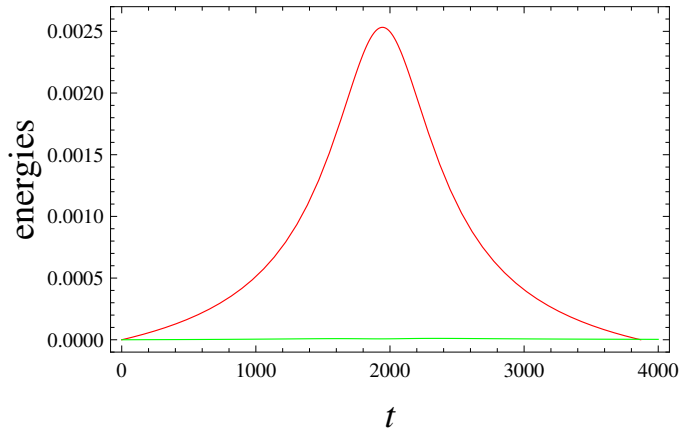
Figure 1.3: Repulsive motion: one particle (P') falls into another (P) that is at rest initially: $ee' = 1$, $c = 1$, $l_0 = 100$, $m = 10$, $m' = 50$, $\omega_0 = 0$, $\omega'_0 = -0.4$; cf. (1.34–1.39). The minimal inter-particle distance $x'(t) - x(t) = 1.2287$ is reached at $t = 255.87$.

(a) $\Delta_{t|0}E$ (red) and $\Delta_{t|0}(E + K')$ (green).

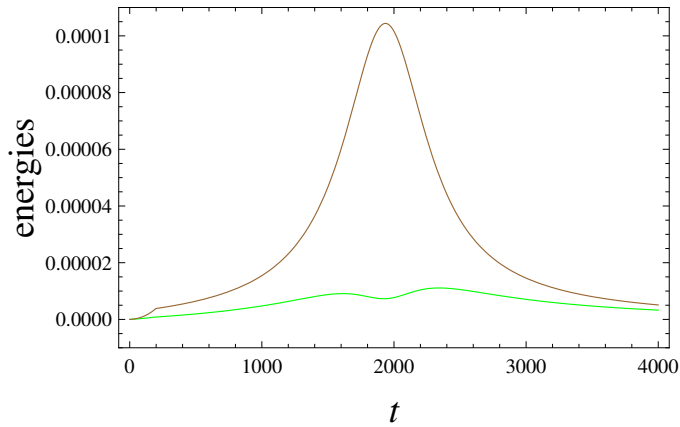
(b) $\omega(t)$ (red) and $\omega'(t)$ (black).

Figs. 1.3 show a scattering process of repelling particles: P' runs on P which is at rest initially. For scattering processes-where particles are free both initially and finally-(1.34–1.37) predict elastic collision, if conditions discussed around (1.30) hold, i.e. the radiation reaction can be neglected.

Figs. 1.4 show a specific elastic collision, where no energy transfers takes place between initial and final (asymptotically-free) states, but there is a non-trivial work-exchange at intermediate times.



(a)



(b)

Figure 1.4: Scattering of particles with $ee' = 1$, $c = 1$, $l_0 = 200$, $m = 5$, $m' = 50$, $\omega_0 = 0.1$, $\omega'_0 = -0.0100499$; cf. (1.34–1.39). The parameter are chosen such that the initial (and the final) kinetic momentum is zero: $m\omega_0/\sqrt{1-\omega_0^2} + m'\omega'_0/\sqrt{1-\omega_0'^2} = 0$. The minimal inter-particle distance $x'(t) - x(t) = 30.57$ is reached at $t = 1944.13$.

(a) Red (upper) curve $\Delta_{t|0}E$. Green (lower) curve: $\Delta_{t|0}(E + K')$; cf. Fig. 1.1(a).

(b) Green (lower) curve: $\Delta_{t|0}(E + K')$. Brown (upper) curve: $\Delta_{t|0}(K + E')$.

Figs. 1.1(a), 1.1(b), 1.2(a), 1.3(a), 1.4(a) and 1.4(b) show that (1.46) holds with a good precision provided that $t_2 - t_1$ is sufficiently large. Everywhere we assume (1.40): Figs. 1.1(c), 1.2(b) and 1.3(b) demonstrate that even for modestly large values of $\frac{m'}{m}$ the motion of P' is weakly perturbed by P .

The definition of work is clarified via Figs. 1.1(b) and 1.4(b): they show that $E + K'$ is a better conserved quantity than $K' + E$; cf. (1.42, 1.43). Hence the definition (1.45, 1.46) is selected by the approximate conservation law argument.

Figs. 1.1(a), 1.1(b) and 1.2(a) show that for a range of initial times E is strictly conserved. Hence (1.46) does not hold and no work can be defined via (1.45). This relates to the fact

that for parameters of Figs. 1.1 and 1.2 the particles P and P' have zero velocities for $t < 0$; cf. (1.38). Due to retardation each particle sees a fixed neighbor for some initial time. This leads to conservation of E for those times. Thus, this example illustrates the causal behavior of work, a desirable feature ensured by the Lorenz gauge. It is absent for the Coulomb gauge (1.9), where ϕ_C propagates instantaneously. This example also shows that the work cannot be defined *only* via (1.45).

Another scenario for violating (1.46) is seen for attracting particles that approach each other closely; see Fig. 1.2(a). Now the inter-particle distance becomes comparable with (1.30). Hence the self-force cannot be neglected, and the considered dynamics is not applicable.

For the elastic collision displayed in Figs. 1.4 the initial overall kinetic momentum is zero $p(0) + p'(0) = 0$. Hence it is zero also finally and there is no overall energy transfer. But Fig. 1.4(a) shows that the work is non-trivial at intermediate times: first the work flows from P' to P, and then goes back by the same amount.

1.5 Gauge-freedom of non-relativistic time-dependent Hamiltonian

The Hamiltonian (1.1) can be deduced from a Lagrangian $\mathcal{L}(x, \dot{x}; t)$ via [11, 44]

$$\mathcal{H}(x, \pi; t) = \pi \dot{x} - \mathcal{L}, \quad \pi \equiv \partial_{\dot{x}} \mathcal{L}. \quad (1.49)$$

The Lagrange equations stay intact if instead of \mathcal{L} one uses another Lagrangian $\hat{\mathcal{L}}$:

$$\hat{\mathcal{L}} = \mathcal{L} + \frac{d\chi(x, t)}{dt}, \quad \frac{d\chi(x, t)}{dt} = \dot{x} \partial_x \chi + \partial_t \chi, \quad (1.50)$$

The corresponding Hamiltonian

$$\hat{\mathcal{H}}(x, \hat{\pi}; t) = \mathcal{H}(x, \pi; t) - \partial_t \chi(x, t), \quad (1.51)$$

differs from (1.49) by a factor that is formally similar to the scalar potential $\phi(\mathbf{x}, t)$ in (1.4). Hence formally the time-dependent Hamiltonian is not defined uniquely.

For the considered non-relativistic situation this non-uniqueness is straightforward to resolve: one finds the time-independent (non-relativistic!) Hamiltonian for the particle and the work-source together, e.g.

$$\mathcal{H}_{\text{tot}}(x, \pi; f, \pi_f) = \mathcal{H}(x, \pi; f) + \mathcal{H}_{\text{source}}(f, \pi_f), \quad (1.52)$$

where π_f and f are the canonical momentum and coordinate of the work-source. No issue similar to (1.51) arises in (1.52), because (1.52) is time-independent (one can still add to (1.52) a constant). Then the physical time-dependent Hamiltonian for the particle is found by neglecting its backreaction onto the source: $\mathcal{H}(x, \pi; t) = \mathcal{H}(x, \pi; f(t))$.

1.6 Standard forms of the energy-momentum tensor

Two versions of the energy-momentum tensor of electromagnetic field (EMF) are known in literature [11, 44]

$$\mathcal{T}^{ik} = \frac{1}{4\pi}(-F^{il}F^k{}_l + \frac{g^{ik}}{4}F_{lm}F^{lm}), \quad (1.53)$$

$$\tilde{\mathcal{T}}^{ik} = \frac{1}{4\pi}(-\partial^i A^l F^k{}_l + \frac{g^{ik}}{4}F_{lm}F^{lm}), \quad (1.54)$$

$$F_{ik} \equiv \partial_i A_k - \partial_k A_i. \quad (1.55)$$

$\tilde{\mathcal{T}}^{ik}$ is deduced from the standard Lagrangian of EMF [11]; see (1.66, 1.69) in section 1.7. \mathcal{T}^{ik} is obtained from $\tilde{\mathcal{T}}^{ik}$ via the so called Belinfante method that renders a symmetric and explicitly gauge-invariant expression [11].

1. First we focus on comparing (1.53) with (1.18, 1.19), because (1.53) is widely accepted as the correct energy-momentum tensor. Then we turn to discussing (1.54).

1.1 Eq. (1.53) does not allow to introduce potential energy for particles [cf. (1.22, 1.24)], because the full conserved energy-momentum tensor of the EMF+matter is defined as [cf. (1.16)] [11]

$$\mathcal{T}^{ik} + \tau^{ik}, \quad \partial_k(\mathcal{T}^{ik} + \tau^{ik}) = 0. \quad (1.56)$$

Hence according to (1.53, 1.56) the matter has only kinetic energy, as can be verified in detail by working out (1.53) analogously to (1.21–1.24). This is why (1.53) indirectly supports the choice of the temporal gauge $\phi = 0$.

1.2 Recall that according to (1.53), $\mathcal{T}^{00} \propto \mathbf{E}^2 + \mathbf{B}^2$ is energy density, and

$$\begin{aligned} c\mathcal{T}^{0\alpha} &= -\frac{c}{4\pi}(\partial^0 A_\beta - \partial_\beta A^0)(\partial^\alpha A^\beta - \partial^\beta A^\alpha) \\ &= \frac{c}{4\pi}\mathbf{E} \times \mathbf{B} \end{aligned} \quad (1.57)$$

is the energy current (Poynting vector), and $\mathcal{T}^{\alpha 0}$ is the momentum density.

The Poynting vector is non-zero also for time-independent fields. This is a known con-

troversty in the standard definition of the EMF energy current: stationary fields-e.g. created by a constant change and permanent magnet, which do not require any energy cost for their maintenance|would lead to permanent flow of energy and constant field momentum [12, 74, 94]. In contrast, (1.23) is zero for time-independent fields [61]. This is an advantage.

We are not aware of direct experimental results which would single out a unique expression for EMF energy current [12, 94–100]. Some experiments point against the universal applicability of the Poynting vector for the EMF energy flow [102].

1.3 Eq. (1.53) does not allow a clear-cut separation between the orbital momentum and spin of EMF. Indeed, due to $\mathcal{T}^{ik} = \mathcal{T}^{ki}$, we get for a free EMF [11]

$$\partial_k \mathcal{M}_{lm}^k = 0, \quad \mathcal{M}_{lm}^k \equiv x_m \mathcal{T}_l^k - x_l \mathcal{T}_m^k. \quad (1.58)$$

Now \mathcal{M}_{lm}^k is conserved, but it has the form of orbital momentum; sometimes it is also interpreted as the full angular momentum leaving unspecified the separate contributions of orbital momentum and spin [11]⁷. In contrast, (1.18, 1.19) lead to well-defined expressions for the angular momentum and spin that are conserved separately for a free EMF; see section 1.8. This section also explains that when EMF couples to matter only the sum of the full orbital momentum (including that of matter) and the EMF spin is conserved.

1.4 Eq. (1.53) and (1.18, 1.19) lead to the same predictions for the (space-integrated) conserved quantities. Indeed, using the Lorenz gauge (1.10) and the equation of motion (1.14) for A^i we get from (1.53, 1.18):

$$\mathcal{T}^{ik} + \tau^{ik} - \mathbb{T}^{ik} = \frac{1}{4\pi} \partial_l B^{ikl}, \quad (1.59)$$

$$B^{ikl} \equiv A^k \partial^i A^l + A^i \partial^k A^l - A^i \partial^l A^k - \frac{g^{ik}}{2} A_m \partial^m A^l. \quad (1.60)$$

Note that (1.59) is not the usual freedom associated with the choice of the energy-momentum tensor [11]. That freedom amounts to $B^{ikl} = -B^{ilk}$, which clearly does not hold with (1.60).

⁷Such quantities can be introduced at the level of \mathcal{M}_{lm}^k ; see e.g. [50]. But this introduction is *ad hoc*; cf. (1.78, 1.77, 1.73, 1.75).

Relations $\partial_k[\mathcal{T}^{ik} + \tau^{ik}] = \partial_k \mathbb{T}^{ik} = 0$ amount to conservation of $\int d^3x [\mathcal{T}^{i0} + \tau^{i0}]$ and $\int d^3x \mathbb{T}^{i0}$ in time. More generally, such a conservation law may be absent, e.g. when some non-electromagnetic forces act on the matter.

At any rate, we want to show that $\mathcal{T}^{ik} + \tau^{ik}$ and \mathbb{T}^{ik} do predict the same values for the full (space-integrated) energy-momentum of the matter+EMF. To this end, consider from (1.59, 1.60) the difference of the two predictions:

$$\begin{aligned} & \int d^3x [\mathcal{T}^{i0} + \tau^{i0}] - \int d^3x \mathbb{T}^{i0} \\ &= \frac{1}{4\pi} \partial_0 \int d^3x B^{i00} + \frac{1}{4\pi} \int d^3x \partial_\alpha B^{i0\alpha}. \end{aligned} \quad (1.61)$$

The second term in (1.61) contains full space-derivatives and amounts to zero under standard boundary conditions. Also, B^{i00} amounts to full space-derivatives,

$$B^{\alpha 00} = \frac{1}{2} \partial^\alpha [A^0 A^0], \quad B^{000} = -\frac{1}{2} \partial_\alpha [A^\alpha A^0], \quad (1.62)$$

where we used the Lorenz gauge condition (1.10). Hence (1.62) implies that $\int d^3x B^{i00} = 0$. Thus, we get from (1.61)

$$\int d^3x [\mathcal{T}^{i0} + \tau^{i0}] = \int d^3x \mathbb{T}^{i0}. \quad (1.63)$$

1.5 Eq. (1.53) predicts a non-negative expression

$$\mathcal{T}^{00} = \frac{1}{8\pi} (\mathbf{E}^2 + \mathbf{B}^2) \quad (1.64)$$

for the energy density of EMF [11]. In contrast, according to (1.18) the energy density of EMF is generally not positive. It is positive for stationary fields, and it is positive for a radiation emitted by a point particle, where (1.18) and (1.53) agree with each other; see section 2.2. The non-positivity should not be regarded as a drawback, e.g. because once for point particles the diverging terms for (1.53) are renormalized away, the energy density of EMF is not anymore strictly positive.

1.6 Another difference between (1.53) and (1.18) for a free EMF is that the zero-trace relation $\mathcal{T}_i^i = 0$ is always true, while T_i^i is generally not zero; cf. (1.19)]. Now $\mathcal{T}_i^i = 0$ is generally related to the zero mass of photon. For photons we also get that $T_i^i = 0$; see section 2.2. However, it is not generally true that a superposition of two or more photons (e.g. bi-photon) has a zero-mass; see e.g. [103]. Physically, this means that we should not expect the zero-trace relation for an arbitrary EMF.

2. We now turn to discussing the features of (1.54).

2.1 Eq. (1.54) is non-symmetric even for the free EMF. Hence the desired relation between the energy current and momentum density is generally violated: $\tilde{\mathcal{T}}^{0\alpha} \neq \tilde{\mathcal{T}}^{\alpha 0}$. This is not physical.

2.2 The symmetry of (1.54) for a free EMF also means that if one introduces the orbital momentum as $\tilde{\mathcal{M}}_{lm}^k \equiv x_m \tilde{\mathcal{T}}_l^k - x_l \tilde{\mathcal{T}}_m^k$, it is generally not conserved: $\partial_k \tilde{\mathcal{M}}_{lm}^k \neq 0$. This is not physical.

2.3 Eq. (1.54) is neither explicitly gauge-invariant, nor it allows to single out any specific gauge ⁸.

2.4 Eq. (1.54) relates to the following energy-momentum tensor for EMF+matter:

$$\partial_k (\tilde{\mathcal{T}}^{ik} + \tau^{ik} + \frac{1}{c} A^i J^k) = 0. \quad (1.65)$$

This follows from $\tilde{\mathcal{T}}^{ik} = \mathcal{T}^{ik} - \frac{1}{4\pi} \partial^l A^i F_l^k$ [see (1.53, 1.54)] and from (1.56). Comparing (1.65) with (1.18), we see that (1.65) predicts analogues of (1.22, 1.24), but without singling out the Lorenz gauge (1.10).

⁸This point can be reformulated as follows [50]. It is based on separating the full potential A_i into a physical (i.e. gauge-invariant) part and the pure gauge: $A_i = A_i^{\text{phys}} + A_i^{\text{pure}}$, where $A_i^{\text{pure}} = \partial_i \chi$ [50]. Expectedly, the modified (i.e. gauge-invariant) analogue of (1.54) is given by the same expression, where $A^l \rightarrow A^{l \text{ phys}}$. The modified expression is now gauge-invariant, but is still not unique, because now there is a freedom in choosing A_i^{phys} .

1.7 Fermi's Lagrangian for free EMF

The purpose of this section is to derive (1.19) from the Fermi's Lagrangian for a free classical electro-magnetic field (EMF) [62, 70, 73]. The standard Lagrangian reads

$$\mathcal{L} = -\frac{1}{16\pi} F_{ik} F^{ik}, \quad F_{ik} \equiv \partial_i A_k - \partial_k A_i. \quad (1.66)$$

where $A^i = (\phi, \mathbf{A})$ is the 4-potential.

For the Lorenz gauge (1.10), an alternative Lagrangian was proposed by Fermi [62, 70, 73]. It is obtained from (1.66) upon using (1.10) and neglecting full derivatives

$$L = -\frac{1}{8\pi} \partial_i A_k \partial^i A^k. \quad (1.67)$$

The equations of motion $\partial_k \frac{\partial L}{\partial[\partial_k A^i]} = \frac{\partial L}{\partial A^i}$ are

$$\partial_k \partial^k A_i = 0, \quad (1.68)$$

which are consistent with the Lorenz gauge (1.10). The latter is to be considered as a condition imposed on (1.67).

Given (1.67) and recalling the standard expression for the the energy-momentum tensor [11, 62]

$$T_i{}^k = \partial_i A_l \frac{\partial L}{\partial[\partial_k A_l]} - \mathcal{L} \delta_i^k, \quad (1.69)$$

we obtain from (1.67):

$$T_i{}^k = -\frac{1}{4\pi} \partial_i A_l \partial^k A^l + \frac{1}{8\pi} \delta_i^k \partial_n A_m \partial^n A^m, \quad (1.70)$$

where δ_i^k is the Kroenecker delta. Eqs. (1.70, 1.68) show that the tensor is symmetric and

holds energy-momentum conservation

$$T_{ik} = T_{ki}, \quad (1.71)$$

$$\partial_k T_i{}^k = 0. \quad (1.72)$$

The invariance of a Lagrangian under rotations implies the following general relation between the energy-momentum tensor and angular momentum tensor [62]:

$$M_{lm}^k = x_m T_l{}^k - x_l T_m{}^k + S_{lm}^k, \quad (1.73)$$

$$S_{lm}^k = \frac{\partial L}{\partial[\partial_k A^m]} A_l - \frac{\partial L}{\partial[\partial_k A^l]} A_m, \quad (1.74)$$

where $T_l{}^k$ is given by (1.69), S_{lm}^k is the internal angular momentum (spin), while $x_m T_l{}^k - x_l T_m{}^k$ is the orbital momentum. Using (1.67) we obtain for the spin tensor [62, 70]

$$S_{lm}^k = -\frac{1}{4\pi} (A_l \partial^k A_m - A_m \partial^k A_l). \quad (1.75)$$

Employing (1.68, 1.71, 1.72) we get that the angular momentum and spin tensor are conserved separately [62, 70]:

$$\partial_k M_{lm}^k = \partial_k S_{lm}^k = 0, \quad (1.76)$$

as should be for a free field. The symmetry (1.71) is crucial for the existence of two separate conservation laws (1.76).

The standard approaches to the energy-momentum tensor of EMF are recalled in section 1.6. The spin and orbital momentum of EMF is reviewed in [50, 104]

1.8 Angular momentum

Here we shall connect the energy-momentum tensor \mathbb{T}^{ik} to the angular momentum tensor.

It is seen from (1.18) that \mathbb{T}^{ik} is not symmetric: $\mathbb{T}^{ik} \neq \mathbb{T}^{ki}$. This asymmetry has a physical

meaning and it relates to the spin of EMF ⁹. Recall the following general relation between the orbital momentum tensor \mathbb{O}_{lm}^k and energy-momentum tensor \mathbb{T}^{ik} [11, 62]

$$\mathbb{O}_{lm}^k = x_m \mathbb{T}_l^k - x_l \mathbb{T}_m^k. \quad (1.77)$$

The orbital momentum of matter is already included into \mathbb{O}_{lm}^k . Due to $\mathbb{T}^{ik} \neq \mathbb{T}^{ki}$, the orbital momentum is not conserved: $\partial_k \mathbb{O}_{lm}^k \neq 0$. This is natural, since it is the full angular momentum $\mathbb{M}_{lm}^k = \mathbb{O}_{lm}^k + S_{lm}^k$ (orbital+spin of EMF) that should be conserved. We can thus deduce the spin tensor S_{lm}^k from the conservation law

$$\partial_k \mathbb{M}_{lm}^k = \partial_k (\mathbb{O}_{lm}^k + S_{lm}^k) = 0. \quad (1.78)$$

Eqs. (1.13–1.78) and the fact that S_{lm}^k should be a quadratic function of A_i imply

$$S_{lm}^k = -\frac{1}{4\pi} (A_l \partial^k A_m - A_m \partial^k A_l). \quad (1.79)$$

This expression has formally the same shape as the spin tensor derived in [62, 70] for a free EMF via the Fermi’s Lagrangian; see section 1.7.

Hence the matter-field coupling leads (as expected) to exchange (1.78) between the orbital momentum and the spin. If this coupling is absent, then \mathbb{T}^{ik} is symmetric; hence \mathbb{O}_{lm}^k and S_{lm}^k are conserved separately. These two points-conservation of $\mathbb{O}_{lm}^k + S_{lm}^k$ under matter-EMF coupling and separate conservation of \mathbb{O}_{lm}^k and S_{lm}^k for free EMF|are specific features of (1.78–1.79) that distinguish it from other proposals for angular momentum of EMF; see [50, 104] for a review of those proposals.

1.9 Derivation of (1.34–1.37)

Consider two interacting point particles P and P’; we denote their parameters by primed and unprimed letters. In (1.13, 1.15), the current J^k divides into two contributions, each of

⁹A non-symmetric energy-momentum tensor implies a generalized gravity; see, e.g. [105–107] for examples of such theories.

them is conserved separately

$$J^k = j^k + j'^k, \quad \partial_k j^k = \partial_k j'^k = 0. \quad (1.80)$$

The EMF field A^k in (1.14, 1.15) also divides into two parts:

$$A^k = a^k + a'^k, \quad \partial_k a^k = \partial_k a'^k = 0, \quad (1.81)$$

$$\partial_i \partial^i a^k = \frac{4\pi}{c} j^k, \quad \partial_i \partial^i a'^k = \frac{4\pi}{c} j'^k. \quad (1.82)$$

Hence a^k (a'^k) is created by j^k (j'^k).

Equations of motion for P and P' are deduced from (1.15) noting that the self-interaction is neglected and the point-particle limit is taken; cf. (1.29) These equations read [75–83]:

$$mc^2 \frac{du^k}{ds} = eu_l f'^{kl}, \quad m'c^2 \frac{du'^k}{ds'} = e'u'_l f^{kl}, \quad (1.83)$$

where

$$f^{kl} = \partial^k a^l - \partial^l a^k, \quad f'^{kl} = \partial^k a'^l - \partial^l a'^k, \quad (1.84)$$

$$ds = cdt\sqrt{1 - v^2/c^2}, \quad ds' = cdt\sqrt{1 - v'^2/c^2}. \quad (1.85)$$

Thus the following (self-interaction-excluded) energy-momentum tensor is conserved [cf. (1.18)]

$$\partial_k \tilde{\mathbb{T}}^{ik} = 0, \quad (1.86)$$

$$\begin{aligned} \tilde{\mathbb{T}}^{ik} = & -\frac{1}{4\pi} [\partial^i a_l \partial^k a'^l + \partial^i a'_l \partial^k a^l - g^{ik} \partial_n a_m \partial^n a'^m] \\ & + \tau^{ik} + \tau'^{ik} + \frac{1}{c} a^i j'^k + \frac{1}{c} a'^i j^k, \end{aligned} \quad (1.87)$$

where τ^{ik} and τ'^{ik} are the energy-momentum tensors of P and P'; see (1.16).

As usual, we shall select the retarded (Liénard-Wiechert) solutions of (1.82); see [11, 44] and section 2.2. In contrast to \mathbb{T}^{ik} that diverges in the point-particle limit, $\tilde{\mathbb{T}}^{ik}$ is already a convergent tensor, i.e. the energy of EMF and particles can be calculated via $\int d^3x \tilde{\mathbb{T}}^{00}(t, \mathbf{x})$.

We focus on the 1D situation, where the particles P and P' move on a line; see (1.31).

The retarded solutions for $a^i = (\phi, A)$ and $a'^i = (\phi', A')$ in (1.82) read [11]:

$$\phi(x', t) = \frac{e}{[x' - x(t - \delta)][1 - \omega(t - \delta)]}, \quad (1.88)$$

$$A(x', t) = \frac{e\omega(t - \delta)}{[x' - x(t - \delta)][1 - \omega(t - \delta)]}, \quad (1.89)$$

$$\phi'(x, t) = \frac{e'}{[x'(t - \delta') - x][1 + \omega'(t - \delta)]}, \quad (1.90)$$

$$A'(x, t) = \frac{e'\omega'(t - \delta')}{[x'(t - \delta') - x][1 + \omega'(t - \delta)]}, \quad (1.91)$$

where the delays $\delta(t)$ and $\delta'(t)$ hold

$$c\delta(t) = x' - x(t - \delta(t)), \quad (1.92)$$

$$c\delta'(t) = x'(t - \delta'(t)) - x. \quad (1.93)$$

To derive the equations of motion from (1.83, 1.88–1.93) recall that f^{kl} [f'^{kl}] in (1.83) is taken at $x' = x'(t)$ [$x = x(t)$]:

$$\dot{p}(t) = -ee' \frac{1 - v'(t - \delta')/c}{1 + v(t - \delta)/c} \frac{1}{[x(t) - x'(t - \delta')]^2}, \quad (1.94)$$

$$\dot{p}'(t) = ee' \frac{1 + v(t - \delta)/c}{1 - v'(t - \delta')/c} \frac{1}{[x'(t) - x(t - \delta)]^2}, \quad (1.95)$$

where

$$p = mv/\sqrt{1 - v^2/c^2}, \quad p' = mv'/\sqrt{1 - v'^2/c^2}, \quad (1.96)$$

$$v(t) = \dot{x}(t) \equiv c \omega(t), \quad v'(t) = \dot{x}'(t) \equiv c \omega'(t). \quad (1.97)$$

We get (1.34–1.37) from (1.92–1.97).

1.10 Solving self-consistently delay-differential equations

1. Let us explain how to solve (1.34–1.38). The method described below was first suggested

in [75]; see also [80] for a recent discussion.

We start with an initial function $\omega'_0(t)$ that holds $\omega'_0(t \leq 0) = \omega'_0$; cf. (1.38). Then (1.34, 1.36) become ordinary differential equations for $\omega(t)$ and $\delta'(t)$. They are solved for $t > 0$ with initial conditions $\omega(0) = \omega_0$ and $\delta'(0)$ from (1.39); cf. (1.38). The solution is denoted by $\omega_0(t)$. This function is extended to $t < 0$ via (1.38): $\omega_0(t < 0) = \omega_0$.

Next, $\omega_0(t)$ is put into (1.35, 1.37), and these equations are solved for $t > 0$, $\omega'(0) = \omega'_0$ and $\delta(0)$ from (1.39). The solution $\omega'_1(t)$ is again extended to $t < 0$ via (1.38): $\omega'_1(t < 0) = \omega'_0$. Iterations are continued till convergence.

2. We turn to solving (1.36, 1.37).

Now the initial function $x'(t) = x'_0(t)$ is defined for $t < t_f$. For solving (1.36) we need to know $\delta'(t_f)$. It is found from (1.33), i.e. from

$$c\delta'_0(t_f) = x'_0(t_f - \delta'(t_f)) - x(t_f). \quad (1.98)$$

Hence this initial condition will change from iteration to another. Now (1.36) can be solved as ordinary differential equations backward in t from t_f to some $T_i \ll t_f$. Then the solution is continued to $t < T_i$ by assuming that $\omega(t) = \omega(T_i)$ for $t < T_i$. This assumption is needed, because it is impossible to integrate numerically from t_f till $-\infty$. Effectively, this means that the particles did not interact in the remote past; or (alternatively) that they interacted so strongly that $\omega(t) = v(t)/c \simeq 1$ for $t < T_i$.

Overall, the solution defines $x_0(t)$ with which we repeat the above step for (1.37), e.g. $x_0(t)$ is put into (1.37), and now we have instead of (1.98): $c\delta_0(t_f) = x'(t_f) - x_0(t_f - \delta_0(t_f))$. The backward solution of ordinary-differential (1.37) is continued as $\omega'(t) = \omega'(T_i)$ for $t < T_i$. Once iterations converged, we assure by direct replacement that (1.36, 1.37) do hold for $T_i \ll t < \tau$.

Chapter 2

Work in the presence of self-interaction ¹

2.1 Two-particle retarded interaction in the presence of self-interaction

Consider two points particles P and P'-with charges e, e' and masses m, m' -interacting via EMF. Let us denote their trajectories and velocities as, respectively, $\mathbf{x}(t), \mathbf{x}'(t)$ and $\mathbf{v} = \dot{\mathbf{x}}(t), \mathbf{v}' = \dot{\mathbf{x}}'(t)$, where dotes mean time-derivatives. We employ $x^i(t) = (t, \mathbf{x}), x'^i(t) = (t, \mathbf{x}')$ and metric $g_{ik} = \text{diag}[1, -1, -1, -1]$. The equations of motion read [11, 44]

$$m \frac{du^k}{ds} = eu_l F'^{kl} + \frac{2e^2}{3} \left[\frac{d^2 u^k}{ds^2} + \frac{du^l}{ds} \frac{du_l}{ds} u^k \right], \quad m' \frac{du'^i}{ds'} = e' u'_l F^{kl} + \frac{2e'^2}{3} \left[\frac{d^2 u'^k}{ds'^2} + \frac{du'^l}{ds'} \frac{du'_l}{ds'} u'^k \right] \quad (2.1)$$

where $ds = \sqrt{1 - v^2} dt, ds' = \sqrt{1 - v'^2} dt, u^k = dx^k/ds, u'^k = dx'^k/ds', F'^{kl} = \partial^k A'^l - \partial^l A'^k, F^{kl} = \partial^k A^l - \partial^l A^k$. Now A^i is the potential generated by P, $\partial_i \partial^i A^k(t, \mathbf{x}) = 4\pi e \dot{x}^k \delta_D(\mathbf{x} - \mathbf{x}(t))$ (δ_D is the Dirac's delta function), in the Lorenz gauge: $\partial_i A^i = 0$. The retarded solutions reads, see next section.

$$A^k(t, \mathbf{x}) = e \dot{x}^k / (|\mathbf{R}| - \mathbf{R}\mathbf{v}), \quad (2.2)$$

¹The results considered in this chapter are published in Ref. [179].

In (2.2) all quantities are taken at the time \hat{t} that is determined from the retardation condition $|\mathbf{R}| \equiv |\mathbf{x} - \mathbf{x}(\hat{t})| = t - \hat{t}$. A^i is obtained from (2.2) by changing the non-primed quantities to the primed ones. The term $\propto \frac{2e^2}{3}$ in (2.1) is the self-force that includes the radiation reaction. This is the exact expression of the self-force in the point-particle limit, i.e after the renormalization of masses [11, 44, 108]. The term $\propto \frac{du'}{ds} \frac{du}{ds}$ in the self-force is the Larmor rate [11, 44, 108].

Let two particles P and P' move on a line. This situation is realized if their initial velocities are collinear. We set for the coordinates of P and P': $x(t_1) \leq x'(t_2)$ for all t_1 and t_2 . Equations of motion read from (2.1, 2.2)

$$\frac{\dot{v}(t)}{[1 - v^2]^{3/2}} = -\frac{ee'}{m} \frac{1}{\delta'^2} \frac{1 - v'(t - \delta')}{1 + v'(t - \delta')} + \frac{2e^2}{3m} \frac{\ddot{v}(1 - v^2) + 3v\dot{v}^2}{[1 - v^2(t)]^3}, \quad (2.3)$$

$$\frac{\dot{v}'(t)}{[1 - v'^2]^{3/2}} = \frac{ee'}{m'} \frac{1}{\delta^2} \frac{1 + v(t - \delta)}{1 - v(t - \delta)} + \frac{2e'^2}{3m} \frac{\ddot{v}'(1 - v'^2) + 3v'\dot{v}'^2}{[1 - v'^2]^3}, \quad (2.4)$$

where $v = v(t)$, $v' = v'(t)$, and where the delays $\delta(t)$ and $\delta'(t)$ arise due to retardation: $\delta(t) = x'(t) - x(t - \delta(t))$, $\delta'(t) = x'(t - \delta'(t)) - x(t)$. We differentiate these equations and use them along with (2.3–2.4):

$$\dot{\delta}'(t) = \frac{v'(t - \delta'(t)) - v(t)}{1 + v'(t - \delta'(t))}, \quad \dot{\delta}(t) = \frac{v'(t) - v(t - \delta(t))}{1 - v(t - \delta(t))}, \quad (2.5)$$

Note the retarded Coulomb interaction $\delta'^{-2} = [x'(t - \delta'(t)) - x(t)]^{-2}$ in the right-hand-side of (2.3).

2.2 Energy momentum-tensor for free radiation

Here we discuss the energy-momentum tensor (1.19) for free radiation. Within this section we put $c = 1$.

Consider a charge e moving on a world-line $z^i(s)$. Define $u^i = dz^i(s)/ds$ for the 4-velocity.

Recall that $u^i u_i = 1$. Let w^i and c^i be defined as follows

$$w^i w_i = -1, \quad u^i w_i = 0, \quad (2.6)$$

$$c^i = u^i + w^i, \quad c^i c_i = 0. \quad (2.7)$$

Given an observation event with 4-coordinates x^i , there is a unique point $z^i(s_{\text{ret}})$, so that the light signal emitted from a $z^i(s_{\text{ret}})$ reached x^i . Define using (2.6, 2.7) [44]:

$$R^i = x^i - z^i(s_{\text{ret}}), \quad R^i R_i = 0, \quad (2.8)$$

$$R^i = \rho c^i, \quad \rho = R^i u_i. \quad (2.9)$$

When x^i changes, $z^i(s_{\text{ret}})$ changes as well. Hence there is a problem of calculating derivatives [44]. There are 3 main formulas here (recall that $\partial_i \equiv \partial/\partial x^i$):

$$\partial_k s_{\text{ret}} = c_k, \quad (2.10)$$

$$\partial_k R^i = \delta_k^i - u^i c_k, \quad (2.11)$$

$$\partial_k \rho = u_k + c_k (R_i a^i - 1), \quad a^i \equiv d^2 x^i(s)/ds^2. \quad (2.12)$$

To derive (2.10, 2.11), note from (2.8): $\partial_k R^i = \delta_k^i - u^i \partial_k s$. This relation together with $R^i R_i = 0$ implies: $R_i \partial_k R^i = 0 = R_k - R^i u_i \partial_k s$. Together with (2.9) this leads to (2.10) and then to (2.11). Eq. (2.12) is deduced from $\partial_k \rho = \partial_k (R^i u_i)$ using $\partial_k u^i = a^i \partial_k s = a^i c_k$.

The Lienard-Wichert potential of a charge e reads

$$A^i = e u^i / \rho. \quad (2.13)$$

Employing (2.10–2.12) we obtain

$$F^{ik} = \partial^i A^k - \partial^k A^i = e(R^i \omega^k - R^k \omega^i), \quad (2.14)$$

$$\omega^i = \frac{a^i}{\rho^2} + \frac{u^i(1 - a_l R^l)}{\rho^3}, \quad (2.15)$$

$$\partial^i A^l \partial^k A_l = \frac{e^2 c^i c^k [a_l a^l + (a_l w^l)^2]}{\rho^2} \quad (2.16)$$

$$- (a_l w^l) \frac{e^2 [c^i w^k + c^k w^i]}{\rho^3} + \frac{e^2 w^i w^k}{\rho^4}, \quad (2.17)$$

$$\partial_k A^l \partial^k A_l = (a_l w^l) \frac{2e^2}{\rho^3} - \frac{e^2}{\rho^4}. \quad (2.18)$$

These expressions determine from (1.19) the energy-momentum tensor of EMF.

Note that the right-hand-side of (2.16) is the only term that scales as ρ^{-2} . This is the term responsible for the energy-momentum of the emitted radiation. It coincides with the radiation energy-momentum tensor obtained from the standard expression (1.53) [44]. In particular, it is symmetric and has zero trace due to (2.7).

2.3 Energy transfer and work

It is expected that due to interaction there is a transfer of energy from one particle to another. We assume that one of the particles (say P') is much heavier than another $m' \gg m$. Hence its motion is perturbed weakly. P' will be the source of work. The definition of work is based *simultaneously* on two concepts: the change $\Delta_{t_2|t_1} E = E(t_2) - E(t_1)$ of the full energy of P [cf. (2.20)] and the change $\Delta_{t_2|t_1} K' = K'(t_2) - K'(t_1)$ of the kinetic energy

$$K' = -m' + m'/\sqrt{1 - v'^2}, \quad (2.19)$$

of P'. The relation of the work to the kinetic energy of P' is due to the fact that this kinetic energy can be fully and immediately transferred to heat, e.g. by stopping the particle via a static target.

The energy of the light particle is defined as its kinetic energy plus the potential energy

in the Lorenz gauge (2.2):

$$E = K + e\phi'(x(t), t) = \frac{m}{\sqrt{1 - v^2(t)}} + \frac{ee'}{\delta'(t)[1 + v'(t - \delta'(t))]}, \quad (2.20)$$

The work transfer from P to P' (or back) can be defined approximately via either $\Delta_{t_2|t_1} E$ or $\Delta_{t_2|t_1} K'$ provided that

$$|\Delta_{t_2|t_1}(E + K')| \ll |\Delta_{t_2|t_1} E|, |\Delta_{t_2|t_1} K'|. \quad (2.21)$$

We shall see that this definition does apply in the relativistic situation and does predict a causal behavior for the energy change. Note the analogy with the non-relativistic situation described by the Newton equations with Coulomb potential. Here there is an exact relation [conservation of energy] $\frac{mv^2(t)}{2} + \frac{ee'}{|x'(t) - x(t)|} = -\frac{m'v'^2(t)}{2} + \text{const}$. If $\frac{m'v'^2(t)}{2}$ is identified with the energy of P, we get an exact correspondence between the two aspects of work. The main drawback of this non-relativistic argument is that the interaction term $\frac{ee'}{|x'(t) - x(t)|}$ can equally well be prescribed to the work-source P'. We see below that the drawback is corrected in the relativistic situation.

Technically, delay-differential equations of motion (2.3–2.5) with the self-force can be solved *only* from the future boundary conditions for coordinates, velocities and accelerations [44]. Hence we pose future conditions ($\dot{v}(t_f) = 0, \dot{v}'(t_f) = 0$) and numerically integrate back up to minus infinity employing a version of the self-consistent method [87]. Similar problems were studied in [84], but without looking at energies, which is our main question here.

The existence and uniqueness of the above (Cauchy) solution is not generally known. There are only certain partial results [87–89, 109], e.g. that the solution exists and it is unique for 1D repelling case, $ee' > 0$, if the final separation $|x(t_f) - x'(t_f)|$ is sufficiently large [81]. We focus on this situation. Hence the final time is chosen so large that the particles do not interact for $t \sim t_f$ and for $t \sim 0$.

In (2.3–2.4) we measure the time and space by units of e^2/m . This leaves free two dimensionless parameters: e/e' that take 1 (repulsive case) and $m'/m \gg 1$. Examples of numerical solution are presented in Figs. 2.1–2.3.

Fig. 2.1 displays a situation, where asymptotically (i.e. when comparing $t = t_f$ with $t = 0$) the particle do not exchange energy; only a small part of the energy is radiated away. However, Fig. 2.1 shows that a sizable exchange of energy occurs for intermediate times, and that this exchange is well described by (2.21). First, the energy (work) flows from the heavy particle to the light one, and then it comes back to the heavy particle (source of work). Some energy is radiated away, hence the heavy particle ends up with a lower kinetic energy at $t = t_f$; see Fig. 2.1. Now $\Delta_{t|0}(E + K')$ slowly decays due to radiated energy. Note that $\Delta_{t|0}(E' + K)$ (kinetic energy of the light particle plus the full energy of the heavy one) is neither a slowly decaying, nor approximately constant. It also does not follow the trend of energy radiation. Thus in contrast to the non-relativistic situation [cf. after (2.21)], our relativistic results clarify also the direction of the energy flow, since in choosing between $\Delta_{t|0}(E' + K)$ and $\Delta_{t|0}(E + K')$ the preference should be given to the latter. Likewise, $\Delta_{t|0}(K' + K)$ (sum of kinetic energies) is not approximately constant; see Fig. 2.1.

Fig. 2.1 shows that $\Delta_{t|0}(E + K')$ is bounded from below by the integrated sum of the Larmor rates [see (2.1)]:

$$\Delta_{t|0}(E + K') \geq \frac{2}{3} \int_0^t d\bar{t} \left[\frac{du^k}{ds} \frac{du_k}{ds} + \frac{du'^k}{ds'} \frac{du'_k}{ds'} \right] \equiv -\frac{2}{3} \int_0^t d\bar{t} \left[\frac{\dot{v}^2(\bar{t})}{(1 - v^2(\bar{t}))^3} + \frac{\dot{v}'^2(\bar{t})}{(1 - v'^2(\bar{t}))^3} \right] \quad (2.22)$$

where the latter sum is naturally dominated by the contribution from the light particle, since the heavy particle is weakly perturbed. Inequality (2.22) holds-at least for sufficiently large t (cf. Fig. 2.3)-for all situations we were able to check. Note that the full amount of the radiated energy is to be determined from $\Delta_{t|0}(E + K')$, and not from the Larmor rates. They can be misleading not only quantitatively, but also qualitatively, e.g. looking at the Larmor rates (for $m' \gg m$) may imply that it is the light particle that loses energy, while for the situation on Fig. 2.1 the radiated energy comes from the heavy particle.

Fig. 2.2 shows that the energy transfer takes place from the heavy to the light particle. This transfer is well described by the potential energy in the Lorenz gauge: (2.21) holds, as seen in Figs. 2.2.

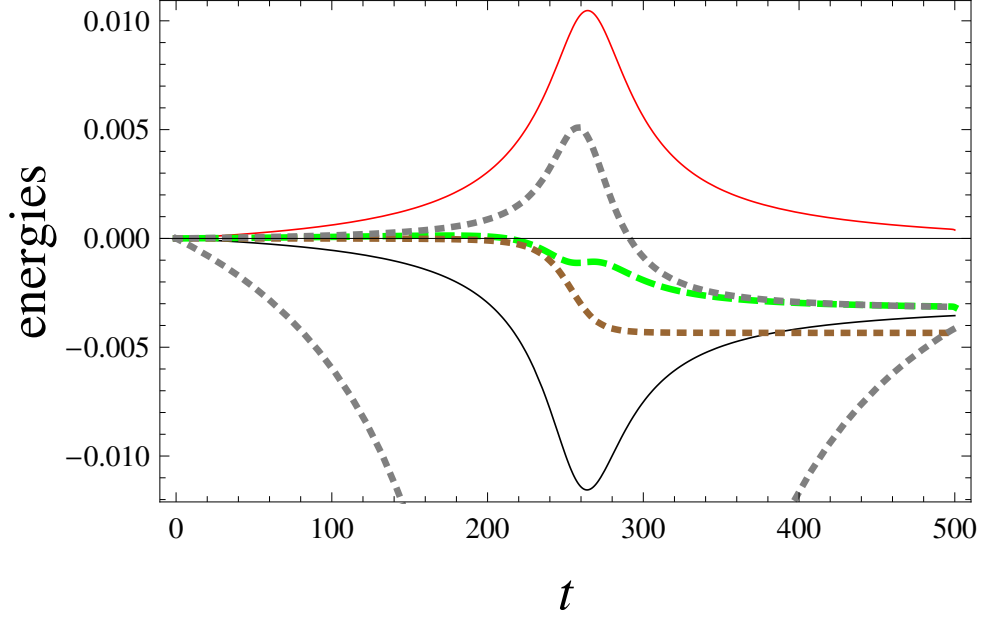


Figure 2.1: For all figures we employ $ee' = 1$, $m'/m = 10$ and the units of the light particle. The infinitely remote time is -10^3 . Cauchy solution for $t_f = 500$, where $v'(t_f) = 0.04$, $v(t_f) = -0.4$, $x'(t_f) - x(t_f) = 100$; $v'(0) = -0.04804$, $v(0) = 0.40117$. From up to down. Upper line $\Delta_{t|0}E$. Upper dotted line $\Delta_{t|0}(E' + K)$. Dashed line $\Delta_{t|0}(E + K')$; cf. (2.19, 2.20). Middle dotted line: the sum of the Larmor rates (2.22). Lower line $\Delta_{t|0}K'$. Lower dotted line $\Delta_{t|0}(K' + K)$.

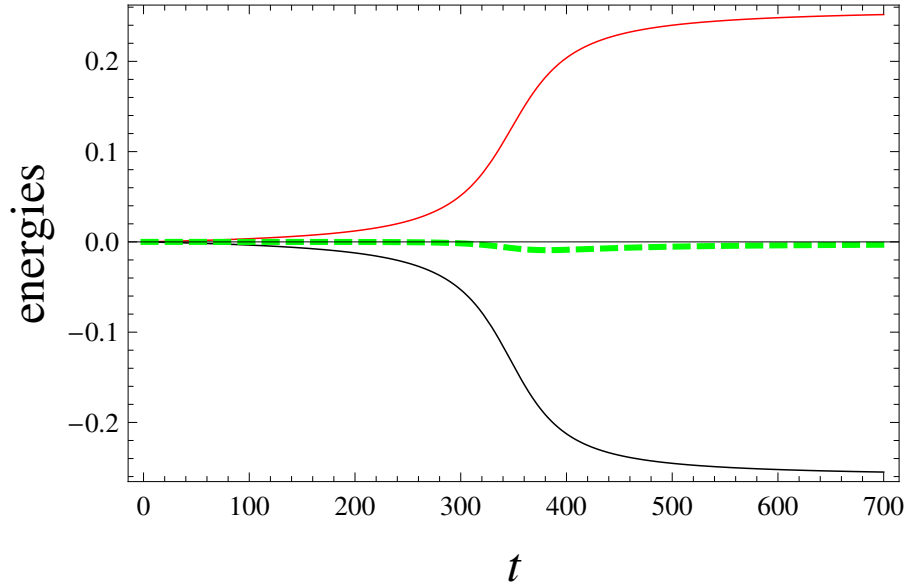


Figure 2.2: Cauchy solution for $t_f = 700$, where $v'(t_f) = -0.3$, $v(t_f) = -0.6$, $x'(t_f) - x(t_f) = 100$; $v'(0) = -0.364289$, $v(0) = 0.0102$. Upper line $\Delta_{t|0}E$. Lower line $\Delta_{t|0}K'$. Dashed line $\Delta_{t|0}(E + K')$.

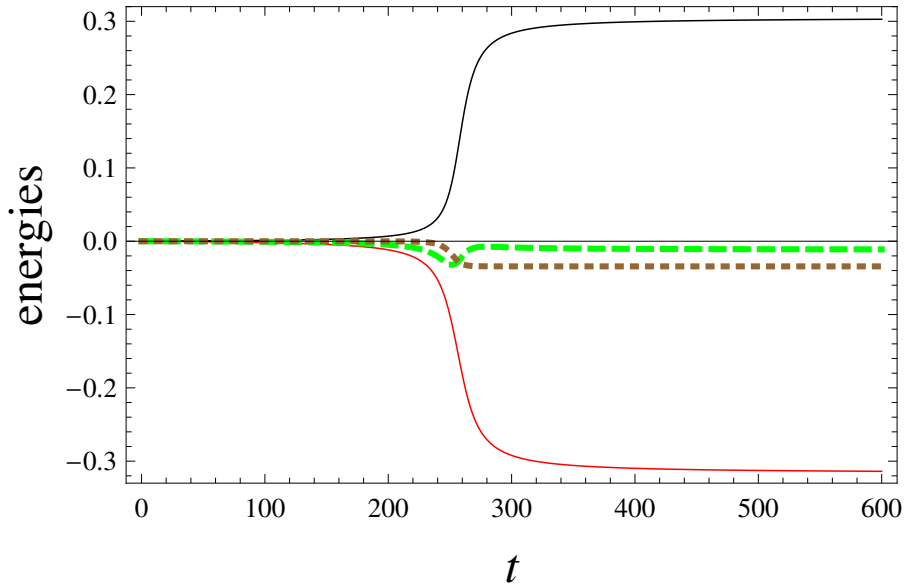


Figure 2.3: Cauchy solution for $t_f = 600$, where $v'(t_f) = 0.3$, $v(t_f) = -0.3$, $x'(t_f) - x(t_f) = 200$; $v'(0) = 0.187263$, $v(0) = 0.677107$.

Lower line $\Delta_{t|0}E$. Upper line $\Delta_{t|0}K'$. Dashed line $\Delta_{t|0}(E + K')$. Dotted line: the sum of the Larmor rates (2.22).

Fig. 2.3 gives an example of the energy transfer from light to the heavy particle. Eq. (2.21) still holds, but a new effect is visible: when the energy transfer starts (at $t \sim 200$), $\Delta_{t|0}(E + K')$ first decreases, and then increases to a slightly smaller value: the transferred energy first goes out of the light particle-hence $\Delta_{t|0}(E + K')$ decreases-and then it arrives at the heavy particle. The small mismatch between those initial and final values is due to the energy that is radiated away. Since $\Delta_{t|0}(E + K')$ is non-monotonic for $t \sim 250$, one can choose times t_2 , t_1 such that $\Delta_{t_2|t_1}(E + K') \approx 0$ ($t_2 \approx 300$, $t_1 \approx 220$), while $\Delta_{t_2|t_1}E$ accounts for the major part of the energy transfer.

Relation (2.21) is confirmed in all other situations we studied, including the case of attractive particles (not shown on figures), where a special treatment of the self-force is necessary.

Chapter 3

Adaptive heat engine ¹

3.1 Introduction

Heat-engines drove the Industrial Revolution and their foundation, *viz.* thermodynamics, became one of the most successful physical theories [110]. Extensions of thermodynamics to stochastic [111, 112] and quantum domain [4] led to new generations of heat engines [4, 112–128]. As everyone could observe, the work-extraction function of macroscopic heat-engines requires external on-line control, e.g. the specific sequence of adiabatic and isothermal processes for the Carnot cycle [14, 110]. Smaller engines may not demand on-line control, i.e. they are autonomous [122–124], but they do demand fitting between internal and environmental parameters [114–121], e.g. because for fixed environment (thermal baths) there are internal parameters, under which the machine acts as a heat-pump or refrigerator performing tasks just opposite to that of heat-engine. Such fitted engines are susceptible to environmental changes, e.g. when the bath temperatures get closer due to the very engine functioning. Car engines treat this problem by abandoning the partially depleted fuel (i.e. the hot bath), and using fresh fuel.

Here we study a rudimentary model of autonomous, adaptive heat engine. Adaptive means that the engine can work for a sufficiently general class of environments, i.e. it needs neither

¹The results considered in this chapter are published in Ref. [180].

on-line control, nor an externally imposed fitting between its internal parameters and the bath temperatures. In particular, the engine can adapt to the results of its own functioning. Hence adaptive engines can be useful for fueling devices via unknown or scarce resources [129].

The major biophysical heat engine, *viz* photosynthesis-which operates between the hot Sun temperature and the low-temperature Earth environment [130]-does have adaptive features that allow its functioning under decreased hot temperature (shadowing) or increased cold temperature (hot whether) [131, 132].

Recently, several physical models concentrated on adaptive sensors, adaptive transport models *etc* [132–140]. These studies clarified thermodynamic costs of adaptation scenarios [132, 135–140]. Other research lines related adaptation with (poly)homeostasis [141] and models of artificial life [14, 142].

For analyzing the adaptation and its resources for heat engines, we need a tractable and realistic model that is much simpler than e.g. its prototypes in photosynthesis. The model ought to consist of the proper heat-engine and a controller that ensures the adaptation; see Fig. 3.1. Together they form an autonomous system.

3.2 Working body

For the heat-engine we choose one of the most known models of quantum/stochastic thermodynamics that was introduced and studied as a model for maser [114–119]. Related models were studied in the context of photovoltaics [125, 126]. The model has three states: $i = 1, 2, 3$. Each state i has energy E_i . Transitions between different states are caused by thermal baths that can provide or accept necessary energies. We assume that the resulting dynamics is described by a Markov master equation [143]:

$$\dot{p}_i \equiv dp_i/dt = \sum_j [\rho_{i \leftarrow j} p_j - \rho_{j \leftarrow i} p_i], \quad i, j = 1, 2, 3, \quad (3.1)$$

where $p_i(t)$ is the probability of the state i at time t , and $\rho_{i \leftarrow j} > 0$ is the transition rate from j to i . We assume for simplicity that each transition $i \leftrightarrow j$ couples with one equilibrium bath at temperature $T_{ij} = T_{ji} = 1/\beta_{ji}$; see Fig. 3.1. The equilibrium nature of each bath imposes

the detailed balance constraint for transitions [143]:

$$\rho_{i \leftarrow j} e^{-\beta_{ij} E_j} = \rho_{j \leftarrow i} e^{-\beta_{ij} E_i}, \quad \beta_{ij} = \beta_{ji}. \quad (3.2)$$

We take one temperature infinite: $\beta_{21} = 0$. This bath is then a work-source, because due to $dS_{21} = \beta_{21} dQ_{21} = 0$ it exchanges energy $dQ_{21} \neq 0$ at zero entropy change $dS_{21} = 0$. The other two thermal baths are the ones necessary for any heat-engine; see Fig. 3.1. Below we ensure its function for a large range of $\beta_{31} \neq \beta_{32}$.

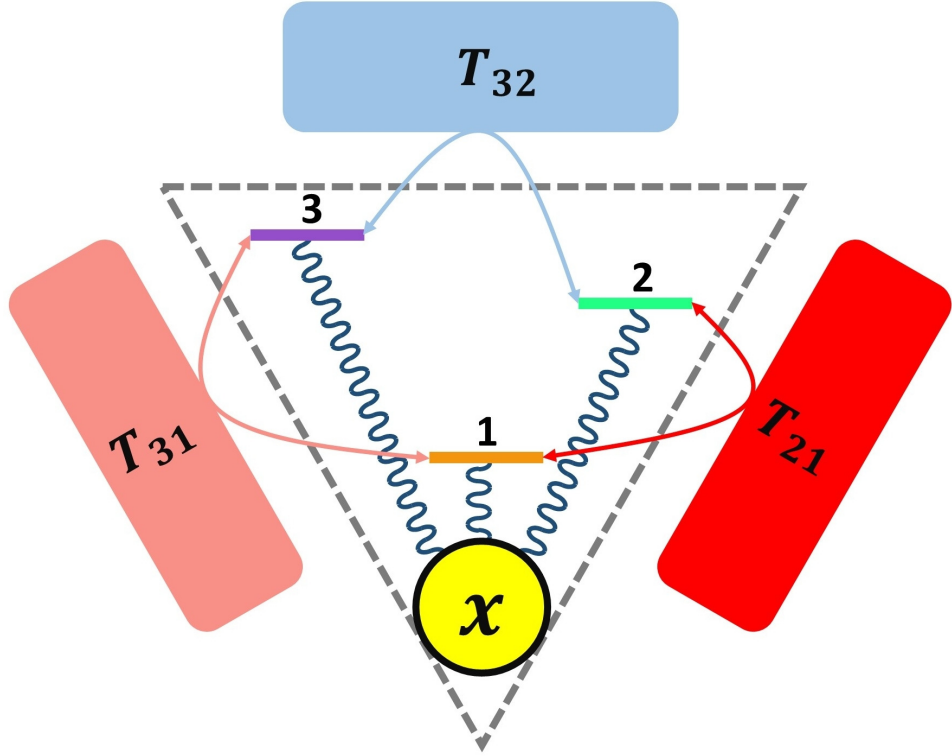


Figure 3.1: A schematic representation of the model. There are three thermal baths at temperatures $T_{32}, T_{31} < T_{21} = \infty$; each one drives a single transition among three engine levels 1, 2, and 3. The bath with temperature $T_{21} = \infty$ is the source of work. A controller x interacts with energies, but does not couple directly with the baths.

Since each bath causes only one transition $i \leftrightarrow j$,

$$J_{ij} = J_{ji} = (E_i - E_j)(\rho_{i \leftarrow j} p_j - \rho_{j \leftarrow i} p_i), \quad (3.3)$$

is the average energy lost (if $J_{ij} > 0$) or gained (if $J_{ij} < 0$) by the bath per time-unit; see (3.1). In the stationary state these energy currents J_{ij} hold $J_{31} + J_{32} + J_{21} = \sum_{i=1}^3 \dot{p}_i E_i = 0$,

as necessary for the average energy conservation. Eq. (3.1) implies for stationary probabilities

$$p_i = \frac{1}{\mathcal{Z}} [\rho_{i \leftarrow j} \rho_{i \leftarrow k} + \rho_{i \leftarrow j} \rho_{j \leftarrow k} + \rho_{i \leftarrow k} \rho_{k \leftarrow j}], \quad (3.4)$$

where \mathcal{Z} ensures $\sum_{i=1}^3 p_i = 1$, and for each $i = 1, 2, 3$ we demand $i \neq j \neq k \neq i$; e.g. $j = 2$ and $k = 3$ for $i = 1$. Using (3.3–3.4) and $\rho_{1 \leftarrow 2} = \rho_{2 \leftarrow 1}$ due to $\beta_{21} = 0$ we get

$$J_{21} = \frac{\hat{E}_2}{\mathcal{Z}} \rho_{2 \leftarrow 1} \rho_{1 \leftarrow 3} \rho_{3 \leftarrow 2} \left[1 - e^{(\beta_{32} - \beta_{31}) \hat{E}_3 - \beta_{32} \hat{E}_2} \right], \quad (3.5)$$

$$J_{31} = -\hat{E}_3 J_{21} / \hat{E}_2, \quad J_{32} = (\hat{E}_3 - \hat{E}_2) J_{21} / \hat{E}_2, \quad (3.6)$$

$$\hat{E}_2 \equiv E_2 - E_1, \quad \hat{E}_3 \equiv E_3 - E_1. \quad (3.7)$$

The heat-engine functioning is defined as [cf. (3.2)]

$$0 > J_{21} = -(E_2 - E_1)(p_2 - p_1)\rho_{1 \leftarrow 2}, \quad (3.8)$$

i.e. the energy goes to the work-source with the *power* $|J_{21}|$. Inequality (3.8) shows that the heat-engine functions via population inversion between energy levels E_1 and E_2 : when driving the transition $1 \leftrightarrow 2$, the work-source gains energy in average. Using (3.5, 3.7) we write (3.8) as

$$\hat{E}_2 [(1 - \theta) \hat{E}_3 - \hat{E}_2] > 0, \quad \theta \equiv \beta_{31} / \beta_{32}. \quad (3.9)$$

Eq. (3.9) demands different temperatures: $\beta_{32} \neq \beta_{31}$. It also demands tuning between the energies \hat{E}_2 , \hat{E}_3 and θ : it is impossible to hold (3.9) for a wide range of θ by means of constant \hat{E}_2 and \hat{E}_3 ; e.g. if (3.9) holds for $1 > \theta$ due to $\hat{E}_3 > \hat{E}_2 > 0$, then it is violated for $1 - \theta < \frac{\hat{E}_2}{\hat{E}_3}$. Tuning is necessary, since for suitable values of \hat{E}_2 and \hat{E}_3 , the machine can function also as a refrigerator or as a heat-pump; see section 3.7 for details.

The efficiency (power divided over the incoming current) η of the engine is given as (see

(3.5, 3.6, 3.9))

$$\eta \equiv \frac{-J_{21}}{\max[J_{31}, J_{32}]} \leq \eta_C \equiv 1 - \min[\theta, \frac{1}{\theta}], \quad (3.10)$$

$$\eta = \max \left[\frac{\hat{E}_2}{\hat{E}_3}, \frac{\hat{E}_2}{\hat{E}_2 - \hat{E}_3} \right] \quad (3.11)$$

where η depends only on energy differences \hat{E}_2 and \hat{E}_3 [see (3.6)], and the Carnot value η_C bounds η from above, as deduced from (3.9). For $\eta \rightarrow \eta_C$ inequality (3.9) saturates, and (3.5, 3.6) show that all J_{ij} nullify (power-efficiency trade-off) [4, 112, 121]; see [144, 145] for most recent discussion of this trade-off.

3.3 The controller

x should ensure adaptation to continuous environmental variations; hence it is continuous. x and i interact via energies $E_i(x)$. The joint probability $p_i(x, t)$ of x and i , $\int dx \sum_i p_i(x, t) = 1$, evolves via the Fokker-Planck plus master equations [cf. (3.1)] [143]:

$$\begin{aligned} \dot{p}_i(x, t) = & \sum_{j=1}^3 [\rho_{i \leftarrow j}(x) p_j(x, t) - \rho_{j \leftarrow i}(x) p_i(x, t)] \\ & + \frac{1}{\gamma} \partial_x [p_i(x, t) E'_i(x)] + D \partial_x^2 p_i(x, t), \quad i = 1, 2, 3, \end{aligned} \quad (3.12)$$

where $E'_i(x) \equiv \frac{dE_i(x)}{dx}$, $\gamma > 0$ is the friction constant, and $D > 0$ is the diffusion constant. $\rho_{i \leftarrow j}(x)$ is specified in (3.22); it holds (3.3) with $E_i \rightarrow E_i(x)$ and $E_j \rightarrow E_j(x)$.

Eq. (3.12) has a wide range of chemical and biological applications [146–160]. It accounts for enzyme dynamics, where a reaction (to be accelerated) is described by a discrete variable i that interacts with a coarse-grained conformational coordinate x of the enzyme [149–158]. The existence of x was inquired from experiments [146–156], and also deduced from microscopic models [157, 158]. Reactions of photosynthesis are also known to interact with conformational degrees of freedom [161]: the main mechanism of the photosynthesis adaptation was located in conformational changes of the thylakoid membrane that bounds light-dependent reactions [131].

Eq. (3.12) has similarities with recent models for quantum heat engines; but there the continuous variable is employed for storing the extracted work [127, 128].

The harmonic choice of interaction energies $E_i(x)$ verified itself well in various applications [149, 150, 155–157, 159, 160]

$$E_i(x) = a(x - b_i)^2 + c_i, \quad i = 1, 2, 3, \quad (3.13)$$

where $a > 0$, b_i and c_i are constants; a is i -independent, since $E_i(x)$ have the same shape for $x \rightarrow \pm\infty$. Eq. (3.13) was explained in [158] via quantum chemistry.

The exact stationary solution $p_i(x)$ of (3.12) is not found. We need an explicit form of $p_i(x)$, since from within $p_i(x)$ we should search for adaptation-friendly shapes of $E_i(x)$. This issue is solved, if we assume in (3.12) that x is slow: $\frac{1}{\gamma}$, $D \ll \rho_{i \leftarrow j}(x)$. This is realistic for enzymes, where x includes large molecular groups whose motion is slow [153–156]. A virtue of the slow limit is that it decreases energy costs related to control, akin to the standard reversibility limit of thermodynamics; see below. Section 3.8 justifies the slow limit. It is implemented by introducing in (3.12) the conditional probability $p_{i|x}(t)$ [162],

$$p_i(x, t) = p_{i|x}(t)p(x, t), \quad \int dx p(x, t) = 1, \quad \sum_{i=1}^3 p_{i|x}(t) = 1,$$

and collecting fast terms:

$$\dot{p}_{i|x} = \sum_{j=1}^3 [\rho_{i \leftarrow j}(x)p_{j|x} - \rho_{j \leftarrow i}(x)p_{i|x}]. \quad (3.14)$$

Slow terms are found from (3.12, 3.14) by summing over i :

$$\dot{p}(x, t) = \frac{1}{\gamma} \partial_x [p(x, t) \sum_{i=1}^3 p_{i|x} E'_i(x)] + D \partial_x^2 p(x, t). \quad (3.15)$$

Since i is fast, $p_{i|x}$ in (3.15) can be taken as time-independent, i.e. $p_{i|x}$ is found from (3.4) upon replacing there $\rho_{ij} \rightarrow \rho_{ij}(x)$ [162]. The stationary probability of x is found from (3.15)

via the zero-current condition $p(x)\sum_{i=1}^3 p_{i|x} E'_i(x) + \gamma D \partial_x p(x) = 0$:

$$p(x) \propto e^{-\Psi(x)/(\gamma D)}, \quad \Psi'(x) \equiv \sum_{i=1}^3 p_{i|x} E'_i(x), \quad (3.16)$$

where $\Psi'(x) = \frac{d\Psi}{dx}$. Using $\sum_{i=1}^3 p_{i|x} = 1$ we define [cf. (3.7)]

$$\Phi'(x) \equiv \sum_{i=2}^3 p_{i|x} \hat{E}'_i(x) = \Psi'(x) - E'_1(x), \quad (3.17)$$

$$\hat{E}_i(x) \equiv E_i(x) - E_1(x). \quad (3.18)$$

3.4 Adaptation

The energies $E_i(x)$ do not depend on β_{31} and β_{32} . We choose $E_i(x)$ as follows. First, there is a unique maximally probable value \hat{x} of x , which is the minimum of the effective potential $\Psi(x)$, i.e. [from (3.16, 3.17)]:

$$\Phi'(\hat{x}) = -E'_1(\hat{x}), \quad \Phi''(\hat{x}) > -E''_1(\hat{x}), \quad (3.19)$$

where the latter condition means stability.

Second, the heat-engine condition $J_{21}(x) < 0$ holds in a vicinity of the maximally probable value \hat{x} [cf. (3.9, 3.18)]:

$$\hat{E}_2(x)[(1 - \theta)\hat{E}_3(x) - \hat{E}_2(x)] > 0, \quad x \simeq \hat{x}, \quad (3.20)$$

Work-extraction should also hold in average [cf. (3.3, 3.2)]:

$$\langle J_{21} \rangle = \rho_{1 \leftarrow 2} \int dx \hat{E}_2(x) p(x) (p_{1|x} - p_{2|x}) < 0. \quad (3.21)$$

Eq. (3.20) implies (3.21), if γD is small enough, because in this limit the probability of x concentrates around \hat{x} ; see (3.16). More generally (e.g. out of the slow limit), the adaptation criterion can be based directly on (3.21).

The adaptation scenario implied by (3.17, 3.20) is as follows. Assume that the machine in its stationary state is already working as a heat-engine for certain bath temperatures β_{31} and β_{32} . If one of them (or both) change, $p_{i|x}$ goes out of the stationary state. As shown by (3.17), this moves \hat{x} to a new value, where according to (3.20) the heat-engine function is recovered. We stress that in this feedback scheme, x does not interact directly with the baths: the change of \hat{x} comes from $p_{i|x}$; see (3.17). Using a feed-forward scheme, where x directly couples with the baths, does not lead to advantages with respect to adaptation, because it changes only friction and diffusion in (3.12); see section 3.9. Section 3.10 studies scenarios, where in addition to the heat-engine function (3.20) the adaptation optimizes the heat-engine efficiency η or its power $|J_{21}|$.

To search for adaptation, we focus on the following class of transition rates [cf. (3.1, 3.3)]:

$$\rho_{i \leftarrow j}(x) = f_{ij}[E_j(x) - E_i(x)], \quad (3.22)$$

where $f_{ij}[y]$ holds (3.3). Eq. (3.22) includes the Kramers' rate $f_{ij}[y] = e^{\beta_{ij}[\Delta_{ij} + \min(y, 0)]}$, where $\Delta_{ij} = \Delta_{ji}$ is the barrier height [143], and $f_{ij}[y] = e^{\beta_{ij}y/2}$ that relates to the discrete-space Fokker-Planck equation [148]. The constraint (3.22) relates to one of conditions of the no-pumping theorem [163, 164]; see section 3.11 that also studies adaptation scenarios which go beyond (3.22).

Eqs. (3.22, 3.18, 3.4) imply that $\rho_{ij}(x)$, the stationary $p_{i|x}$, and $\Phi'(x)$ in (3.17) depend on $E_1(x)$ only via $\hat{E}_3(x)$ and $\hat{E}_2(x)$. Hence we study $\Phi'(x)$ for given $\hat{E}_3(x)$ and $\hat{E}_2(x)$, look for a domain where (3.20) holds, and then define \hat{x} via (3.19) by choosing a suitable $E_1(x)$ that does not depend on β_{31} and on β_{32} . This is achieved by plotting $\Phi'(x)$ as a function of x under different values of β_{31} and β_{32} .

Note that (3.20) confines the shape of $\hat{E}_2(x)$: since (3.20) should hold for $\theta \rightarrow 1$, there exists x_0 such that $\hat{x} \rightarrow x_0$ for $\theta \rightarrow 1$, and $\hat{E}_2(x_0) = 0$. In the vicinity of x_0 , $\hat{E}_3(x)$ is either finite or goes to zero slower than $\hat{E}_2(x)$, so that (3.20) still holds for $\theta \rightarrow 1$ and $\hat{x} \rightarrow x_0$.

3.5 Restricted adaptation.

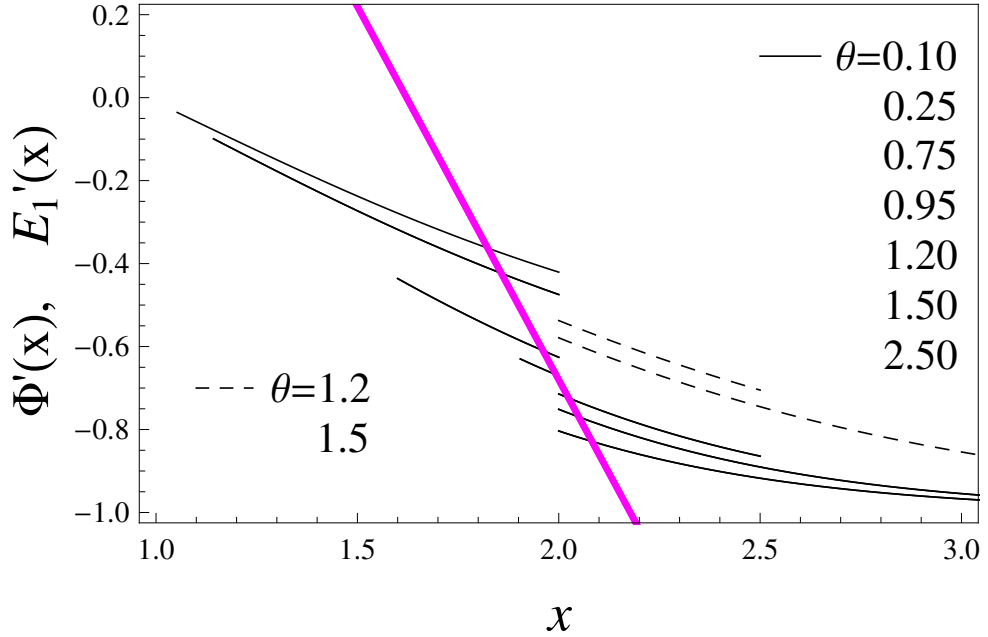


Figure 3.2: Restricted adaptation scenario. $\Phi'(x)$ given by (3.17, 3.22) with $f_{ij}[y] = e^{\beta_{ij}y/2}$. (Similar results hold for all other physical choices of $f_{ij}[y]$; see (3.22) and 3.10) We assume $\hat{E}_3(x) = -x$, $\hat{E}_2(x) = x - 2$; see (3.18, 3.13). Now heat-engine conditions (3.20) hold for $x > 2$ if $\theta > 2$, and for $x \in (\frac{2}{2-\theta}, 2)$ if $\theta < 2$. Normal (resp. dashed) curves: $\Phi'(x)$ for x that support (3.20) under $\beta_{32} = 1$ (resp. $\beta_{32} = 0.7$) and various $\theta = \beta_{31}/\beta_{32}$. They are indicated from the top to the bottom in the right (resp. left). The magenta (bold) curve shows $-E_1'(x)$, where $E_1'(x) = 1.8(x - 2) + 0.680289$; cf. (3.13). Intersections of $-E_1'(x)$ with $\Phi'(x)$ determine \hat{x} . Conditions (3.19) hold for all normal curves, and none of dashed curves.

Let us first assume that one temperature (say β_{31}) takes arbitrary positive values, while another one (β_{32}) is fixed. Adaptation is necessary here, since $\theta = \beta_{31}/\beta_{32}$ is an arbitrary positive number, hence (3.20) cannot be valid for x -independent E_i . Applying the above method, we deduce that (3.17, 3.20) for adaptation can be satisfied for the experimentally motivated choice (3.13) for $E_i(x)$; see Fig. 3.2.

Since the validity domain (3.20) of the heat-engine shrinks to a point for $\theta \rightarrow 1$, we need progressively smaller values of $D\gamma$ in (3.16) for ensuring the average work-extraction (3.21) under $\theta \rightarrow 1$. If the diffusion of x is caused by an equilibrium bath, we get $D\gamma = T$ in (3.12) [143], and the temperature T of this bath should be sufficiently low for (3.21) to hold. If this is the lowest temperature, there is a heat current J_A towards it tending to increase it; see section 3.14. Hence this low temperature is a resource; see [135–140] for related results. In

the slow limit, $J_A = \mathcal{O}(\frac{1}{\gamma})$ can be much smaller than the energy currents J_{ij} of the heat-engine. Eqs. (3.6, 3.9 3.10) imply that $J_{ij} \rightarrow 0$ for high efficiencies $\eta \rightarrow \eta_C$. In that case J_A stays finite and is the dominant energy current.

3.6 Full adaptation

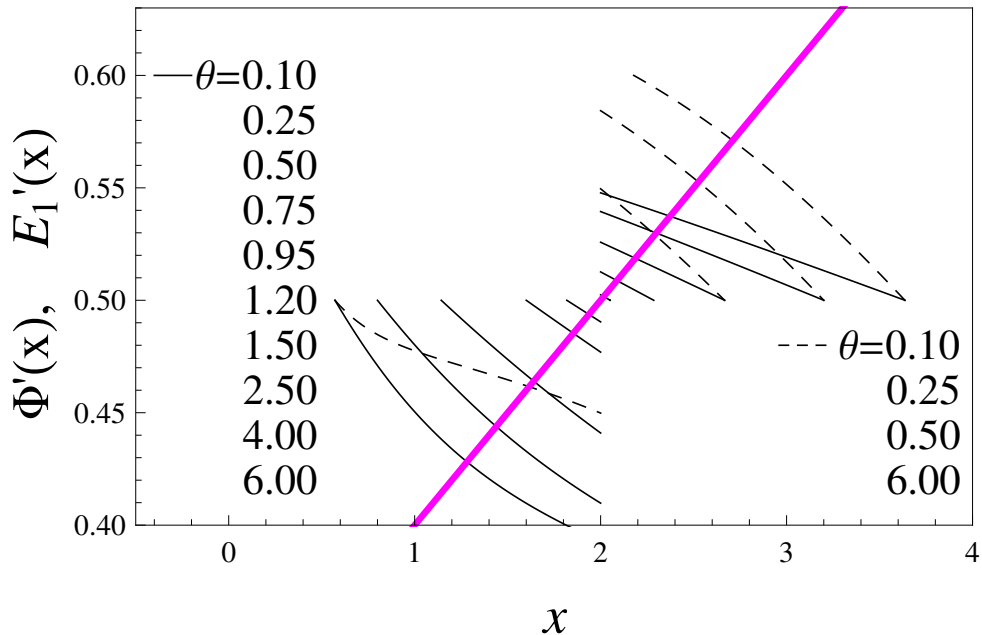


Figure 3.3: Full adaptation scenario ($\gamma < 0$). $\Phi'(x)$ with $f_{ij}[y] = e^{\beta_{ij}y/2}$ for varying β_{31} and fixed β_{32} ; cf. Fig. 3.2. We assume $\hat{E}_3(x) = x/2$, $\hat{E}_2(x) = x - 2$, and (3.20) holds for $x \in (\frac{4}{1+\theta}, 2)$. Normal (resp. dashed) curves: $\Phi'(x)$ for x that support (3.20) under $\beta_{32} = 1$ (resp. $\beta_{32} = 3$) and various $\theta = \beta_{31}/\beta_{32}$, as indicated from the top to the bottom in the left (resp. right). The magenta (bold) curve shows $-E_1'(x)$, where for the considered range of x , $E_1'(x) = -0.1(x - 2) - 0.5$. Adaptation conditions (3.23) hold for all curves, and for all β_{31} , β_{32} .

Let now *both* β_{31} and β_{32} vary. Fig. 3.2 shows that the set-up which worked for a fixed β_{32} does not apply: adaptation conditions (3.19) break down in a vicinity of $\theta = 1$. Topologically, changing both β_{32} and β_{31} destroys fine-tuned equality in (3.19); see Fig. 3.2.

In section 3.13 we argue that adaptation conditions (3.19) cannot hold together, if both β_{31} and β_{32} vary, *and* if $\frac{d}{dy}f_{ij}[y] \geq 0$; see (3.22). The latter holds for all physical examples we are aware of, and means that the transition from one energy to another is facilitated, if the lower energy increases or the higher energy decreases.

The only way we found for recovering adaptation is to assume that x is subject to a

negative friction: $\gamma < 0$. Note that the $\gamma < 0$ and $D > 0$ situation is stable, since (3.15) does predict relaxation to (3.16).

One way to achieve $\gamma < 0$ is to subject x to a negative-temperature (population-inverted) thermal bath: $\beta < 0$. Eqs. (3.12) with $\gamma \propto \beta < 0$ is then an effective description of quasi-continuous, but discrete degrees of freedom; see section 3.8. Negative temperatures are known for various systems whose energies are bounded from above [165–170]. Now $\beta < 0$ is a resource, since when coupled to positive temperatures, β tends to increase [165, 166]. Physically, $\beta < 0$ means a reservoir of stored energy, and the fact that β decreases means that this energy is spent for adaptation.

Other examples of negative friction include negative resistance of electric circuits [171], negative viscosity of driven fluids [172], and the negative absolute mobility for Brownian systems [173–175].

Now $D\gamma < 0$ in (3.16), and the most probable \hat{x} means that inequalities in (3.19) are reversed. New adaptation conditions are (3.20) and [instead of (3.19)]

$$\Phi'(\hat{x}) = -E_1'(\hat{x}), \quad \Phi''(\hat{x}) < -E_1''(\hat{x}). \quad (3.23)$$

These conditions can be satisfied, as seen in Fig. 3.3. In contrast to the previous scenario, now $\Phi'(x)$ is very robust with respect to changing β_{31} and β_{32} , i.e. the adaptation is achieved for *all* β_{31} and β_{32} (excluding a $|\gamma D|$ -dependent vicinity of $\beta_{31} = \beta_{32}$). Though the choice of $E_1(x)$ is more flexible than for the previous restricted adaptation scenario, it cannot belong to the set (3.13) of harmonic functions. For $\gamma D < 0$, x should change in a bounded domain; otherwise for the natural shape of energies ($E_i(x) \rightarrow \infty$ for $x \rightarrow \pm\infty$) one gets a non-normalizable $p(x)$ in (3.16).

3.7 Functioning regimes of the machine (heat-engine, refrigerator, heat-pump)

Eq.(3.2) defines J_{ij} as the average energy lost (if $J_{ij} > 0$) or gained (if $J_{ij} < 0$) by the thermal bath at temperature $1/\beta_{ij}$. Here $(ij) = (21), (31), (32)$.

Thus J_{ij} are the energy currents. Recall that $\beta_{21} = 0$ is the source of work, and hence the corresponding bath is the source of work. The energy conservation in the stationary state implies: $J_{21} + J_{31} + J_{32} = 0$.

Now neglecting the possibility that some of J_{ij} could be zero we get the following 4 regimes:

$$J_{21} < 0, \tag{3.24}$$

$$J_{21} > 0, J_{32} < 0, J_{31} < 0, \tag{3.25}$$

$$J_{21} > 0, J_{32} < 0, J_{31} > 0, \tag{3.26}$$

$$J_{21} > 0, J_{32} > 0, J_{31} < 0. \tag{3.27}$$

Eq. (3.24) refers to the heat engine regime, where the energy goes to the work-source.

Within (3.25) the energy (work) coming from the source of work heats up both thermal baths. This regime did not get a special name, because it is rarely useful.

If $T_{32} > T_{31}$, (3.26) means refrigeration: thanks to the work consumption ($J_{21} > 0$), the lower-temperature bath loses energy. Eq. (3.27) implies pumping, where the hotter bath loses energy. Note that the heat-engine and refrigerator are devices that function against their natural thermal gradients. (The natural gradient for the infinite-temperature bath is to lose energy. Analogously, it is natural that the lowest temperature bath gains energy and not loses it.) The heat-pump regime is useful as far as the natural gradient is enhanced by the injection of work.

If $T_{32} < T_{31}$, then the heat-pumping and refrigeration regime interchange: now (3.27) refers to refrigeration, while (3.26) refers to heat-pumping.

3.8 Derivation of the Fokker-Planck equation and justification of the slow limit

3.8.1 Fokker-Planck equation

Eq.(3.14) was studied in the limit, where x is slow. Here we shall show that this limit emerges naturally from the dynamics of two discrete random variables, when one of them becomes quasi-continuous. In this context, we also study the applicability of the slow limit.

Consider the following master equation for two discrete degrees of freedom i and α :

$$\begin{aligned} \dot{p}_{i\alpha} &= \sum_{j=1}^3 [\rho_{i\leftarrow j|\alpha} p_{j\alpha} - \rho_{j\leftarrow i|\alpha} p_{i\alpha}] \\ &+ \sum_{\gamma=1}^N [\omega_{\alpha\leftarrow\gamma|i} p_{i\gamma} - \omega_{\gamma\leftarrow\alpha|i} p_{i\alpha}], \end{aligned} \quad (3.28)$$

$$i = 1, 2, 3, \quad \alpha = 1, \dots, N,$$

where $p_{i\alpha}$ is the joint probability of i and α , and $\rho_{i\leftarrow j|\alpha}$ and $\omega_{\alpha\leftarrow\gamma|i}$ are transition probabilities.

We shall make three assumptions. First is that transitions between α and γ are governed by a thermal bath at temperature $T = 1/\beta$. Hence the detailed balance holds:

$$\omega_{\alpha\leftarrow\gamma|i} e^{-\beta E_{i\gamma}} = \omega_{\gamma\leftarrow\alpha|i} e^{-\beta E_{i\alpha}}, \quad (3.29)$$

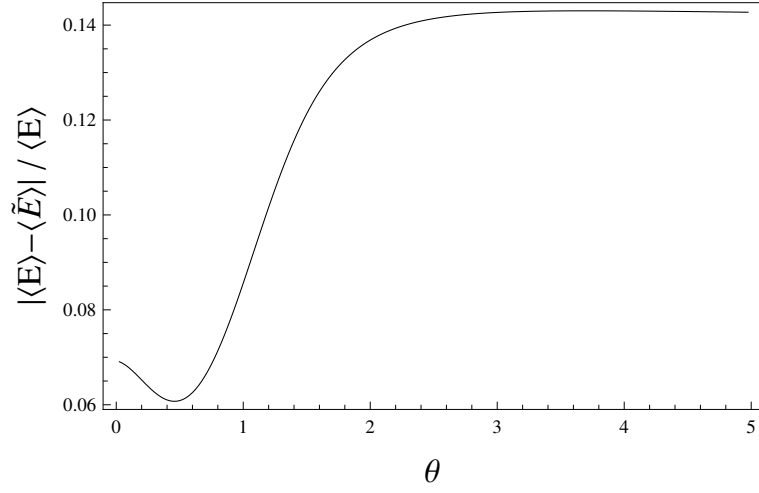
where $E_{i\gamma}$ is the energy of the state $(i\gamma)$. As a concrete example of the rates (3.29) we take:

$$\omega_{\gamma+1\gamma|i} = \frac{1}{\tau} e^{\frac{\beta}{2}(E_{i\gamma} - E_{i\gamma+1})}, \quad (3.30)$$

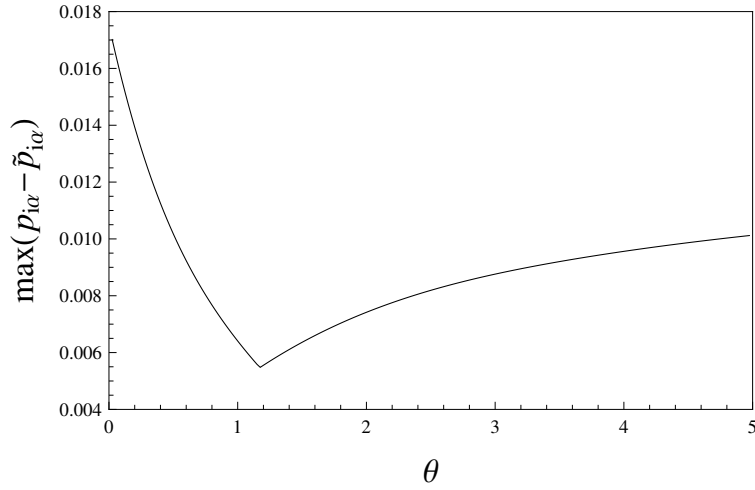
where τ is a constant characteristic time.

Second we shall assume that the states α make up a one-dimensional chain:

$$\begin{aligned} \omega_{\alpha\leftarrow\gamma} &= [1 - \delta_{\alpha 1}] \delta_{\alpha-1\gamma} \omega_{\alpha\leftarrow\alpha-1} \\ &+ [1 - \delta_{\alpha N}] \delta_{\alpha+1\gamma} \omega_{\alpha\leftarrow\alpha+1}, \quad \alpha = 1, \dots, N, \end{aligned} \quad (3.31)$$



(a)



(b)

Figure 3.4: (a) $\langle E \rangle = \sum_{i=1}^3 \sum_{\alpha=1}^N p_{i\alpha} E_{i\alpha}$ is the stationary average energy as a function of $\theta = \beta_{31}/\beta_{32}$ calculated from (3.28, 3.30, 3.31) for $\beta_{32} = 1$, $N = 100$, $\tau = 2$, $\beta = 0.5$ and $E_{i\alpha} = i\alpha^2$. $\langle \tilde{E} \rangle = \sum_{i=1}^3 \sum_{\alpha=1}^N \tilde{p}_{i\alpha} E_{i\alpha}$ is the stationary average energy calculated via the probabilities $\tilde{p}_{i\alpha}$ under the slow limit; see (3.43–3.45). Now (a) shows the relative difference $\frac{\langle E \rangle - \langle \tilde{E} \rangle}{\langle E \rangle}$ between $\langle E \rangle$ and $\langle \tilde{E} \rangle$. It is seen that the validity of the slow limit (as measured by the magnitude of $\frac{\langle E \rangle - \langle \tilde{E} \rangle}{\langle E \rangle}$) gets worst for $\theta \rightarrow 0$ and $\theta \rightarrow \infty$. This is natural because low temperatures of the heat-engine baths freeze some of its motions and tend to make it less fast, i.e. low temperatures act against the slow limit.

(b) $p_{i\alpha}$ are the stationary probabilities calculated from (3.28, 3.30, 3.31) for the same parameters as in (a), but $\tau = 1$, $\beta = 2$. $\tilde{p}_{i\alpha}$ are the slow-limit stationary probabilities calculated from (3.43, 3.44, 3.45). The figure shows $\max_{i\alpha} |p_{i\alpha} - \tilde{p}_{i\alpha}|$, which is another measure for the validity of the slow limit. We again see that the validity of the slow limit gets worst for $\theta \rightarrow 0$ and $\theta \rightarrow \infty$.

where $\delta_{\alpha\gamma} = 1$ if $\alpha = \gamma$, and $\delta_{\alpha\gamma} = 0$ if $\alpha \neq \gamma$.

Third, we shall assume that α is quasi-continuous, i.e. $N \gg 1$ and $E_{i\alpha+1} - E_{i\alpha}$ is small.

Hence we have

$$E_{i\gamma} \rightarrow E_i(x), \quad E_{i\gamma+1} \rightarrow E_i(x) + \epsilon E'_i(x), \quad (3.32)$$

where x is a continuous parameter, ϵ is a small parameter (step of the chain), and where $E'_i(x) \equiv \frac{d}{dx} E_i(x)$.

Let us recall how one obtains the Fokker-Planck equation in the continuous limit; see e.g. [148]. We expand (3.30) as

$$\tau\omega_{\gamma+1\gamma|i} = 1 + \frac{\beta}{2}(E_{i\gamma} - E_{i\gamma+1}) + \mathcal{O}(\epsilon^2), \quad (3.33)$$

and write the last term in (3.28) as

$$\sum_{\gamma} [\omega_{\alpha\gamma|i} p_{i\gamma} - \omega_{\gamma\alpha|i} p_{i\alpha}] \quad (3.34)$$

$$= \beta[\zeta_{i\alpha+1} - \zeta_{i\alpha}] + [\xi_{i\alpha+1} - \xi_{i\alpha}], \quad (3.35)$$

where we denoted

$$\zeta_{i\alpha+1} \equiv \frac{1}{\tau}(E_{i\alpha+1} - E_{i\alpha}) \frac{p_{i\alpha} + p_{i\alpha+1}}{2}, \quad (3.36)$$

$$\xi_{i\alpha+1} \equiv \frac{1}{\tau}(p_{i\alpha+1} - p_{i\alpha}). \quad (3.37)$$

Hence (3.35) can be written as

$$(3.35) = \beta \epsilon \zeta'_i(x) + \epsilon \xi'_i(x). \quad (3.38)$$

Eqs. (3.36, 3.37) imply

$$\zeta_i(x) = \frac{\epsilon}{\tau} p_i(x) E'_i(x), \quad \xi_i(x) = \frac{\epsilon}{\tau} p'_i(x). \quad (3.39)$$

Eqs. (3.28) and (3.34–3.39) lead to the Fokker-Planck equation:

$$\begin{aligned} \dot{p}_i(x) = & \sum_j [\rho_{i \leftarrow j}(x) p_j(x) - \rho_{j \leftarrow i}(x) p_i(x)] \\ & + \frac{\epsilon^2}{\tau} \partial_x [\beta p_i(x) E'_i(x) + p'_i(x)], \end{aligned} \quad (3.40)$$

where τ is the characteristic time that was introduced in (3.30), and where ϵ^2 emerged due to the continuous limit.

Eq. (3.40) coincides with Eq. (3.12), where we denote

$$D = \epsilon^2/\tau, \quad \gamma^{-1} = \epsilon^2\beta/\tau. \quad (3.41)$$

Note that the Fokker-Planck equation naturally comes out with the slow limit due to ϵ in (3.40).

3.8.2 Fokker-Planck equation for a negative temperature

Note from (3.41) that $D > 0$, since $\tau > 0$. The latter follows from the positivity of probability in (3.30). The sign of γ coincides with that of β . The degree of freedom α is discrete, hence it can have a negative temperature: $\beta < 0$ [165–167, 169, 170]. Note that if in (3.28) both i and α have the same negative temperature, then the stationary probability reads:

$$p_{i\alpha} = \frac{1}{Z} e^{-\beta E_{i\alpha}}, \quad Z = \sum_{i=1}^3 \sum_{\alpha=1}^N e^{-\beta E_{i\alpha}}. \quad (3.42)$$

It is consistent provided that N is finite (though possibly large).

3.8.3 Checking the slow limit

One way of studying the applicability of the slow limit is to start with a finite N in (3.28, 3.31), and then to compare numerically the stationary solution of (3.28) obtained under the slow limit in (3.28) with the exact stationary solution of (3.28). Implementing the slow limit

directly within (3.28, 3.31) we get for the stationary solution:

$$\tilde{p}_{i\alpha} = \tilde{p}_\alpha \tilde{p}_{i|\alpha}, \quad (3.43)$$

where the conditional probability $\tilde{p}_{i|\alpha}$ is found from

$$\sum_j [\rho_{i\leftarrow j|\alpha} \tilde{p}_{j|\alpha} - \rho_{j\leftarrow i|\alpha} \tilde{p}_{i|\alpha}] = 0, \quad (3.44)$$

and where the stationary probability of α reads

$$\tilde{p}_\alpha = \frac{1}{Z} \prod_{\gamma=1}^{\alpha-1} \frac{\Omega_{\gamma+1|\gamma}}{\Omega_\gamma \gamma+1}, \quad \Omega_{\alpha\gamma} \equiv \sum_i \omega_{\alpha\gamma|i} \tilde{p}_{i|\gamma}. \quad (3.45)$$

Here Z is found from $\sum_\alpha \tilde{p}_\alpha = 1$.

Figs. 3.4(a) and 3.4(b) compare the outcome of solving (3.28, 3.31) numerically with predictions of (3.43–3.45). For the numerics we adopted $\rho_{i\leftarrow j|\alpha} = e^{\frac{1}{2}\beta_{ij}[E_{j\alpha} - E_{i\alpha}]}$ in (3.28).

It is seen that the agreement of the numerical solution with the slow limit prediction is fair, even for moderately large values of N and for $\tau \leq 2$ (these values of τ means that no attempt is made to introduce the slow limit “by hands”, i.e. due to a large τ). The agreement does improve significantly for larger values of N and/or larger values of τ .

3.9 Feedforward does not provide advantages for adaptation

The feedback control studied in above amounts to an autonomous scheme, where the controller x does not interact directly with the thermal bath, but it achieves the heat-engine functioning due to the interaction with the probabilistic state $p_{i|x}$ of the heat-engine.

Within a feedforward control scheme, we try to have for x certain anticipatory features: it will couple to both thermal baths at temperatures $T_{31} = 1/\beta_{31}$ and $T_{32} = 1/\beta_{32}$, whose changing temperatures damage the heat-engine functioning. Thus a feedforward scheme tries to implement a temperature sensor via x ; see [176] for a general discussion on the differences

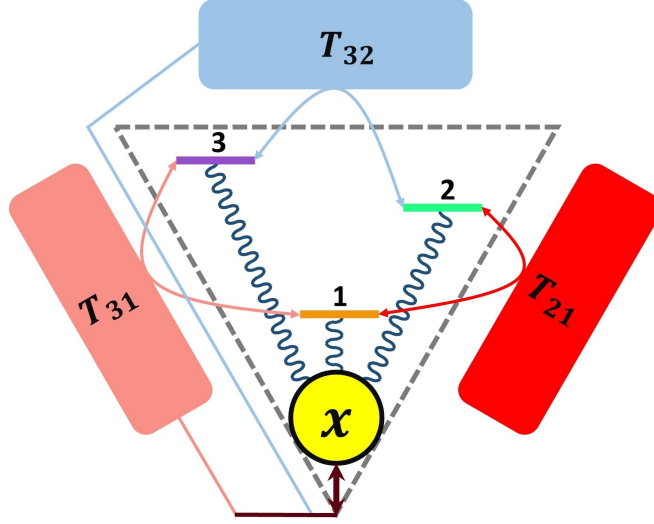


Figure 3.5: A schematic representation of the model with the feedforward control. There are three thermal baths at temperatures $T_{32} < T_{31} < T_{21} = \infty$; each one drives a transition among three engine states 1, 2, and 3. x is a controller that changes energies of states, and also does interact directly with the two baths;

between feedback and feedforward control.

Now x couples directly to the baths at temperatures $T_{31} = 1/\beta_{31}$ and $T_{32} = 1/\beta_{32}$ ². This amounts to adding in Eq. (3.12) the following terms

$$\sum_{\alpha=31,32} \gamma_{\alpha}^{-1} [\partial_x [p_i(x, t) E'_i(x)] + T_{\alpha} \partial^2 p_i(x, t)], \quad (3.46)$$

where γ_{α} is the friction constant due to the coupling with the bath α , and the detailed balance with respect to this coupling is naturally assumed.

Using (3.46), Eq. (3.12) becomes

$$\begin{aligned} \dot{p}_i(x, t) = & \sum_j [\rho_{i \leftarrow j}(x) p_j(x, t) - \rho_{j \leftarrow i}(x) p_i(x, t)] \\ & + \left(\frac{1}{\gamma} + \frac{1}{\gamma_{32}} + \frac{1}{\gamma_{31}} \right) \partial_x [p_i(x, t) E'_i(x)] \\ & + \left(D + \frac{T_{32}}{\gamma_{32}} + \frac{T_{31}}{\gamma_{31}} \right) \partial_x^2 p_i(x, t). \end{aligned} \quad (3.47)$$

Eq. (3.47) coincides with Eq.(3.14), after we take effective friction and diffusion. In particular,

²A naive possibility for a feedforward control would amount just to taking \hat{E}_2 and \hat{E}_3 as functions of the bath temperatures. For our purposes this is not legitimate, since we need a physical coupling of the controller x to thermal baths.

the stationary probability density $p(x)$ of x reads (within the adiabatic approximation)

$$p(x) \propto e^{-\Psi(x)/\sigma}, \quad \sigma = \frac{D + \sum_{\alpha=31,32} \gamma_{\alpha}^{-1} T_{\alpha}}{\gamma^{-1} + \sum_{\alpha=31,32} \gamma_{\alpha}^{-1}}, \quad (3.48)$$

where $\Psi(x)$ is still defined by Eq. (3.16). Hence the maximally probable value \hat{x} does not change.

We conclude that the feed-forward scheme does not provide real advantages for adaptation³. The origin of this result should be sought in the form (3.46) of the coupling between x and the baths. For a discrete x this coupling is more flexible (i.e. less constrained) and there may be more possibilities for a feed-forward adaptation [136]. However, x had to be continuous, if we want to ensure that the system adapts to continuously changing bath temperatures T_{31} and T_{32} .

3.10 Heat-engine adaptation: symmetric vs. Kramers rates

For simplicity we have concentrated on the symmetric transition rates

$$\rho_{i \leftarrow j}(x) = e^{\frac{1}{2}\beta_{ij}[E_j(x) - E_i(x)]}, \quad (3.49)$$

where β_{ij} is the inverse temperature of the bath that drives the transition (3.49). Figs. 3.2 and 3.3 demonstrate (resp.) the restricted and full adaptation situation by showing $\Phi'(\hat{x})$ and \hat{x} for (3.49).

The aim of this section is to show that basically the same results are valid for the Kramers rates [143]:

$$\rho_{i \leftarrow j}(x) = e^{\beta_{ij}\Delta(x) + \min[0, \beta_{ij}(E_j(x) - E_i(x))]}, \quad (3.50)$$

³A small advantage may be that σ in (3.48) can be smaller than γD , i.e. the direct coupling to the baths can under specific conditions make the density of x more narrow.

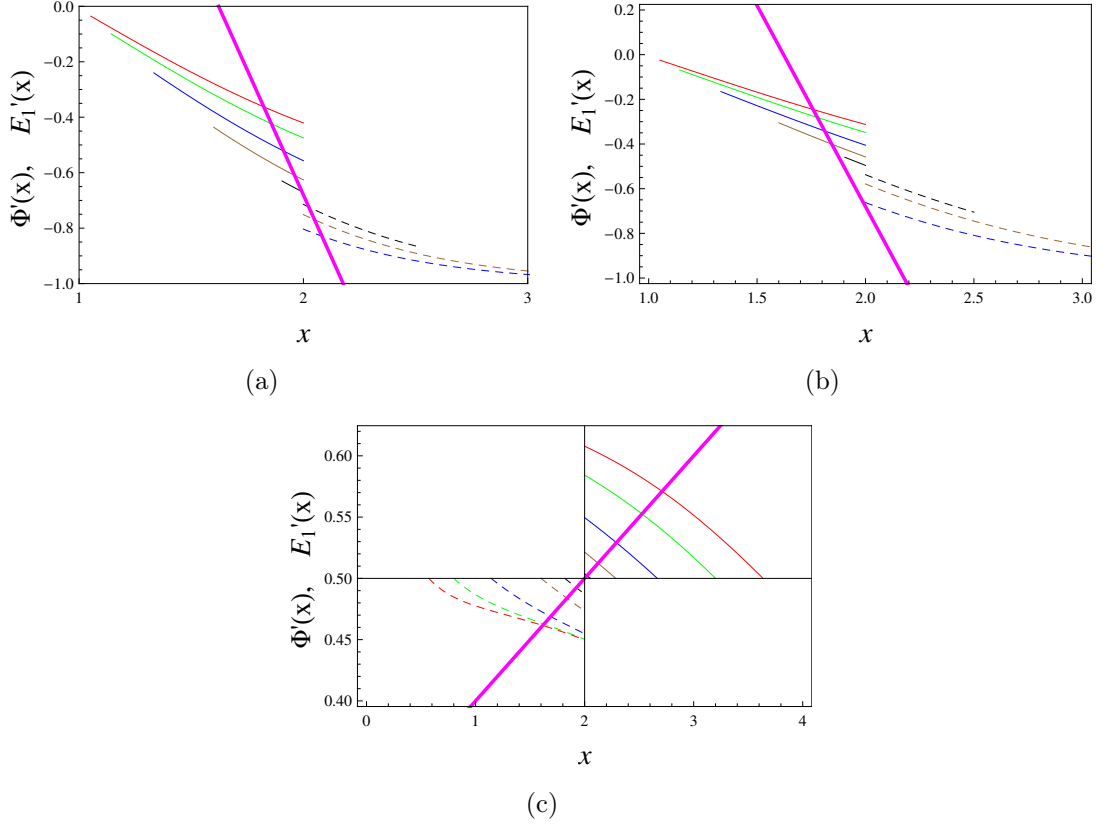


Figure 3.6: (a) $\Phi'(x)$ with $f_{ij}[y] = e^{\beta_{ij}y/2}$ for varying β_{31} and fixed $\beta_{32} = 1$ (restricted adaptation scenario). We assume $\hat{E}_3(x) = -x$, $\hat{E}_2(x) = x - 2$, and (3.20) holds for $x > 2$ if $\theta > 2$, for $\frac{2}{2-\theta} > x > 2$ if $1 < \theta < 2$, and for $\frac{2}{2-\theta} < x < 2$ if $\theta < 1$. $\Phi'(x)$ is shown for various $\theta = \beta_{31}/\beta_{32}$ and those x that support (3.20): $\theta = 0.1$ (red curve), $\theta = 0.25$ (green), $\theta = 0.5$ (blue), $\theta = 0.75$ (brown), $\theta = 0.95$ (black), $\theta = 1.2$ (black-dashed), $\theta = 1.5$ (brown-dashed), $\theta = 2.5$ (blue-dashed). The magenta curve shows $-E_1'(x)$, where $E_1'(x) = 1.8(x-2) + 0.680289$. Intersections of $-E_1'(x)$ with $\Phi'(x)$ determine \hat{x} .

(b) The same as in Fig. 3.6(a), but for $\beta_{32} = 0.7$. It is seen that for θ close to 1, no heat-engine functioning exists (i.e. (3.20) does not hold): the magenta curve does not cross the curves with $\theta = 0.95$, $\theta = 1.2$ and $\theta = 1.5$.

(c) Adaptation for a negative friction $\gamma < 0$, $\beta_{32} = 3$ and varying β_{13} . The same parameters as in Fig. 3.6(a), but now $\hat{E}_3(x) = x/2$. Conditions (3.20) amount to $\frac{4}{1+\theta} > x > 2$ if $\theta < 1$, and to $\frac{4}{1+\theta} < x < 2$ if $\theta > 1$. $\Phi'(x)$ is shown for: $\theta = 0.1$ (red curve), $\theta = 0.25$ (green), $\theta = 0.5$ (blue), $\theta = 0.75$ (brown), $\theta = 0.95$ (black), $\theta = 1.2$ (black-dashed), $\theta = 1.5$ (brown-dashed), $\theta = 2.5$ (blue-dashed), $\theta = 4$ (green-dashed), $\theta = 6$ (red-dashed). The magenta curve shows $-E_1'(x)$, where for the considered range of x , $E_1'(x)$ is approximated as $E_1'(x) = -0.1(x-2) - 0.5$.

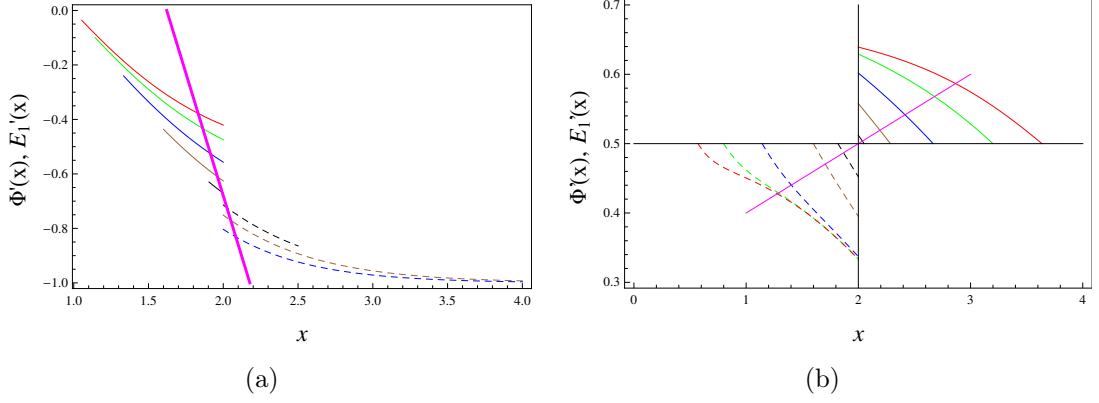


Figure 3.7: (a) and (b) are the analogues of (resp.) Fig. 3.6(a) and Fig. 3.6(c), but with the Kramers rates (3.50) under $\Delta = 1$.

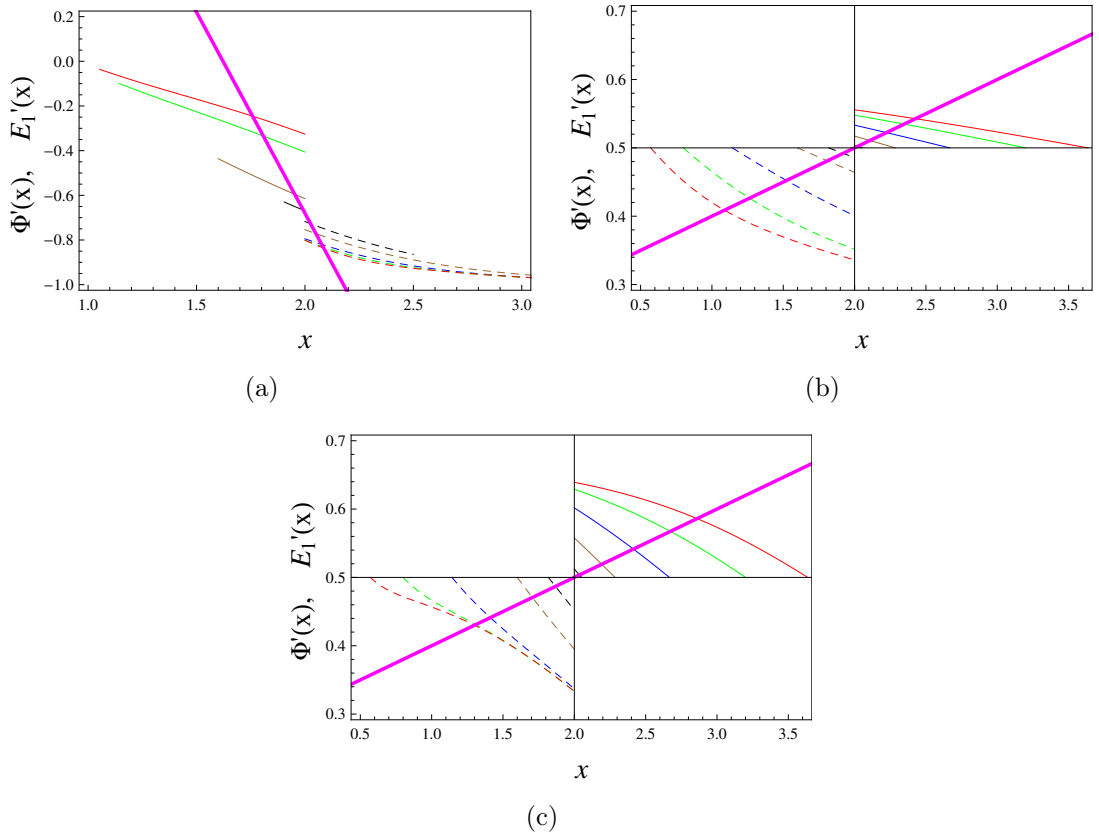


Figure 3.8: (a) and (b) are the analogues of (resp.) Fig. 3.6(a) and Fig. 3.6(c) [also, respectively, of Fig. 3.2 and Fig. 3.3], but with the rates given by (3.56) under $F_{ij} = 1$.

(c) is the analogue of (b), but with $\beta_{32} = 3$.

For (a): $\hat{E}_1(x) = 0.9(x - 2)^2 + 0.680289(x - 2)$, $\hat{E}_2(x) = x - 2$, $\hat{E}_3(x) = -x$.

For (b) and (c): $\hat{E}_1(x) = -0.05(x - 2)^2 - 0.5(x - 2)$ (in the considered range of x), $\hat{E}_2(x) = x - 2$, $\hat{E}_3(x) = x/2$.

where Δ is the energy barrier that separates the states i and j . Here we assumed for simplicity that the barrier Δ does not depend on i and j , and it does not depend on x .

Figs. 3.7(a) and 3.7(b) show that the adaptive functioning of the heat-engine with the Kramers rate (3.50) is very similar to that of the symmetric rates (3.49); cf. Figs. 3.2 and 3.3 with (resp.) Figs. 3.7(a) and 3.7(b).

3.11 Relations with the no-pumping theorem

The Kramers rate (3.50) can be re-written as

$$\rho_{i \leftarrow j}(x) = e^{\beta_{ij}(E_j(x) - F_{ij}(x))}, \quad F_{ij}(x) = F_{ji}(x), \quad (3.51)$$

$$F_{ij}(x) \equiv \max[E_i(x), E_j(x)] - \Delta_{ij}(x). \quad (3.52)$$

The authors of [163, 164] employed (3.51, 3.52) and proved the following no-pumping theorem (which we somewhat simplify for our purposes). Let us assume that the following three conditions hold:

(i) $x = x(t)$ in (3.51, 3.52) are time-dependent periodic function with a period τ : $x(t) = x(t + \tau)$.

(ii) F_{ij} in (3.52) is x -independent (hence time-independent).

(iii) All temperatures in (3.51) are equal, $\beta_{ij} = \beta$.

Then the time-averaged probability current generated by such an external field $x(t)$ nullify (no external pumping) [163, 164]:

$$\int_T^{T+\tau} ds I_{i \leftarrow j}(s) = 0, \quad (3.53)$$

$$I_{i \leftarrow j}(s) \equiv \rho_{i \leftarrow j}(s)p_j(s) - \rho_{j \leftarrow i}(s)p_i(s), \quad (3.54)$$

where T is sufficiently large for the system to forget about its initial state.

Now condition (ii) above does relate with conditions (3.21) that we assumed for the

adaptive heat engine. Indeed if these conditions are written for the Kramers rate we get:

$$\Delta_{ij}(E_j(x) - E_i(x)) = \Delta_{ji}(E_j(x) - E_i(x)). \quad (3.55)$$

Now this is not compatible with (3.52), where F_{ij} is x -independent.

Thus, whenever F_{ij} is x -independent the method presented above for studying adaptation does not apply, i.e. we do not know how to search systematically for $E_i(x)$ that achieves adaptation.

However, it can be checked directly that once the functions $E_i(x)$ that achieved adaptation were found via condition (3.20) are sufficient for adaptation if the rates are given as

$$\rho_{i \leftarrow j}(x) = e^{\beta_{ij}(E_j(x) - F_{ij})}, \quad F_{ij} = F_{ji}, \quad (3.56)$$

with barriers $F_{ij} = F_{ji}$ that do not depend on x . For instance the message of Figs. 3.2 and 3.3 is fully reproduced when using (3.56); see Figs. 3.8(a), 3.8(b) and 3.8(c).

Thus condition (3.20) is useful for searching for adaptation, but a violation of this condition does not mean that the adaptation is impossible.

3.12 Efficiency and power

The adaptation was employed merely for supporting the heat-engine functioning. There are two important characteristics of any heat-engine|*viz.* efficiency and power|and we now show how the adaptation with respect to the heat-engine functioning should be modified to account also for their optimization.

We recall features of efficiency and power starting (for simplicity) with the case without any controller x .

The following formulas hold for the energy current J_{ij} of the heat bath at temperature

$T_{ij} = 1/\beta_{ij}$ ($i, j = 1, 2, 3$):

$$J_{21} = \frac{\hat{E}_2}{\mathcal{Z}} \rho_{2\leftarrow 1} \rho_{1\leftarrow 3} \rho_{3\leftarrow 2} \left[1 - e^{(\beta_{32} - \beta_{31})\hat{E}_3 - \beta_{32}\hat{E}_2} \right], \quad (3.57)$$

$$J_{31} = -\frac{\hat{E}_3 J_{21}}{\hat{E}_2}, \quad J_{32} = \frac{(\hat{E}_3 - \hat{E}_2) J_{21}}{\hat{E}_2}, \quad (3.58)$$

$$\hat{E}_2 \equiv E_2 - E_1, \quad \hat{E}_3 \equiv E_3 - E_1, \quad (3.59)$$

Recall that $\beta_{21} = 0$, i.e. the bath at this temperature is the source of work. Thus the work-extraction power is $|J_{21}|$. Now the efficiency η of the heat-engine is defined as

$$\eta = -\frac{J_{21}}{J_{31}} = \frac{\hat{E}_2}{\hat{E}_3}, \quad \text{if } \beta_{31} < \beta_{32}, \quad (3.60)$$

$$= -\frac{J_{21}}{J_{32}} = \frac{\hat{E}_2}{\hat{E}_2 - \hat{E}_3}, \quad \text{if } \beta_{31} > \beta_{32}. \quad (3.61)$$

Indeed, if $\beta_{31} < \beta_{32}$, the energy lost (per time-unit) by the high-temperature thermal bath is J_{31} , hence definition (3.60) follows. Likewise, for $\beta_{31} > \beta_{32}$ we obtain (3.61).

It is seen that the efficiency η depends only on the energy differences \hat{E}_2 and \hat{E}_3 . This is a feature of the present class of heat-engines. The Carnot bound

$$\eta < \eta_C \equiv 1 - \min\left[\theta, \frac{1}{\theta}\right], \quad \theta \equiv \frac{\beta_{31}}{\beta_{32}}, \quad (3.62)$$

follows from (3.60, 3.61) when demanding $J_{21} < 0$ (i.e. the heat-engine functioning) and using (3.57).

Eqs. (3.60, 3.61, 3.62) show the notorious power-efficiency trade-off: when η tends to its maximal (Carnot) value, the work-extraction power $-J_{21}$ nullifies due to $(1 - \theta)\hat{E}_3 - \hat{E}_2 \rightarrow 0$ in (3.57).

Let us now study the work power $-J_{21}$ in more detail. To this end, we specify the transition rates $\rho_{i\leftarrow j}$, taking for simplicity

$$\rho_{i\leftarrow j} = e^{\frac{1}{2}\beta_{ij}[E_j - E_i]}, \quad (3.63)$$

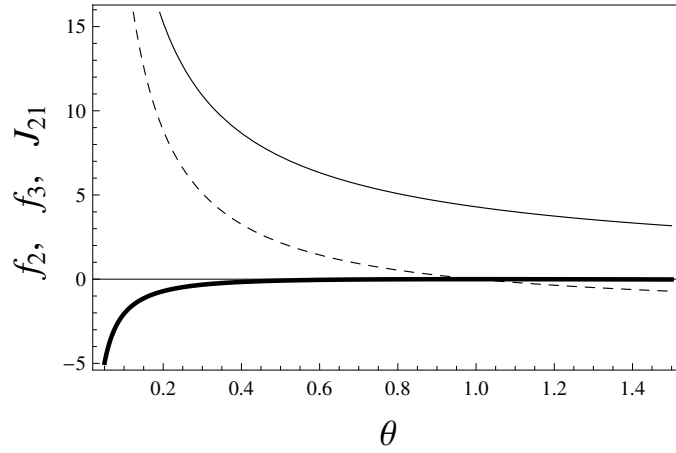


Figure 3.9: Functions $f_2(\theta)$ (dashed curve) and $f_3(\theta)$ (full curve) that determine the values of \hat{E}_2 and \hat{E}_3 which minimize J_{21} (i.e. maximize the power of the heat-engine); see (3.66). The minimized $J_{21}(\theta)$ for $\beta_{32} = 1$ (thick curve).

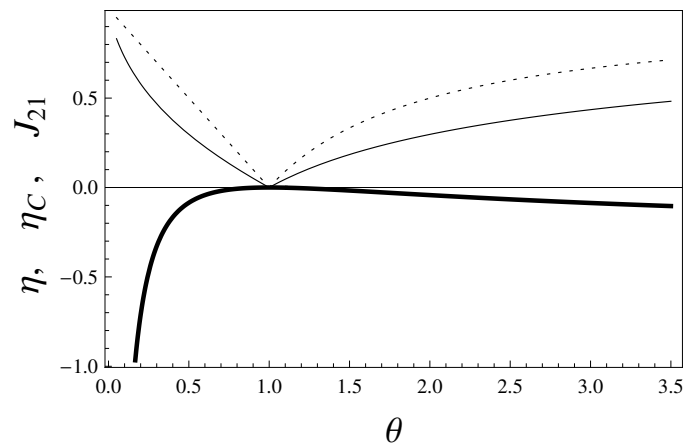


Figure 3.10: The efficiency $\eta(\theta)$ at the maximal power (full curve), the Carnot efficiency $\eta_C = 1 - \min(\theta, \frac{1}{\theta})$, and the minimized $J_{21}(\theta)$ at $\beta_{32} = 1$ (thick curve); see (3.62) and (3.60, 3.61).

which were already employed above; cf. also Figs. 3.2 and 3.3. We get from (3.57, 3.63)

$$J_{21} = \frac{1}{\hat{z}} \hat{E}_2 e^{\beta_{32}[(1-\theta)\hat{E}_3 - \hat{E}_2]}, \quad (3.64)$$

$$\begin{aligned} \hat{z} \equiv & 1 + e^{\beta_{32}[(1-\theta)\hat{E}_3 - \hat{E}_2]} (1 + 2e^{\frac{\beta_{31}}{2}\hat{E}_3}) \\ & + e^{-\beta_{31}\hat{E}_3} + e^{-\frac{\beta_{31}}{2}\hat{E}_3} + e^{\frac{\beta_{32}}{2}[\hat{E}_3 - \hat{E}_2]} (2 + e^{-\beta_{31}\hat{E}_3}). \end{aligned} \quad (3.65)$$

It is seen from (3.64, 3.65) that the minimum (i.e. the optimum with the respect to the heat-engine function) of the J_{21} is achieved for

$$\hat{E}_2 = T_{32}f_2(\theta), \quad \hat{E}_3 = T_{32}f_3(\theta), \quad (3.66)$$

where $T_{32} = 1/\beta_{32}$ and f_2 and f_3 are one-variable functions deduced from (3.64, 3.65).

Fig. 3.9 shows the shape of $f_2(\theta)$ and $f_3(\theta)$. Fig. 3.10 studies the efficiency at the maximum power that is obtained from (3.60, 3.64, 3.65). This figure also compares the Carnot (maximal) efficiency with the efficiency at the maximal power. Both Fig. 3.9 and Fig. 3.10 display the optimized J_{21} , which is seen to be a symmetric function of $\theta - 1$ only for $\theta \approx 1$.

3.12.1 Adaptation of efficiency

Let us now include the controller x . $E_i(x)$ contain interaction energies that depend both on x and on i . Hence also $\rho_{i \leftarrow j}(x)$ and $J_{21}(x)$ depend on x . Let us first focus on the case, where γD is so small that we can restrict ourselves with $x \approx \hat{x}$, where \hat{x} is the maximally probable value of x ; see (3.19).

Now to the heat-engine functioning conditions

$$\hat{E}_2(\hat{x})[(1-\theta)\hat{E}_3(\hat{x}) - \hat{E}_2(\hat{x})] > 0, \quad (3.67)$$

we add conditions of the efficiency maximization that read from (3.60, 3.61, 3.67):

$$(1-\theta)\hat{E}_3(\hat{x}) - \hat{E}_2(\hat{x}) \approx 0. \quad (3.68)$$

Fig. 3.11 shows an example for the efficiency adaptation. This is the same example as in Fig. 3.2, but $E_1(x)$ is chosen so that both (3.68) and (3.67) hold. Note that it is impossible to take $(1 - \theta)\hat{E}_3(\hat{x}) - \hat{E}_2(\hat{x}) = 0$ [cf. (3.68)], even though this provides the global maximum ($\eta = \eta_C$) for the efficiency η . Indeed, this will lead to $J_{21} = 0$ [see (3.57)], hence the engine is useless. Yet another (not less important) reasons for the above impossibility is that we consider a small γD , where the whole distribution of x reduces to its maximally probable value \hat{x} . But since γD is necessarily non-zero, the density $p(x)$ of x does have certain width, and taking (3.68) too close to zero will mean that for certain values of x we loose the very heat-engine function.

3.12.2 Adaptation of power

We turn to the situation, where the adaptation not only supports the heat-engine functioning, but also maximizes the power $-J_{21}$. First of all, (3.66) show that the *full* minimization of J_{21} amounts to two independent conditions, and they cannot generically be satisfied via one controller variable x . Second, conditions (3.66) that minimize J_{21} strongly depend on the concrete form of transition rates

Hence we should look for adaptation scenarios that optimize the power partially and (simultaneously) sufficiently independent on the form of $\rho_{i \leftarrow j}$.

Thus to simplify the situation, we shall look at J_{21} in the high-temperature regime, where both β_{32} and β_{31} are sufficiently small. Recalling that $\beta_{21} = 0$, we see that this regime relates to the linear non-equilibrium thermodynamics (all inverse temperatures are small). Eq. (3.57) implies for this regime:

$$J_{21}(\hat{x}) = -\rho \beta_{32} \hat{E}_2(x) [(1 - \theta)\hat{E}_3(x) - \hat{E}_2(x)], \quad (3.69)$$

where $\rho > 0$ is constant that is found from the infinite-temperature limit of $\rho_{i \leftarrow j}$.

It is seen that the minimization of (3.69) over $\hat{E}_2(x)$ is achieved for

$$\hat{E}_2(x) = \frac{1}{2}(1 - \theta)\hat{E}_3(x), \quad (3.70)$$

where J_{21} reads

$$J_{21}(\hat{x}) = -\frac{\rho}{4} \beta_{32} (1 - \theta)^2 \hat{E}_3^2(\hat{x}), \quad (3.71)$$

where we already took $x = \hat{x}$. Within the high-temperature regime we cannot minimize (3.71) also over \hat{E}_3 , because this will take us out of this regime. Hence the regime naturally leads to a partial power optimization.

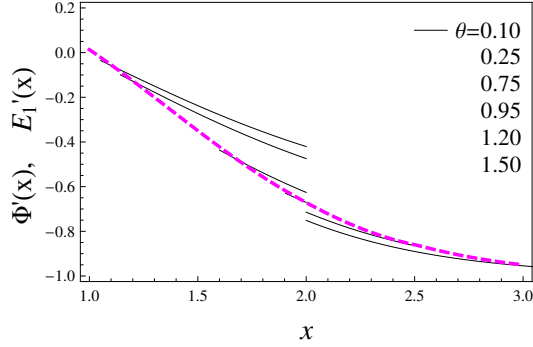


Figure 3.11: Efficiency adaptation.

$\Phi'(x)$ under rates (3.63) for varying β_{31} and fixed $\beta_{32} = 1$ (restricted adaptation scenario). We assume $\hat{E}_3(x) = -x$, $\hat{E}_2(x) = x - 2$, and (3.67) holds for $x > 2$ if $\theta > 2$, for $\frac{2}{2-\theta} > x > 2$ if $1 < \theta < 2$, and for $\frac{2}{2-\theta} < x < 2$ if $\theta < 1$. $\Phi'(x)$ is shown for various $\theta = \beta_{31}/\beta_{32}$, as indicated on the right from top to bottom.

The magenta (dashed) curve shows $-E_1'(x)$; it is chosen so that both (3.67) and (3.68) hold. Intersections of $-E_1'(x)$ with $\Phi'(x)$ determine \hat{x} . The magenta curve passes on the edges of $\Phi'(x)$, i.e it passes through $\approx \frac{2}{2-\theta}$ that for the present choice of \hat{E}_2 and \hat{E}_3 fulfils (3.68).

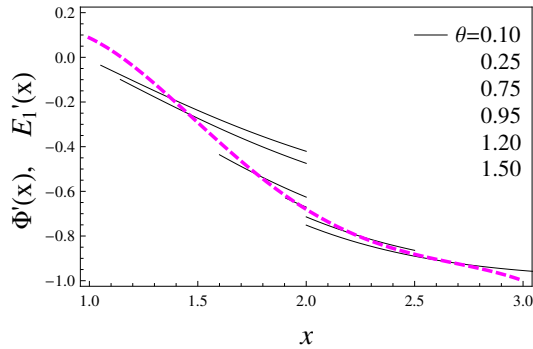


Figure 3.12: Power adaptation.

The same as for Fig. 3.11, but the magenta (dashed) curve $-E_1'(x)$ is chosen so that both (3.67) and (3.70) hold, i.e. the magenta curve passes through $\frac{4}{3-\theta}$ that for the present choice of $\hat{E}_2(x) = x - 2$ and $\hat{E}_3(x) = -x$ fulfils (3.70).

Note that the adopted value $\beta_{32} = 1$ is sufficiently small for the high-temperature result (3.69) to apply.

Thus the adaptation with a partial optimization of power will be defined via (3.67) and

(3.70). Fig. 3.12 shows the same example as in Fig. 3.11, but now the energy $E_1(x)$ is chosen so as to achieve this partial optimization.

3.13 No-go statement for adaptation

Let us recall from Eq. (3.16–3.19) the adaptation conditions:

$$\hat{E}_2(\hat{x})[(1 - \theta)\hat{E}_3(\hat{x}) - \hat{E}_2(\hat{x})] > 0, \quad (3.72)$$

$$\hat{E}_i(x) \equiv E_i(x) - E_1(x), \quad (3.73)$$

$$\Phi'(\hat{x}) = -E_1'(\hat{x}), \quad (3.74)$$

$$\Phi''(\hat{x}) > -E_1''(\hat{x}), \quad (3.75)$$

where

$$\Phi'(x) \equiv \sum_{i=2}^3 p_{i|x} \hat{E}_i'(x). \quad (3.76)$$

Recall that $p_{i|x}$ in (3.76) is defined via Eq. (3.4) that we write in an expanded form:

$$p_{1|x} = \frac{1}{\mathcal{Z}} [\rho_{1\leftarrow 2} \rho_{1\leftarrow 3} + \rho_{3\leftarrow 2} \rho_{1\leftarrow 3} + \rho_{2\leftarrow 3} \rho_{1\leftarrow 2}], \quad (3.77)$$

$$p_{2|x} = \frac{1}{\mathcal{Z}} [\rho_{2\leftarrow 1} \rho_{2\leftarrow 3} + \rho_{3\leftarrow 1} \rho_{2\leftarrow 3} + \rho_{2\leftarrow 1} \rho_{1\leftarrow 3}], \quad (3.78)$$

$$p_{3|x} = \frac{1}{\mathcal{Z}} [\rho_{3\leftarrow 1} \rho_{3\leftarrow 2} + \rho_{2\leftarrow 1} \rho_{3\leftarrow 2} + \rho_{1\leftarrow 2} \rho_{3\leftarrow 1}], \quad (3.79)$$

where \mathcal{Z} ensures $p_{1|x} + p_{2|x} + p_{3|x} = 1$, and where $\rho_{i\leftarrow j} = \rho_{i\leftarrow j}(x)$.

Our aim is to show that (3.72, 3.74, 3.75) and (3.76) are not compatible if both β_{31} and β_{32} vary. To this end, we shall determine the form of $\Phi'(x)$ for $\theta \equiv \beta_{31}/\beta_{32} \simeq 1$. For $\theta \rightarrow 1$, we have $\hat{x} \rightarrow x_0$, where

$$\hat{E}_2(x_0) = 0. \quad (3.80)$$

Eq. (3.80) follows from the fact that (3.72) should hold both for $\theta < 1$ and also $\theta > 1$. For simplicity we assume that $\hat{E}_3(x_0) \neq 0$; otherwise, the arguments below generalize straightforwardly.

Now we assume that $\hat{x} \sim x_0$ due to $\theta \sim 1$. We get for $\Phi'(x)$ in the first order of $\hat{x} - x_0$:

$$\Phi'(\hat{x}) = \Phi''(x_0)(\hat{x} - x_0) + \Phi'(x_0). \quad (3.81)$$

Here $\Phi''(x_0)$ and $\Phi'(x_0)$ are functions of β_{31} and β_{32} . We should work them out for $\beta_{31} \sim \beta_0$ and $\beta_{32} \sim \beta_0$, where β_0 is some reference value between β_{31} and β_{32} , e.g. $\beta_0 = (\beta_{31} + \beta_{32})/2$. Neglecting quantities that are higher than linear over $\hat{x} - x_0$, $\beta_0 - \beta_{31}$ and $\beta_0 - \beta_{32}$, we get from (3.81)

$$\begin{aligned} \Phi'(\hat{x}) &= \Phi''(x_0) |_{\beta_{31}=\beta_{32}=\beta_0} (\hat{x} - x_0) \\ &\quad + \Phi'(x_0) |_{\beta_{31}=\beta_{32}=\beta_0} + b, \end{aligned} \quad (3.82)$$

$$b \equiv \sum_{\alpha=31,32} (\beta_\alpha - \beta_0) \partial_{\beta_\alpha} \Phi'(x_0) |_{\beta_{31}=\beta_{32}=\beta_0}. \quad (3.83)$$

Taking $\hat{x} \rightarrow x_0$ in (3.74) we get

$$\Phi'(x_0) |_{\beta_{31}=\beta_{32}=\beta_0} = -E'_1(x_0). \quad (3.84)$$

Once $E'_1(x)$ does not depend on β_{31} and β_{32} , $\Phi'(x_0) |_{\beta_{31}=\beta_{32}=\beta}$ should not depend on β_0 ; see (3.84).

Let us work out implications of this fact. Eqs. (3.77–3.79) show that under $\beta_{31} = \beta_{32} = \beta_0$ and (3.80), we get equilibrium probabilities

$$p_{1|x_0} |_{\beta_{31}=\beta_{32}=\beta_0} = p_{2|x_0} |_{\beta_{31}=\beta_{32}=\beta_0} = \frac{1}{Z}, \quad (3.85)$$

$$p_{3|x_0} |_{\beta_{31}=\beta_{32}=\beta_0} = \frac{e^{-\beta_0 \hat{E}_3(x_0)}}{Z}. \quad (3.86)$$

Hence we obtain

$$\Phi'(x_0) |_{\beta_{32}=\beta_{31}=\beta_0} = \frac{\hat{E}'_2(x_0) + \hat{E}'_3(x_0)e^{-\beta_0\hat{E}_3(x_0)}}{2 + e^{-\beta_0\hat{E}_3(x_0)}}. \quad (3.87)$$

This expression is not a function of β_0 only for

$$\hat{E}'_2(x_0) = 2\hat{E}'_3(x_0), \quad (3.88)$$

where

$$\Phi'(x_0) |_{\beta_{31}=\beta_{32}=\beta_0} = \hat{E}'_3(x_0). \quad (3.89)$$

Now using (3.88, 3.76) and the fact that $\hat{E}_2(x)$ and $\hat{E}_3(x)$ do not depend on β_{31} and β_{32} , we get from (3.83)

$$b = \hat{E}'_3(x_0) \sum_{\alpha=31,32} (\beta_\alpha - \beta) \partial_{\beta_\alpha} [p_{2|x_0} - p_{1|x_0}]. \quad (3.90)$$

To work out (3.90) via (3.77–3.79), we recall that we assumed for the transition rates $\rho_{i \leftarrow j}(x)$ [see Eq. (3.22)]:

$$\rho_{i \leftarrow j}(x) = f_{ij}[E_j(x) - E_i(x)], \quad (3.91)$$

where $f_{ij}[y]$ holds the detailed balance conditions [see Eq. (3.2)]:

$$f_{ij}(y) = f_{ji}(-y)e^{\beta_{ij}y}. \quad (3.92)$$

Combining (3.90) with (3.91) and with (3.77–3.79), we get

$$p_{2|x_0} - p_{1|x_0} = \frac{1}{Z(x_0)} [f_{32}(\hat{E}_3(x_0))f_{31}(-\hat{E}_3(x_0)) - f_{31}(\hat{E}_3(x_0))f_{32}(-\hat{E}_3(x_0))], \quad (3.93)$$

$$b = \frac{\hat{E}_3(x_0)\hat{E}'_3(x_0)}{Z(x_0)} \sum_{\alpha=31,32} \frac{\beta_0 - \beta_\alpha}{\beta_0} \psi_\alpha[\hat{E}_3(x_0)], \quad (3.94)$$

where we denoted

$$f'_{ij}[y] \equiv \frac{d}{dy} f_{ij}[y], \quad (3.95)$$

$$\psi_{31}[x] \equiv f'_{31}[x]f_{32}[-x] + f'_{31}[-x]f_{32}[x], \quad (3.96)$$

$$\psi_{32}[x] \equiv -f'_{32}[-x]f_{31}[x] - f'_{32}[x]f_{31}[-x]. \quad (3.97)$$

Now let us assume the following inequality

$$f'_{ij}[y] \geq 0. \quad (3.98)$$

This inequality is clearly not implied by the detailed balance condition (3.92). It means that the transition from a lower energy to a higher energy is facilitated, if the lower energy increases or the higher energy decreases. This inequality holds for all physical examples we are aware of. It thus should be regarded as an additional and physically well-motivated condition that we impose on the present set-up.

Eqs. (3.95–3.98) imply

$$\psi_{31}[\hat{E}_3(x_0)] \geq 0, \quad \psi_{32}[\hat{E}_3(x_0)] \leq 0. \quad (3.99)$$

Recalling that β_0 is in between of β_{31} and β_{32} we see from (3.94, 3.99)

$$\text{sign}[b] = \text{sign}[\hat{E}_3(x_0)\hat{E}'_3(x_0)(1 - \theta)] \quad (3.100)$$

Let us now return to (3.72) and work it out in the considered first-order over $\hat{x} - x_0$ and

$1 - \theta$:

$$\hat{E}'_2(x_0)(\hat{x} - x_0)[(1 - \theta)\hat{E}_3(x_0) - \hat{E}'_2(x_0)(\hat{x} - x_0)] \geq 0. \quad (3.101)$$

Next, we put (3.82) into (3.74), expand in the latter $E'_1(\hat{x})$ for $\hat{x} \sim x_0$, and employ (3.84):

$$[\Phi''(x_0)|_{\beta_{31}=\beta_{32}=\beta_0} + E''_1(x_0)](\hat{x} - x_0) + b = 0. \quad (3.102)$$

On the other hand, (3.75) leads to

$$\Phi''(x_0)|_{\beta_{31}=\beta_{32}=\beta_0} + E''_1(x_0) > 0. \quad (3.103)$$

Hence (3.102, 3.103) mean that $\text{sign}[b(\hat{x} - x_0)] < 0$, which implies from (3.100)

$$\text{sign}[\hat{E}_3(x_0)(1 - \theta)\hat{E}'_2(x_0)(\hat{x} - x_0)] < 0. \quad (3.104)$$

Eq. (3.101) and (3.104) contradict each other, hence no adaptation is possible.

3.14 Slow current

Eq. (3.12) shows that the dynamics of the controller x amounts to drift and diffusion. Let us assume that they originate from an equilibrium thermal bath at temperature $T = 1/\beta$. Then the fluctuation-dissipation relation implies $T = \gamma D$, where $\gamma > 0$ is the damping constant, and $D > 0$ is the diffusion constant. Starting from Eq. (3.12), we define the energy lost/gain by the thermal bath at temperature T :

$$J_A = \frac{1}{\gamma} \sum_{j=1}^3 \int dx E_j(x) \partial_x [p_j(x, t) E'_j(x) + T p'_j(x, t)], \quad (3.105)$$

where we recall that $E'_i(x) \equiv \frac{dE_i(x)}{dx}$. Indeed, (3.105) is that part of the overall energy change $\sum_{j=1}^3 \int dx E_j(x) \dot{p}_j(x)$ that is driven by the bath at the temperature T .

In the stationary state we integrate (3.105) by parts, and get

$$J_A = -\frac{1}{\gamma} \sum_{j=1}^3 \int dx E'_j(x) [p_j(x) E'_j(x) + T p'_j(x)], \quad (3.106)$$

where the stationary probability is

$$p_i(x) = p_{i|x} p(x), \quad p(x) \propto e^{-\beta \Psi(x)}, \quad (3.107)$$

$$\Psi(x) = \sum_i p_{i|x} E'_i(x), \quad (3.108)$$

where $p_{i|x}$ is defined via (3.77–3.79).

For very small temperatures we deduce $J_A < 0$ from (3.106), i.e. the thermal bath at temperature T gains energy. Note that $J_A = \mathcal{O}(\frac{1}{\gamma})$, i.e. it is small in the slow limit. However, for $\beta_{32} \approx \beta_{31}$ also all other energy currents are small, hence J_A can become the dominant energy current in the system. Our numerical results show that for $\beta_{32} \approx \beta_{31} < \beta$, we get $J_A < 0$.

3.15 External force that generates negative friction

Recall Eqs. (3.12, 3.15). We generalize them so that Eq. (3.15) reads

$$\begin{aligned} \dot{p}(x, t) = & \frac{1}{\gamma} \partial_x [p(x, t) \Psi'(x)] + \frac{T}{\gamma} \partial_x^2 p(x, t) \\ & + \partial_x [p(x, t) G'(x)], \end{aligned} \quad (3.109)$$

where we assume that x couples with a thermal bath at temperature T ,

$$\gamma > 0, \quad (3.110)$$

is the friction constant, and $G'(x) = \frac{d}{dx} G(x)$ is an external force. If now we set

$$G(x) = -\frac{2}{\gamma} \Psi(x), \quad (3.111)$$

the resulting joint influence of $G(x)$ and $\Psi(x)$ is equivalent to a negative friction.

The average energy Π dissipated per unit of time due to the external force $G'(x)$ can be estimated via the change of the free energy

$$F = \int dx p(x, t) [\Psi(x) + T \ln p(x, t)], \quad (3.112)$$

of x due to the external part (3.109) of the dynamics

$$\Pi = \int dx \partial_x [p(x, t) G'(x)] [\Psi(x) + T \ln p(x, t)]. \quad (3.113)$$

In the stationary state:

$$\Pi = - \int dx p(x) G'(x) [\Psi'(x) + T \frac{d}{dx} \ln p(x)] \quad (3.114)$$

$$= \gamma \int dx p(x) [G'(x)]^2, \quad (3.115)$$

where $p(x) \propto \exp[-(\Psi(x) + \gamma G(x))/T]$. Using (3.111) we finally obtain:

$$\Pi = \frac{1}{\gamma} \int dx p(x) [\Psi'(x)]^2. \quad (3.116)$$

3.16 Non-equilibrium features and fragility

Above we saw that the heat-engine functioning is fragile in the sense that changing even one bath temperature puts the machine out of the heat-engine functioning. But not all non-equilibrium features are fragile in this sense, as we shall now show.

Recall the Markov equation (3.1) and consider the probability current

$$I_{i \leftarrow j} = \rho_{i \leftarrow j} p_j - \rho_{j \leftarrow i} p_i \quad (3.117)$$

from state j to i ; cf. the definition of $I_{3 \leftarrow 1}$ with the definition of the energy current $J_{i > j}$ given

by Eq. (3.3). In the stationary regime $I_{i \leftarrow j}$ is read-off from (3.4–3.8):

$$I_{1 \leftarrow 2} = I_{3 \leftarrow 1} = I_{2 \leftarrow 3} = \frac{\rho_{3 \leftarrow 1} \rho_{2 \leftarrow 3} \rho_{1 \leftarrow 2}}{\mathcal{Z}} \times (1 - e^{(\beta_{32} + \beta_{31})[E_3 - E_1] - \beta_{32}[E_2 - E_1]}), \quad (3.118)$$

where we took into account $\rho_{1 \leftarrow 2} = \rho_{2 \leftarrow 1}$ due to $\beta_{21} = 0$, and where \mathcal{Z} is the normalization factor defined via Eq. (3.4).

Now consider a *cyclic* transformation of the probability, e.g. between states $1 \leftarrow 2 \leftarrow 3 \leftarrow 1$. Cycles are related to quasi-deterministic motion; they are the building blocks of metabolic processes [112].

The cycle $1 \leftarrow 2 \leftarrow 3 \leftarrow 1$ is determined by positivity of three probability currents $I_{1 \leftarrow 2}$, $I_{3 \leftarrow 1}$ and $I_{2 \leftarrow 3}$. As shown by (3.118), the cycle can hold for all β_{32} and β_{31} by taking $E_3 = E_1$ and $E_2 > E_1$.

Thus the cyclic motion as such is not a fragile feature. Note that even we can still design adaptation schemes that tend to put the value of the above probability current within certain limits. But it is important to stress that the cyclic motion as such does not need adaptation, since it is not fragile.

3.17 Coupling between heat-engine and controller has to be informative in the Bayesian sense

The effect of heat-engine adaptation obtained above was related to assuming that E_i are correlated random variables with the density

$$P(E_1, E_2, E_3) = \int dx p(x) \prod_{k=1}^3 \delta(E_k - E_k(x)), \quad (3.119)$$

and with specific forms of $E_i(x)$. Here $p(x)$ is the probability density of x .

To see why such assumptions are necessary, take an extreme case, where the probability density of energies $\Pi(E_1, E_2, E_3)$ is *non-informative* in terms of the Bayesian statistics [5, 120].

Since we do not have prior expectations about correlations between random variables E_1 , E_2 and E_3 , they are taken as independent [5]

$$\Pi(E_1, E_2, E_3) = \prod_{k=1}^3 \Pi(E_k). \quad (3.120)$$

Also, since E_k can assume either sign, the non-informative density $\Pi(E_k)$ is the homogeneous one [5]:

$$\Pi(E_k) = \frac{1}{2A} \Theta[E_k + A] \Theta[A - E_k], \quad \int dx \Pi(x) = 1, \quad (3.121)$$

where $\Theta[x]$ is the step function: $\Theta[x \leq 0] = 0$, $\Theta[x > 0] = 1$, and where $A > 0$ serves for regularizing the homogeneous density, it will not influence final results.

Recall that the heat-engine functioning conditions read

$$(1 - \theta)\hat{E}_3 > \hat{E}_2 > 0, \quad \text{or} \quad (1 - \theta)\hat{E}_3 < \hat{E}_2 < 0, \quad (3.122)$$

$$\hat{E}_k \equiv E_k - E_1, \quad \theta \equiv \beta_{31}/\beta_{32}. \quad (3.123)$$

Employing (3.121) we calculate from (3.122) the probability of the heat-engine functioning:

$$\int_{-A}^A \frac{dE_1 dE_2 dE_3}{8A^3} \left(\Theta[\hat{E}_2] \Theta[(1 - \theta)\hat{E}_3 - \hat{E}_2] + \Theta[-\hat{E}_2] \Theta[-(1 - \theta)\hat{E}_3 + \hat{E}_2] \right) = \frac{1 - \min[\theta, \frac{1}{\theta}]}{3}. \quad (3.124)$$

This probability is generally lower than $\frac{1}{3}$. Hence it is not surprising that we found numerically that the current J_{21} averaged over $\Pi(E_1, E_2, E_3)$ is positive, i.e. the random-structure machine does not function as a heat-engine.

Thus the coupling between structure and function, which is encoded in $P(E_1, E_2, E_3)$ must be informative in the above sense.

Conclusion

Let's shortly summarize the results obtained in this thesis.

We started by arguing that the problem of defining and interpreting the thermodynamic work done on a charged particle by time-dependent electromagnetic field (EMF) is still open. In particular, the definition of the thermodynamic work is not automatic, since the time-dependent Hamiltonian (1.4) of the particle is not gauge-invariant. Hence deeper physical reasons are needed for coming up with a consistent definition of work. We stress that previous attempts [11, 44, 46, 47, 53, 54] did not resolve this problem. In particular, it was not clear how to formulate the first law (that relates the work to the energy of the EMF-source), and how to connect with the mechanic work (force times displacement). All these issues are relevant for relativistic statistical thermodynamics [177].

The solution of the problem was sought along the following lines:

- The definition of work ought to emerge from a consistent energy-momentum tensor of the overall system (particles+EMF). In particular, this ensures that the definition is relativistically covariant. The standard energy-momentum tensor of EMF does not apply to this problem, since it implies that the particle does not have a potential energy and hence indirectly supports the choice of the temporal gauge $\phi = 0$ that leads to unacceptable conclusions for the definition of the thermodynamic work; see in introduction.

- The definition should hold the first law (work-energy theorem) that relates the energy of the work-recipient with the energy of the work-source.

We carried out this program|within lacunae listed below|and showed that the physically meaningful definition emerges from the Lorenz gauge of EMF. It comes from the energy-

momentum tensor (for matter+EMF) that is proposed in section 1.2. This tensor is gauge-invariant and holds several necessary features. Its differences and similarities with the standard energy-momentum tensor are discussed in section 1.2 and 1.6. The thermodynamic work can be defined via the particle's Hamiltonian in the Lorenz gauge. To an extent we were able to check, it is only in this gauge that the thermodynamic work is relativistically consistent and relates to the gauge-invariant kinetic energy of the source of EMF. The latter can also be recovered as the mechanic work done by Lorentz force acting on the source, thereby establishing a relation between the thermodynamic and mechanic work.

We verified the first law (1.46) also for the case, when the self-interaction is included in the dynamics of system. The energy transfer direction is well defined also in this case.

Our motivation was and is to understand how to define work for particles interacting with/via a non-stationary EMF. Besides its obvious importance in non-equilibrium statistical mechanics.

We studied a model for an adaptive heat engine that can function under scarce or unknown resources. The engine is consisted of working body and controller, which are feed-back connected. Several physical limitations for the adaptation concept were uncovered. They relate to the prior information available about the environment, i.e. whether both bath temperatures vary or one of them is fixed. It is shown that the adaptation mechanism is valid both for symmetric and Kramer's rates. Feed-forward mechanism doesn't provide any advantage of adaptation mechanism. The efficiency and power adaptation is also presented in this thesis. It is shown that if there is no any information (in Bayesian terms) about the probability density of energy levels of working body, then the machine mainly doesn't work as a heat engine.

Bibliography

- [1] R. Balian, *From Microphysics to Macrophysics*, I (Springer, Berlin, 1992).
- [2] J.C. Maxwell, *Tait's Thermodynamics*, Nature, **17**, 257 (1878).
- [3] J.W. Gibbs, *Elementary Principles in Statistical Mechanics*, New Haven, (1914).
- [4] G. Mahler, *Quantum Thermodynamic Processes*, Pan Stanford, Singapore, (2015).
- [5] E.T. Jaynes, *Prior probabilities*, IEEE Transactions on systems science and cybernetics, **4**, 227 (1968).
- [6] J. D. Bekenstein, *Bekenstein-Hawking entropy*, Scholarpedia, **3**, 7375 (2008).
- [7] F. Schlögl, *Probability and Heat*, (Vieweg, Braunschweig/Wiesbaden, 1989).
- [8] G. Lindblad, *Non-Equilibrium Entropy and Irreversibility*, D. Reidel, Dordrecht, (1983).
- [9] Th.M. Nieuwenhuizen and A.E. Allahverdyan, *Statistical thermodynamics of quantum Brownian motion: Construction of perpetuum mobile of the second kind*, Phys. Rev. E **66**, 036102 (2002)
- [10] Yu. G. Pavlenko, *Hamiltonian methods in electrodynamics and quantum mechanics*, Moscow University Press, (1985).
- [11] L.D. Landau and E.M. Lifshitz, *The Classical Theory of Fields*, 4th ed., Pergamon Press, Oxford, (1975).
- [12] R.P. Feynman, R.B. Leighton and M. Sands, *The Feynman Lectures on Physics*, Addison-Wesley, Reading, MA, (1964); chapter 27.

- [13] L.I. Mandelshtam, *Lectures on optics, relativity theory and quantum mechanics*, Moscow, Nauka, (1972).
- [14] S. Kauffman, *Molecular autonomous agents*, Phil. Trans. R. Soc. A **361**, 1089 (2003).
- [15] W. Brittin and G. Gamow, *Negative entropy and photosynthesis*, Proceedings of the National Academy of Sciences **47**, 724-727 (1961).
- [16] R.C. Jennings, E. Engelmann, F. Garlaschi, A. P. Casazza, and G. Zucchelli, *Photosynthesis and negative entropy production*, Biochimica et Biophysica Acta **1709**, pp.251-255 (2005).
- [17] R.M. MacNab, *An entropy-driven engine-the bacterial flagellar motor*. In: Oplatka, A., Balaban, M., (Eds), Biological Structures and Coupled Flows. Academic Press, New York, pp. 147-160 (1979).
- [18] K. Matsuno, *Physics underlying the formation of protocells*, J. Biol. Physics **20**, 117-121 (1995).
- [19] K. Matsuno, *A possible prebiotic heat engine*, Origins Life Evol. Biospheres **26**, 458 (1996).
- [20] A.W.J. Muller, *Thermoelectric energy conversion could be an energy source of living organisms*, Phys. Lett. 96 A, 319-321 (1983)
- [21] W.J. Muller, *Thermosynthesis by biomembranes: energy gain from cyclic temperature changes*, J. Theor. Biol. **115**, 429-453 (1985).
- [22] A.W.J. Muller and D. Schulze-Makuch, *Sorption heat engines: simple inanimate negative entropy generators*, Physica A **362**, 369-381 (2006).
- [23] V. N. Kompanichenko, *Inversion Concept of the Origin of Life*, Orig. Life Evol. Biosph. **42**, 153-178 (2012).
- [24] A.V. Melkikh, *Quantum information and the problem of mechanisms of biological evolution*, BioSystems, 115, 33-45 (2014).
- [25] A.V. Melkikh, *Can an organism adapt itself to unforeseen circumstances?*, arXiv preprint cs/0604009 (2006).

- [26] A.V. Melkikh, *The Modern Theory of Evolution from the Viewpoint of Statistical Physics*,
arXiv preprint q-bio/0603005 (2006).
- [27] A.V. Melkikh, *The No Free Lunch Theorem and hypothesis of instinctive animal behavior*,
Artificial Intelligence Research **3**, 43 (2014).
- [28] R.L. Lehrman, *Energy is not the ability to do work* ,
Phys. Teach. **11**, 15 (1973).
- [29] H.S. Leff and A.J. Mallinckrodt, *Stopping objects with zero external work: Mechanics meets thermodynamics* ,
Am. J. Phys. **61**, 121 (1993).
- [30] M. Esposito, U. Harbola, and S. Mukamel, *Nonequilibrium fluctuations, fluctuation theorems, and counting statistics in quantum systems* ,
Rev. Mod. Phys. **81**, 1665 (2009).
- [31] C. Jarzynski, *Nonequilibrium work relations: foundations and applications*,
Eur. Phys. J. B **64**, 331 (2008).
- [32] M. Campisi, P. Hanggi, and P. Talkner, *Erratum: Colloquium: Quantum fluctuation relations: Foundations and applications*,
Rev. Mod. Phys. **83**, 771 (2011).
- [33] P. Skrzypczyk, A. J. Short, S. Popescu, Nat. Commun. **5**, 4185 (2014).
- [34] A.E. Allahverdyan, *Nonequilibrium quantum fluctuations of work*,
Phys. Rev. E **90**, 032137 (2014).
- [35] R. Gallego, J. Eisert, and H. Wilming, *Defining work from operational principles*,
arXiv:1504.05056.
- [36] P. Talkner and P. Hanggi, *Aspects of Work*, arXiv:1512.02516.
- [37] F. Plastina *et al.*, *Irreversible Work and Inner Friction in Quantum Thermodynamic Processes*,
Phys. Rev. Lett. **113**, 260601 (2014).
- [38] A. E. Allahverdyan, K. V. Hovhannisyan, D. Janzing, and G. Mahler, *Thermodynamic limits of dynamic cooling*,
Phys. Rev. E **84**, 041109 (2011).
- [39] J.M.G. Vilar, and J.M. Rubi, *Failure of the Work-Hamiltonian Connection for Free-Energy Calculations*,
Phys. Rev. Lett. **100**, 020601 (2008);

- J.M.G. Vilar, and J.M. Rubi, *Reply*,
 Phys. Rev. Lett. **101**, 098902 (2008);
 J.M.G. Vilar, and J.M. Rubi, *Reply*,
 Phys. Rev. Lett. **101**, 098904 (2008).
- [40] L. Peliti, *Comment on “Failure of the Work-Hamiltonian Connection for Free-Energy Calculations”*,
 Phys. Rev. Lett. **101**, 098903 (2008).
 L. Peliti, *On the work-Hamiltonian connection in manipulated systems*,
 J. Stat. Mech.: Theory. Exp. P05002 (2008).
- [41] E.N. Zimanyi and R. J. Silbey, *The work-Hamiltonian connection and the usefulness of the Jarzynski equality for free energy calculations*,
 J. Chem. Phys. **130**, 171102 (2009).
- [42] J.M.G. Vilar, and J.M. Rubi, *Work-Hamiltonian connection for anisoparametric processes in manipulated microsystems*,
 J. Non-Equilib. Thermodyn. **36**, 123 (2011).
- [43] J. Horowitz and C. Jarzynski, *Comment on “Failure of the Work-Hamiltonian Connection for Free-Energy Calculations”*,
 Phys. Rev. Lett. **101**, 098901 (2008).
- [44] B. Kosyakov, *Introduction to the Classical Theory of Particles and Fields*,
 Springer, Berlin, (2007).
- [45] K.-H. Yang, *Gauge transformations and quantum mechanics I. Gauge invariant interpretation of quantum mechanics*,
 Annals of Physics, **101**, 62 (1976).
- [46] D.H. Kobe, E.C.T. Wen and K.H. Yang, *Power operator in quantum mechanics*,
 Phys. Rev. D **26**, 1927 (1982).
- [47] D.H. Kobe and K.H. Yang, *Gauge-invariant non-relativistic limit of an electron in a time-dependent electromagnetic field*,
 J. Phys. A: Math. Gen. **13**, 3171 (1980).
- [48] J. A. Sanchez-Monroy, J. Morales, and E. Zambrano, *Energy operator for non-relativistic and relativistic quantum mechanics revisited*,
 arxiv.org/1208.1425.
- [49] D. J. Griffiths, *Resource letter EM-1: Electromagnetic momentum*,
 Am. J. Phys. **80**, 7 (2012).

- [50] E. Leader and C. Lorcé, *The angular momentum controversy: What's it all about and does it matter?*,
Phys. Rep. **541**, 163 (2014).
- [51] H. R. Reiss, *Limitations of gauge invariance*,
arXiv:1302.1212v1.
- [52] H. R. Reiss, *On a modified electrodynamics*,
J. Mod. Optics **59**, 1371 (2012).
- [53] J. E. Sipe, *New Hamiltonian for a charged particle in an applied electromagnetic field*,
Phys. Rev. A, **27**, 615 (1983)
- [54] W.-M. Sun, X.-S. Chen, X.-F. Lü, and F. Wang, *Gauge-invariant hydrogen-atom Hamiltonian*,
Phys. Rev. A, **82**, 012107 (2010).
- [55] A. M. Stewart, *Vector potential of the Coulomb gauge*,
Eur. J. Phys. **24**, 519 (2003).
- [56] J.A. Heras, *A short proof that the Coulomb-gauge potentials yield the retarded fields*,
Eur. J. Phys. **32**, 213 (2011).
- [57] B.J. Wundt and U. D. Jentschura, *Sources, potentials and fields in Lorenz and Coulomb gauge: Cancellation of instantaneous interactions for moving point charges*,
Annals of Physics **327**, 1217 (2012).
- [58] J. A Heras and G. Fernandez-Anaya, *Can the Lorenz-gauge potentials be considered physical quantities?*,
arXiv:1012.1063v1.
- [59] V. P. Dmitriyev, *On vector potential of the Coulomb gauge*,
Eur. J. Phys. **25**, L23 (2004).
- [60] L-C. Tu, J. Luo and G.T. Gillies, *The mass of the photon*,
Rep. Prog. Phys. **68**, 77 (2005).
- [61] H.E. Puthoff, *Electromagnetic Potentials Basis for Energy Density and Power Flux*,
arxiv.org/pdf/0904.1617.
- [62] N.N. Bogoliubov and D.V. Shirkov, *Introduction to theory of Quantized Fields*,
J. Wiley, NY, (1980).
- [63] S. Deffner and A. Saxena, *Quantum work statistics of charged Dirac particles in time-dependent fields*,
Phys. Rev. E **92**, 032137 (2015)

- [64] J.I. Jimenez-Aquino, F.J. Uribe and R.M. Velasco, *Work-fluctuation theorems for a particle in an electromagnetic field*,
J. Phys. A **43**, 255001 (2010)
- [65] A. Saha and A. M. Jayannavar, *Nonequilibrium work distributions for a trapped Brownian particle in a time-dependent magnetic field*,
Phys. Rev. E **77**, 022105 (2008).
- [66] P. Pradhan, *Nonequilibrium fluctuation theorems in the presence of a time-reversal symmetry-breaking field and nonconservative forces*,
Phys. Rev. E **81**, 021122 (2010).
- [67] A. Saha, S. Lahiri, and A.M. Jayannavar, *Classical diamagnetism revisited*,
Modern Physics Letters B **24**, 2899 (2010)
- [68] G. Rousseaux, *Lorenz or Coulomb in Galilean electromagnetism?*,
Europhys.Lett. **71**, 15 (2005).
- [69] J. Larsson, *Electromagnetics from a quasistatic perspective*,
Am. J. Phys. **75**, 230 (2007).
- [70] A.B. van Oost, Eur. Phys. J. D, **8**, 9 (2000).
- [71] V. Fock and B. Podolsky, *On the quantization of electromagnetic waves and the interaction of charges on Dirac theory*,
Sov. Phys **1**, 801 (1932).
- [72] A.V. Gritsunov, *Self-sufficient potential formalism in describing electromagnetic interactions*,
Radioelectronics and Communications Systems, **52**, 649 (2009).
- [73] E. Fermi, Rend. Lincei **9**, 881 (1929).
- [74] E. M. Pugh and G. E. Pugh, *Physical significance of the Poynting vector in static fields*,
Am. J. Phys. **35**, 153 (1967).
- [75] J.L. Synge, *On the electromagnetic two-body problem*,
Proc. Roy. Soc. London A **177**, 118 (1940).
- [76] R.C. Stabler, *A possible modification of classical electrodynamics*,
Phys. Lett. **8**, 185 (1964).
- [77] F.H.J. Cornish, *Classical radiation theory and point charges*,
Proc. Phys. Soc. **86**, 427 (1965).
- [78] D. Leiter, J. Phys. A, **3**, 89 (1970).

- [79] R.G. Beil, *Alternate formulations of classical electrodynamics*,
Phys. Rev. D, **12**, 2266 (1975)
- [80] J. Franklin and C. LaMont, *The Motion of a Pair of Charged Particles*,
Brazilian Journal of Physics **44**, 119 (2014).
- [81] S.B. Kirpichev and P. A. Polyakov, *On the formulation of initial-value problems for systems consisting of relativistic particles*,
Journal of Mathematical Sciences, **141**, 1051 (2007).
- [82] R.D. Driver, *A two-body problem of classical electrodynamics: the one-dimensional case*,
Ann. Phys. **21**, 122 (1963).
- [83] R.D. Driver and M.J. Norris, *Note on uniqueness for a one-dimensional two-body problem of classical electrodynamics*,
Ann. Phys. **42**, 347 (1967).
- [84] J. Huschilt, W. E. Baylis, D. Leiter, and G. Szamosi, *Numerical solutions to two-body problems in classical electrodynamics: straight-line motion with retarded fields and no radiation reaction*,
Phys. Rev. D **7**, 2844 (1973).
- [85] J. C. Kasher, *Taylor-series method for two-body problems in classical electrodynamics: One-dimensional repulsive motion with retarded fields and no radiation reaction*,
Phys. Rev. D **12**, 1729 (1975).
- [86] R. D. Driver, *Ordinary and Delay Differential Equations*,
Springer-Verlag, New York, (1977).
- [87] S.P. Travis, *Existence theorem for a backwards two-body problem of electrodynamics*,
Phys. Rev. D **11**, 292 (1975).
- [88] D.P. Hsing, Phys. Rev. D **16**, 974 (1977).
- [89] V.I. Zhdanov, *Convergence of iteration method in the relativistic two-body problem, taking into account the retardation of interactions*,
J. Phys. A: Math. Gen. **24**, 5011 (1991).
- [90] A. Bellen and M. Zennaro, *Numerical methods for delay differential equations*,
Oxford University Press, Oxford,(2003).
- [91] P.C. Aichelburg and H. Grosse, *Exactly soluble system of relativistic two-body interaction*,
Phys. Rev. D **16**, 1900 (1977).
- [92] A. Gamba, *Physical quantities in different reference systems according to relativity*,
Am. J. of Phys. **35**, 83 (1967).

- [93] V.N. Strel'tsov, *On the relativistic length*,
Foundations of Physics, **6**, 293 (1976).
- [94] C. Jeffries, *A New Conservation Law for Classical Electrodynamics*,
SIAM Rev. **34**, 386 (1992).
- [95] J. Slepian, *Energy and energy flow in the electromagnetic field*,
J. Appl. Phys. **13**, 512 (1942).
- [96] C.S. Lai, *Alternative choice for the energy flow vector of the electromagnetic field*,
Am. J. Phys. **49**, 841 (1981).
- [97] P. C. Peters, *Objections to an alternate energy flow vector*,
Am. J. Phys. **50**, 1165 (1982).
- [98] R. H. Romer, *Alternatives to the Poynting vector for describing the flow of electromagnetic energy*,
Am. J. Phys. **50**, 1166 (1982).
- [99] D. H. Kobe, *Energy flux vector for the electromagnetic field and gauge invariance* Am.
J. Phys. **50**, 1162 (1982).
- [100] U. Backhaus and K. Schafer, *On the uniqueness of the vector for energy flow density in electromagnetic fields* ,
Am. J. Phys. **54**, 279 (1986)
- [101] C.J. Carpenter, *Electromagnetic energy and power in terms of charges and potentials instead of fields* ,
IEE Proc. **136**, 55 (1989).
- [102] A. Chubykalo, A. Espinoza, R. Tzonchev, *Experimental test of the compatibility of the definitions of the electromagnetic energy density and the Poynting vector*,
Eur. Phys. J. D **31**, 113 (2004).
- [103] A.M. Gabovich and N. A. Gabovich, *How to explain the non-zero mass of electromagnetic radiation consisting of zero-mass photons*,
Eur. J. Phys. **28**, 649 (2007).
- [104] L. Allen, M.J. Padgett, and M. Babiker, *The orbital angular momentum of light*,
Progress In Optics **XXXIX**, 39, 291 (1999).
- [105] A. Trautman, *Spin and torsion may avert gravitational singularities*,
Nature **242**, 7 (1973).
- [106] D.W. Sciama, *Mathematical Proceedings of the Cambridge Philosophical Society*, **54**,
No. 01 (Cambridge University Press, 1958).

- [107] K. Hayashi and A. Bregman, *Poincaré gauge invariance and the dynamical role of spin in gravitational theory*,
Annals of Physics, **75**, 562 (1973).
- [108] E. N. Glass, J. Huschilt, and G. Szamosi, *Physical interpretation of the Lorentz–Dirac equation*,
Am. J. Phys. **52**, 445 (1984).
- [109] R.D. Driver, *A " backwards " two-body problem of classical relativistic electrodynamics*,
Phys. Rev. **178**, 2051 (1969).
- [110] H.B. Callen, *Thermodynamics and an introduction to thermostatistics*,
John Wiley & Sons, NY, (1985).
- [111] K. Sekimoto, *Stochastic Energetics*
, Springer-Verlag, Berlin (2010).
- [112] U. Seifert, *Stochastic thermodynamics, fluctuation theorems and molecular machines*,
Rep. Prog. Phys. **75**, 126001 (2012).
- [113] D. Chowdhury, *Resource Letter PBM-1: Physics of biomolecular machines*,
Am. J. Phys. **77**, 583 (2009).
- [114] H.E.D. Scovil and E.O. Schultz-DuBois, *Three-level masers as heat engines*,
Phys. Rev. Lett., **2**, 262 (1959).
- [115] J. E. Geusic, E. O. Schulz-DuBios, and H. E. D. Scovil, *Quantum Equivalent of the Carnot Cycle*,
Phys. Rev., **156**, 343 (1967).
- [116] V.K. Konyukhov and A.M. Prokhorov, *Uspekhi Fiz. Nauk*, **119**, 541 (1976).
- [117] E. Geva and R. Kosloff, *Three-level quantum amplifier as a heat engine: A study in finite-time thermodynamics*,
Phys. Rev. E **49**, 3903 (1994).
- [118] E. Boukoza and D. Tannor, *Three-Level Systems as Amplifiers and Attenuators: A Thermodynamic Analysis*,
Phys. Rev. Lett., **98**, 240601 (2007).
- [119] R. Uzdin, A. Levy, and R. Kosloff, *Equivalence of Quantum Heat Machines, and Quantum-Thermodynamic Signatures*,
Phys. Rev. X **5**, 031044 (2015).
- [120] G. Thomas and R.S. Johal, *Expected behavior of quantum thermodynamic machines with prior information*,
Phys. Rev. E **85**, 041146 (2012).

- [121] A. E. Allahverdyan, K. V. Hovhannisyan, A. V. Melkikh, and S. G. Gevorkian, *Carnot Cycle at Finite Power: Attainability of Maximal Efficiency*, Phys. Rev. Lett. **111**, 050601 (2013).
- [122] N. Linden, S. Popescu, and P. Skrzypczyk, *The smallest possible heat engines*, arxiv.1010.6029.
- [123] A.S.L. Malabarba, A.J. Short, and P. Kammerlander, *Clock-driven quantum thermal engines*, New J. Phys. **17**, 045027 (2015).
- [124] M.F. Frenzel, D. Jennings, and T. Rudolph, *Quasi-autonomous quantum thermal machines and quantum to classical energy flow*, New J. Phys. **18**, 023037 (2016).
- [125] M.O. Scully, *Quantum photocell: Using quantum coherence to reduce radiative recombination and increase efficiency*, Phys. Rev. Lett. **104**, 207701 (2010).
- [126] Marlan O. Scully, Kimberly R. Chapin, Konstantin E. Dorfman, Moochan Barnabas Kim, and Anatoly Svidzinsky, *Quantum heat engine power can be increased by noise-induced coherence*, PNAS, **108**, 15097 (2011).
- [127] O. Abah, J. Roßnagel, G. Jacob, S. Deffner, F. Schmidt-Kaler, K. Singer, and E. Lutz, *Single-Ion Heat Engine at Maximum Power*, Phys. Rev. Lett. **109**, 203006 (2012).
- [128] K. Zhang, F. Bariani, and P. Meystre, *Quantum Optomechanical Heat Engine*, Phys. Rev. Lett. **112**, 150602 (2014).
- [129] Damiano La Manna, Vincenzo Li Vigni, Eleonora Riva Sanseverino, Vincenzo Di Dio, Pietro Romano, *Reconfigurable electrical interconnection strategies for photovoltaic arrays: A review*, Renewable and Sustainable Energy Reviews, **33**, 412 (2014).
- [130] E. Albarran-Zavala and F. Angulo-Brown, *A simple thermodynamic analysis of photosynthesis*, Entropy, **9**, 152 (2007).
- [131] S. Falk *et al.*, *Photosynthetic adjustment to temperature*, in *Photosynthesis and the environment*, ed. by N.R. Baker Springer, Netherlands, 1996, pp. 367-385,.

- [132] I. Rojdestvenski, M. G. Cottam, G. Oquist and N. Huner, *Thermodynamics of complexity*,
Physica A **320**, 318 (2003).
- [133] T. Friedlander and N. Brenner, *Adaptive response by state-dependent inactivation*,
PNAS, **106**, 22558 (2009).
- [134] M. Inoue and K. Kaneko, *Dynamics of coupled adaptive elements: Bursting and intermittent oscillations generated by frustration in networks*,
Phys. Rev. E **81**, 026203 (2010).
- [135] G. Lan, P. Sartori, S. Neumann, V. Sourjik, Y. Tu, *The energy-speed-accuracy trade-off in sensory adaptation*,
Nature Phys. **8**, 422 (2012).
- [136] A. E. Allahverdyan and Q.A. Wang, *Adaptive machine and its thermodynamic costs*,
Phys. Rev. E **87**, 032139 (2013).
- [137] A. C. Barato, D. Hartich, and U. Seifert, *Information-theoretic versus thermodynamic entropy production in autonomous sensory networks*,
Phys. Rev. E **87**, 042104 (2013).
- [138] A. C. Barato, D. Hartich, and U. Seifert, *Efficiency of cellular information processing*,
New J. Phys. **16**, 103024 (2014).
- [139] S. Bo, M. Del Giudice, and A. Celani, *Thermodynamic limits to information harvesting by sensory systems*,
Journal of Statistical Mechanics: Theory and Experiment, P01014 (2015).
- [140] P. Sartori and Y. Tu, *Free energy cost of reducing noise while maintaining a high sensitivity*,
Phys. Rev. Lett. **115**, 118102 (2015).
- [141] D. Markovic and C. Gros, *Self-organized chaos through polyhomeostatic optimization*,
Phys. Rev. Lett. **105**, 068702 (2010).
- [142] S. McGregor and N. Virgo, in *Advances in Artificial Life: Darwin Meets von Neumann*,
Springer, Berlin, (2009), pp. 230-237 .
- [143] N.G. van Kampen, *Stochastic Processes in Physics and Chemistry*,
Elsevier, Amsterdam, (2007).
- [144] K. Proesmans, B. Cleuren, and C. Van den Broeck, *Power-efficiency-dissipation relations in linear thermodynamics*,
Phys. Rev. Lett. **116**, 220601 (2016).

- [145] N. Shiraishi, K. Saito, and H. Tasaki, *Universal trade-off relation between power and efficiency for heat engines*, arXiv:1605.00356 (2016).
- [146] R. Zwanzig, *Rate processes with dynamical disorder*, Acc. Chem. Res. **23**, 148 (1990).
- [147] H. Frauenfelder, P.G. Wolynes, and R.H. Austin, *Biological physics*, Rev. Mod. Phys. **71**, S419 (1999).
- [148] N. Agmon and J.J. Hopfield, *Transient kinetics of chemical reactions with bounded diffusion perpendicular to the reaction coordinate: intramolecular processes with slow conformational changes*, J. Chem. Phys. **78**, 6947 (1983).
- [149] M. Kurzynski, *The thermodynamic machinery of life*, (Springer-Verlag, Berlin 2010).
- [150] L.A. Blumenfeld and A.N. Tikhonov, *Biophysical Thermodynamics of Intracellular Processes*, Springer, Berlin, (1994).
- [151] H.-P. Lerch, A.S. Mikhailov, and B. Hess, *Conformational-relaxation models of single-enzyme kinetics*, PNAS, **99**, 15410 (2002).
- [152] H.-P. Lerch, R. Rigler, A.S. Mikhailov, *Functional conformational motions in the turnover cycle of cholesterol oxidase*, PNAS, **102**, 10807 (2005).
- [153] C. Bustamante, Y.R. Chemla, N.R. Forde, and D. Izhaky, *Mechanical processes in biochemistry*, Annu. Rev. Biochem. **73**, 705 (2004).
- [154] Z.D. Nagel and J.P. Klinman, *A 21st century revisionist's view at a turning point in enzymology*, Nat. Chem. Biol. **5**, 543 (2009).
- [155] K.V. Shaitan and A.B. Rubin, *Stochastic dynamics and electron-conformation interactions in proteins*, Biofizika, **30**, 517 (1984).
- [156] K.V. Shaitan, *Dynamics of electron-conformational transitions and new approaches to the physical mechanisms of functioning of biomacromolecules*, Biophysics, **39**, 993 (1994)

- [157] A. L. Borovinskiy and A. Yu. Grosberg, *Design of toy proteins capable of rearranging conformations in a mechanical fashion*, J. Chem. Phys. **118**, 5201 (2003).
- [158] V.A. Kovarskii, *Quantum processes in biological molecules. Enzyme catalysis*, Physics-Uspekhi **42**, 797 (1999).
- [159] Alexander O.Goushcha, Valery N.Kharkyanen, Gary W.Scott, Alfred R.Holzwarth, *Self-Regulation Phenomena in Bacterial Reaction Centers. I. General Theory*, Biophys. J., **79**, 1237 (2000).
- [160] L.N. Christophorov, A.R. Holzwarth, V.N. Kharkyanen, and F. van Mourik, *Structure-function self-organization in nonequilibrium macromolecular systems*, Chemical Physics **256**, 45 (2000).
- [161] A.I. Berg *et al.*, *CONFORMATIONAL REGULATION OF ACTIVITY IN PHOTOSYNTHETIC MEMBRANES OF PURPLE BACTERIA* Molecular Biology **13**, 58 (1979).
- [162] A.E. Allahverdyan and Th.M. Nieuwenhuizen, *Steady adiabatic state: Its thermodynamics, entropy production, energy dissipation, and violation of Onsager relations*, Phys. Rev. E, **62**, 845 (2000).
- [163] S. Rahav, J. Horowitz and C. Jarzynski, *Directed flow in nonadiabatic stochastic pumps*, Phys. Rev. Lett. **101**, 140602 (2008).
- [164] D. Mandal and C. Jarzynski, *A proof by graphical construction of the no-pumping theorem of stochastic pumps*, J. Stat. Mech. P10006 (2011).
- [165] N.F. Ramsey, *Thermodynamics and Statistical Mechanics at Negative Absolute Temperatures*, Phys. Rev. **103**, 20 (1956).
- [166] S. Machlup, *Negative temperatures and negative dissipation*, Am. J. Phys. **43**, 991 (1975).
- [167] A.G. Butkovskii and Yu.I. Samoilenko, *Control of Quantum Mechanical Processes*, Springer, Berlin, (1991).
- [168] H. Schmidt and G. Mahler, *Control of local relaxation behavior in closed bipartite quantum systems*, Phys. Rev. E **72**, 016117 (2005).
- [169] N. Brunner, N. Linden, S. Popescu, and P. Skrzypczyk, Phys. Rev. E **85**, 05111 (2012).

- [170] S. Braun, P. Ronzheimer, M. Schreiber, S. S. Hodgman, T. Rom, I. Bloch, and U. Schneider, *Negative absolute temperature for motional degrees of freedom*, Science, **339**, 52 (2013).
- [171] See https://en.wikipedia.org/wiki/Negative_resistance
- [172] V.P. Starr, *Physics of negative viscosity phenomena*, McGraw-Hill, (1968).
- [173] B. Cleuren and C. Van den Broeck, *Random walks with absolute negative mobility*, Phys. Rev. E. **65**, 030101(R) (2002).
- [174] A. Haljas, R. Mankin, A. Sauga, E. Reiter, *Anomalous mobility of Brownian particles in a tilted symmetric sawtooth potential*, Phys. Rev. E. **70**, 041107 (2004).
- [175] J. Spiechowicz, J. Luczka, P. Hanggi, *Absolute negative mobility induced by white Poissonian noise*, Journal of Statistical Mechanics: Theory and Experiment P02044 (2013).
- [176] I. Tyukin, *Adaptive Nonlinear Systems* Cambridge University Press, Cambridge, UK, (2011).
- [177] M. Requardt, *Thermodynamics meets Special Relativity - or what is real in Physics?*, arXiv preprint arXiv:0801.2639.
- [178] A E Allahverdyan and S G Babajanyan, *Electromagnetic gauge-freedom and work*, J. Phys. A: Math. Theor. **49** 285001, (2016)
- [179] S.G. Babajanyan, *Work and energy for particles in electromagnetic field*, Phys. Atom. Nucl. Vol.80, N 4, p.822-826 (2017).
- [180] A.E. Allahverdyan, S.G. Babajanyan, N.H. Martirosyan, and A.V. Melkikh, *Adaptive Heat Engine*, Phys. Rev. Lett. **117**, 030601, (2016)